

Institut für Organische Chemie und Biochemie
der Technischen Universität München

**Carbohydrates and SAAs in Drug-Design: Synthesis of Selective $\alpha 4\beta 7$ -Integrin
Antagonists and Cyclodextrin Mimetics**

Elsa Locardi

Vollständiger Abdruck der von der Fakultät für Chemie der Technischen Universität
München zur Erlangung des akademischen Grades eines

Doktors der Naturwissenschaften

genehmigten Dissertation.

Vorsitzender: Univ.-Prof. Dr. St. J. Glaser

Prüfer der Dissertation:

1. Univ.-Prof. Dr. H. Kessler
2. Univ.-Prof. Dr. B. Holzmann
3. apl. Prof. Dr. L. Moroder

Die Dissertation wurde am 17.10.2002 bei der Technischen Universität München
eingereicht und durch die Fakultät für Chemie am 09.12.2002 angenommen.

ai miei genitori

There are many people who have directly and indirectly contributed to this work. First of all I would like to thank my thesis supervisor Prof. Dr. Horst Kessler. He has been a great source of encouragement throughout this work. I would like to especially thank him for the amount of scientific freedom he gave me and for his brilliant ideas and very precise and critical comments which added considerably to the quality of this thesis.

A lot of colleagues in the working group of Professor Kessler have contributed to the pleasure of my staying at the Institute. It would be difficult to mention all the names but I would certainly like to mention a few:

I am especially indebted to my lab mates Dr. Claudia Biro, Dr. Jürgen Boer, Ulrich Hersel and Dr. Matthias Stöckle for making my stay here a wonderful experience. They have been fantastic people to work with, both in the fields of chemistry and outside it.

I also thank the other doctoral and postdoctoral fellows at the Institute for the friendly atmosphere and the fruitful discussions. In particular, I am very grateful to Dr. Sibylle Gruner and Dr. Martin Sukopp for being an immense source of joy and for making me very often laugh.

I would like to express my gratitude to Dr. Jürgen Boer who contributed to this study not only by numerous discussions and critical remarks, but also supporting me through all stages of it.

I would like to thank Dr. Gerd Gemecker and Dr. Rainer Haeßner for their advice on the NMR hardware and software.

I am also grateful to Armin Modlinger for his support with many organizational aspects of the work, in particular for getting the HRMS.

My sincerest thanks go to Maria Kranawetter for preparative HPLC purifications, Burghard Cordes for recording MS-spectra, Evelyn Bruckmaier and Marianne Machule for secretarial assistance.

I am also indebted to Sonia Cesana and Dr. Luciana Marinelli for the critical inspection and reading of this work and for being great friends.

I would like to thank Prof Dr. Bernhard Holzmann for his collaboration and Anja Schuster for measuring the biological activities of the sugar analogs.

Last, but definitely not the least I would like to thank my family for the patience they have shown during the course of my studies. I would like to especially thank my parents for the kind of encouragement and support they have provided me - and their constant blessings for my success.

Index

1	Introduction.....	1
2	Biological Implications of α 4-Integrins	3
2.1	α 4 β 7 integrin as therapeutic targets	4
2.2	Cell adhesion molecules (CAMs).....	6
3	Carbohydrates and Sugar Amino Acids in Drug-Design	10
3.1	Naturally occurring sugar amino acid (SAA).....	10
3.2	Carbohydrate-based peptidomimetics.....	12
3.3	SAA oligomers as carbohydrate mimetics.....	13
3.4	Carbohydrate and SAA as scaffolds	15
4	Cyclic Homo-Oligomers from Sugar Amino Acids: Synthesis, Conformational Analysis and Significance.....	24
4.1	Synthesis in solution and on solid phase of the oligomers containing Gum	24
4.2	Conformational analysis by NMR	27
4.3	Molecular modeling.....	30
4.4	Cyclodextrin-like complexation behavior of the cyclic hexamer.....	34
5	Synthesis and SAR of Mannose-Based Peptidomimetics Blocking Selectively Integrin α 4 β 7 Binding to MAdCAM-1	39
5.1	Design and synthesis of the mannose-based peptidomimetics	39
5.2	Structure Activity Relationship for the Biased Mannose-Based Library	49
5.3	Structure activity relationship.....	54
6	Summary	57
7	Zusammenfassung.....	60
8	Experimental Section	63
8.1	General methods	63
8.2	Synthesis of the oligomers containing Gum	63

8.3	Synthesis of individual mannose-based compounds	71
8.4	Conformational analysis of the cyclodextrin mimetics	121
8.5	Binding studies of the cyclodextrin mimetics	122
8.6	Biological evaluation of the mannose-based library	122
8.7	Conformational analysis of the mannose-based library.....	124
9	References.....	126

Abbreviations

1D, 2D	mono-dimensional, two-dimensional
Å	angstrom, 10^{-10} m
Ac	acetyl
ACN	acetonitrile
ADME	absorption, distribution, metabolism, excretion
Boc	<i>tert.</i> -butoxycarbonyl
br	broad
BSA	bovine serum albumin
Bu	<i>n</i> -butyl
BuLi	<i>n</i> -butyllithium
cat.	catalytic
CDA	cyclohexane-1,2-diacetal
conc.	concentrated
COSY	correlated spectroscopy
d	doublet or days
dd	doublet of doublet
δ	chemical shift
dist.	distillated
DCC	<i>N,N'</i> -dicyclohexylcarbodiimide
DCM	dichloromethane
DIC	<i>N,N'</i> -diisopropylcarbodiimide
DIPEA	diisopropylethylamine
DME	1,2-dimethoxyethane
DMF	<i>N,N</i> -dimethylformamide
DMSO	dimethylsulfoxide
<i>E. coli</i>	<i>escherichia coli</i>
EDCI	<i>N</i> -ethyl- <i>N,N'</i> -(dimethylaminopropyl)-carbodiimide
EDT	1,2-ethanedithiole
ELISA	enzyme linked immuno sorbent assay
eq.	equivalent

ESI	electro spray ionization
Et	ethyl
ECM	extracellular matrix
Fmoc	9-fluorenylmethoxycarbonyl
Fmoc-ONSu	(<i>N</i> -fluorenylmethoxycarbonyloxy)- <i>N</i> -succinimide
g	gram
Gum	Glucosyluronic acid methylamine
h	hour
HATU	<i>O</i> -(7-azabenzotriazole-1-yl)- <i>N,N,N',N'</i> , - tetramethyluronium-hexafluorophosphate
HFIP	hexafluoroisopropanol
HIV	human immunodeficiency virus
HOAc	acetic acid
HOAt	1-hydroxy-7-azabenzotriazole
HOBt	1-hydroxybenzotriazole
HOSu	<i>N</i> -hydroxysuccinimide
HPLC	high performance liquid chromatography
Hz	hertz
IC	inhibitory capacity
Ig	immunoglobulin
K	kelvin
kDa	kilodalton
L	liter
LDA	lithiumdiisopropylamide
LHMDS	lithium-bis(trimethylsilyl)amide
J	scalar coupling constant
m	multiplet
M	molar
mAb	monoclonal antibody
MD	molecular dynamic
Me	methyl
MeIm	<i>N</i> -methylimidazole

Abbreviations

MeOH	methanol
MHz	megahertz
min.	minutes
mL	milliliter
mm	millimeter
MMA	<i>N</i> -methylmercaptoacetamide
mmol	millimol
MMP	metallomatrixproteinase
MS	mass spectroscopy
MSNT	1-(mesityl-2-sulfonyl)-3-nitro-1H-1,2,4-triazole
MW	molecular weight
μmol	micromol
N	normal
nm	nanometer
nM	nanomolar
NMM	<i>N</i> -methylmorpholine
NMP	<i>N</i> -methylpyrrolidone
NMR	nuclear magnetic resonance
NOE	nuclear Overhauser enhancement
NOESY	nuclear Overhauser enhancement spectroscopy
PDA	phenanthrene-9,10-diacetals
PEG	polyethyleneglycol
Ph	phenyl
pm	picometer
ppm	parts per million
q	quartet
QSAR	quantitative structure activity relationship
rMD	restraint molecular dynamics
fMD	free molecular dynamics
RP-HPLC	reversed phase high performance liquid chromatography
RP	reversed phase
R _t	retention time

RT	room temperature
s	singlet
SPPS	solid phase peptide synthesis
SPR	surface plasmon resonance
t	triplet
<i>t</i> Bu	<i>tert.</i> -butyl
TBTU	<i>O</i> -(1 <i>H</i> -benzotriazol-1-yl)- <i>N,N,N',N'</i> -tetramethyluronium-hexafluoroborate
TCP	tritylchloride polystyrene resin
TEA	triethylamine
TFA	trifluoroacetic acid
TFE	1,1,1-trifluoroethanol
TEMPO	2,2,6,6-tetramethyl-1-piperidinyloxy
TFMSA	trifluoromethanesulfonic acid
TG	tentagel
TGF	transforming growth factor
THF	tetrahydrofuran
TIPS	triisopropylsilane
TLC	thin layer chromatography
TMS	trimethylsilyl
Trt, Trityl	triphenylmethyl
uPA	urokinase plasminogen activator
uPAR	urokinase plasminogen activator receptor
UV	Ultraviolet
VEGF	vascular endothelial growth factor
VN	vitronectin
Xaa	general aminoacid

In this work the nomenclature is based upon the *Chemical Abstracts* (Chemical Abstracts, 'Index Guide', 77, 210) and the *IUPAC-IUB-commission* (Eur. J. Biochem. **1984**, 138, 9-37).

1 Introduction

Structure Activity Relationship (SAR) studies on biopolymers have led to an increasing interest in the potentials of their synthetic analogues in order to modify pharmacokinetics and metabolic stability of the natural drugs. Peptides and oligosaccharides are attractive targets for mimicry due to their involvement in a complexity of biological processes.

Sugar Amino Acids (SAAs),¹ carbohydrates bearing an amino group and a carboxyl group, are ideal peptidomimetic scaffolds^{2,3} since they may function as structural pharmacophores,⁴ and are attractive building blocks for the incorporation of a sugar moiety into combinatorial libraries using standard peptide coupling techniques.⁵⁻⁹

Oligomers of pyranose sugar amino acids, first introduced by Fuchs and Lehmann^{10,11} have been proposed to mimic oligosaccharide¹² and oligonucleotide^{13,14} backbone structures *via* amide bond linkages. However, cyclic sugar amino acid homo-oligomers have not been reported before our contributions.^{15,16} Herein, the synthesis and the conformational preferences of linear and cyclic, water soluble oligomers containing *Glucosyluronic acid methylamine* (Gum)⁴ as repetitive unit is presented.

This work focused on the potentials of small oligomeric sequences with backbones of specific folding patterns and functionalities as novel artificial receptors. We assumed that a cyclic array of desired ring-size and defined secondary structure, of alternating carbohydrate moieties and amide groups might lead to exquisite specificity of recognition and catalysis. An application of this concept, presented here, is the mimicry of cyclodextrin (CD) inclusion complexes.¹⁷⁻²¹

Another aspect treated in this work is the use of sugars for rational combinatorial development of anti-inflammatory drugs.

The infiltration of leukocytes to the site of inflammation contributes to the pathogenesis of a number of human autoimmune diseases and results from a series of adhesive and activating events involving multiple receptor-ligand interactions. The inflammatory processes leading to tissue damage and disease are mediated in part by the $\alpha 4$ integrins, $\alpha 4\beta 1$ and $\alpha 4\beta 7$, expressed on the leukocyte cell surface. These

glycoprotein receptors modulate cell adhesion *via* interaction with their primary ligands, vascular cell adhesion molecule-1 (VCAM-1) and mucosal addressin cell adhesion molecule-1 (MAdCAM-1), expressed in the affected tissue.

As part of our ongoing research in the development of $\alpha 4\beta 7$ integrin antagonists, we are interested in peptidomimetics based on a rigid scaffold to allow the display of essential side chains in a suitable binding conformation while eliminating backbone amide bonds and therefore improving pharmacokinetic parameters of the drug. So far only a few research groups succeeded in the transition from bioactive peptides to small molecules inhibitors using rigid scaffolds like cyclohexane.²²⁻²⁷ In this work another successful application of this concept is presented. Based on a D-mannose core we developed in a rational combinatorial approach a potent and selective inhibitor of the $\alpha 4\beta 7$ /MAdCAM interaction.

A peptide based structure-activity study was carried out previously in our laboratory leading to a number of potent and selective $\alpha 4\beta 7$ inhibitors.²⁸ Cyclic hexapeptides were designed and synthesized in an effort to mimic the MAdCAM's LDT binding motif by incorporation into a rigid peptide core that adopts only specific conformations. These compounds were later used as templates for the design of a non-peptidic $\alpha 4\beta 7$ antagonist based on β -D-mannose as rigid scaffold, carrying the Leu, Asp and Thr mimetics at 6,1 and 2-positions of the pyranoside, respectively. The mannose core mimicked the bioactive conformation of the constrained peptides displaying the aspartic acid at the $i + 1$ position of a β -turn. Unfortunately, the designed mannopyranoside had no inhibitory activity against $\alpha 4\beta 7$ /MAdCAM interaction, but one analogue, where the Thr side chain is replaced by the Ser side chain, demonstrated inhibition of VCAM mediated binding of $\alpha 4\beta 1$ Jurkat cells ($IC_{50} \cong 3.7$ mM).²⁹ Our interest in $\alpha 4\beta 7$ integrin antagonists prompted us to investigate here the possibility of changing the selectivity and enhancing the potency of this carbohydrate peptidomimetic, as well as of shortening the synthetic strategy.

2 Biological Implications of α 4-Integrins

Integrins are cell surface transmembrane glycoprotein receptors consisting of one α and one β subunit. At present, the existence of 18 different α and 8 unique β subunits are assured composing 24 different known integrin receptors (Figure 2-1).³⁰ They are involved in numerous biological processes³¹ which include wound healing,³² blood clot formation,³³ gene regulation,³⁴ and normal immune responses against invading bacteria, viruses or other pathogens.³⁵

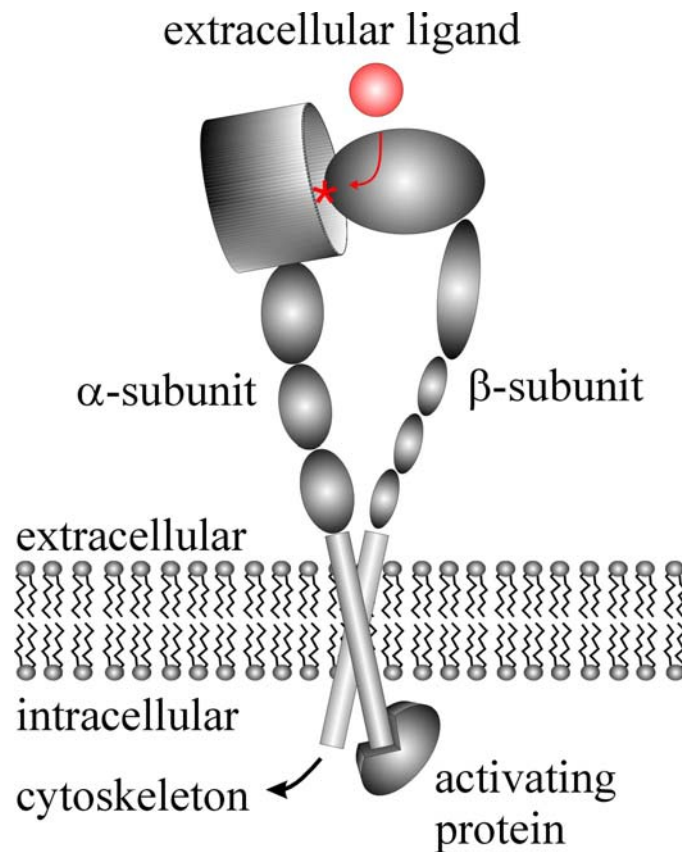


Figure 2-1: *Structure of integrins.*

Through interactions with selectins, extracellular matrix proteins (EMPs), and cell adhesion molecules (CAMs), integrins can function as tissue specific cell adhesion receptors.³⁶ In fact, differential expression of integrins can regulate cell's adhesive properties allowing specific leukocyte populations to be recruited to different organs in response to a variety of inflammatory signals. These signals include various

chemoattractants, which serve as homing beacons for leukocytes, and cytokines such as TNF α which stimulate leukocyte proliferation.

The family of the integrins shows tremendous differences in their biological function and ligand specificity. For most integrins, the mechanism of ligand recognition appears to be critically dependent upon one of two short peptide motifs: RGD and LDV.^{37,38} Several extracellular matrix molecules express the RGD motif in an invariant form and are ligands for a number of integrins (*e.g.* $\alpha 5\beta 1$, $\alpha \text{IIb}\beta 3$, $\alpha \nu\beta 1$, $\alpha \nu\beta 3$).³⁹⁻⁴³ In contrast, the LDV motif exhibits sequence variation. For example, the leukocyte integrins $\alpha 4\beta 1$ and $\alpha 4\beta 7$ recognize an LDVP motif in fibronectin (Fn)⁴⁴⁻⁴⁸, an IDSP sequence in the *N*-terminal domain of IgCAM vascular cell adhesion molecule-1 (VCAM-1),⁴⁹⁻⁵⁵ and an LDTS sequence in a second IgCAM, mucosal addressin cell adhesion molecule-1 (MAdCAM-1).⁵⁶⁻⁵⁹

2.1 $\alpha 4\beta 7$ integrin as therapeutic targets

We focused here on $\alpha 4\beta 7$ integrins which form together with $\alpha 4\beta 1$ the group of the $\alpha 4$ integrins. Both receptors are expressed on most leukocyte cell types. In fact, $\alpha 4$ integrins play essential roles in leukocyte migration and adhesion in the gastrointestinal (GI) tract and surrounding tissue.^{36,60,61} The most important endogenous ligands for $\alpha 4$ integrins are VCAM-1 and fibronectin.^{60,62} The related MAdCAM-1 is recognized by $\alpha 4\beta 7$ but is a poor ligand for $\alpha 4\beta 1$.^{56,63}

The role of $\alpha 4$ integrins and their CAM ligands in leukocyte migration and adhesion during inflammatory processes is shown in Figure 2-2. Interaction of $\alpha 4$ integrins on the leukocyte cell surface with VCAM and/or MAdCAM expressed in the vascular endothelium of the affected tissues initiates attachment and rolling of the leukocyte to the capillary wall, transmigration into the underlying tissue, and subsequent proliferation of inflammatory cells.

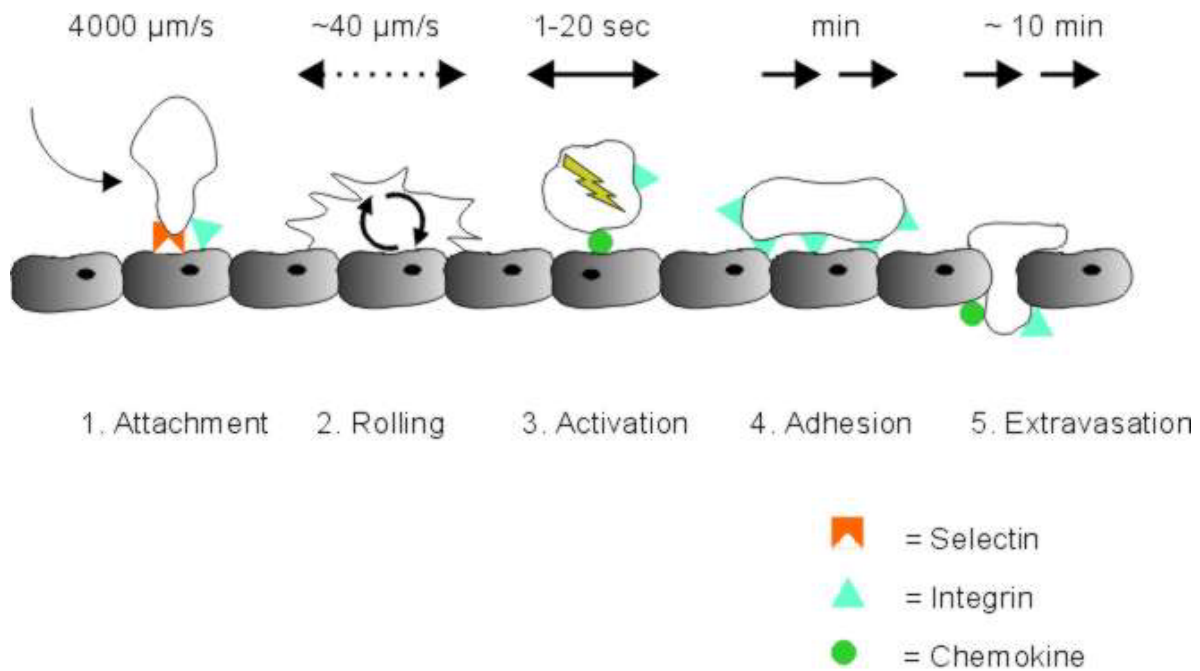


Figure 2-2: *The five distinct steps leading to leukocyte accumulation and tissue damage during inflammatory processes. 1. Selectins mediate reversible attachment of circulating leukocytes to the vessel wall. 2. Additional interaction of $\alpha 4$ integrins (expressed on the leukocyte surface) with VCAM and/or MAdCAM (expressed on the endothelial cells lining the blood vessels), mediates stronger tethering and the leukocyte begins rolling along the vessel wall. 3. Subsequent interaction with chemokines results in activation of the integrin receptors to a higher affinity state. 4. Integrin activation results in firm adhesion of the leukocyte followed by 5. extravasation into the underlying tissue.*

In particular, the gut specific trafficking of lymphocytes from the vascular to gastrointestinal mucosa and lymphoid tissues is mediated by adhesive interactions with MAdCAM-1 and the homing receptor, $\alpha 4\beta 7$.^{56,57,64} MAdCAM-1 specifically binds both human and mouse lymphocytes that express the homing receptor, $\alpha 4\beta 7$, and participates in the homing of these cells to the mucosal endothelium.^{58,65} Organ specific adhesion of normal lymphocytes and lymphoma cells to high endothelial venules of Peyer's patches is mediated by $\alpha 4\beta 7$ integrins.⁶⁶⁻⁶⁸ In mouse models it was demonstrated that antibodies specific for $\beta 7$ integrins and/or MAdCAM-1 block recruitment of lymphocytes to inflamed colon and reduce significantly the severity of colonic inflammatory disease.⁶⁹ Moreover, antibodies against $\beta 7$ integrins protected

mice from the development of insulin-dependent diabetes.⁷⁰ Therefore, the $\alpha 4\beta 7$ /MAdCAM-1 adhesions pathway represents a potent and organ specific target for therapeutic modulation of inflammatory diseases of the gastrointestinal tract such as colitis and autoimmune diabetes.

2.2 Cell adhesion molecules (CAMs)

Differences in the expression profiles of VCAM and MAdCAM provide the most convincing evidence for the role of $\alpha 4$ integrins in autoimmune diseases.⁵⁹ Both proteins are normally expressed in the gastrointestinal tract,⁷¹ however VCAM expression extends into peripheral organs,³² while MAdCAM expression is confined to organs of the gut.⁷²

Although VCAM and MAdCAM are multi-domain transmembrane glycoproteins, their integrin binding sites are thought to reside primarily within their *N*-terminal domain based on previous directed mutagenesis studies.^{50,52,73} These studies revealed that both VCAM and MAdCAM contain a critical aspartic acid residue located within a tripeptide sequence (IDS in VCAM and LDT in MAdCAM). The two ligands differ in binding specificity as already mentioned, in that VCAM interacts with both $\alpha 4\beta 1$ and $\alpha 4\beta 7$, and MAdCAM is highly specific for $\alpha 4\beta 7$.

The molecular basis for MAdCAM's specificity is unknown, however, a recent study demonstrated that fusion of MAdCAM's second domain with the first domain of VCAM resulted in a hybrid protein that was selective for $\alpha 4\beta 7$ and suggested that MAdCAM's specificity might be conferred primarily by its second domain.^{58,74}

The X-ray crystal structures of the two *N*-terminal Ig domains of VCAM-1 (Figure 2-3)^{75,76} and MAdCAM-1 (Figure 2-4)⁷⁴ have recently been solved. Both domains adopt a β - β sandwich topology, composed of an anti-parallel array of β -strands.

However, there are significant differences in both the first and second domains. For example, a protruding, highly acidic loop found in the second domain of MAdCAM (the DE-loop) might explain its lack of affinity for $\alpha 4\beta 1$ if unfavorable electrostatic and steric interactions were created (Figure 2-4). In addition, the analogous DE loop in VCAM (Figure 2-3) contains two positively charged residues (Arg¹⁴⁶-Lys¹⁴⁷) in replacement of the two negatively charged residues in MAdCAM (Glu¹⁴⁸-Glu¹⁴⁹).

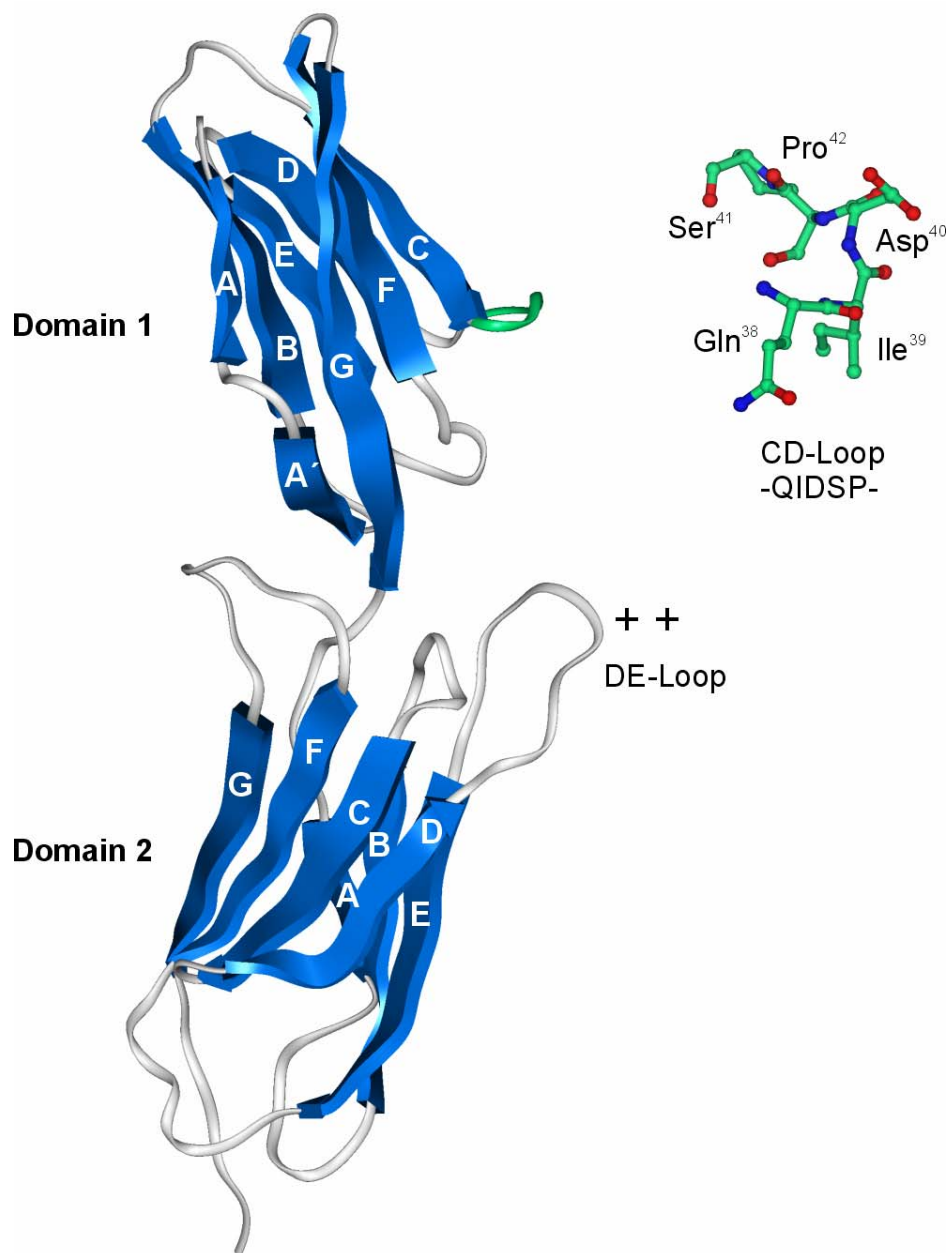


Figure 2-3: X-ray crystal structures of the two N-terminal Ig domains of VCAM-1.^{75,76}

There are also substantial differences in MAdCAM and VCAM's first domain. An obvious difference is that the aforementioned LDT binding epitope in MAdCAM and the analogous IDS epitope in VCAM are both located in a hairpin turn connecting two β strands, which is shifted by approximately 11 Å when the two protein backbones are superimposed.⁷³ These strands form a loop analogous to the complementarity determining loop 3 (CDR3) based on standard immunoglobulin nomenclature. Since both VCAM and MAdCAM require an aspartic acid in their respective CD loops for

high affinity binding and both ligands bind to $\alpha 4\beta 7$ at low nM concentration, these differences could also play a role in determining MAdCAM's specificity for $\alpha 4\beta 7$.

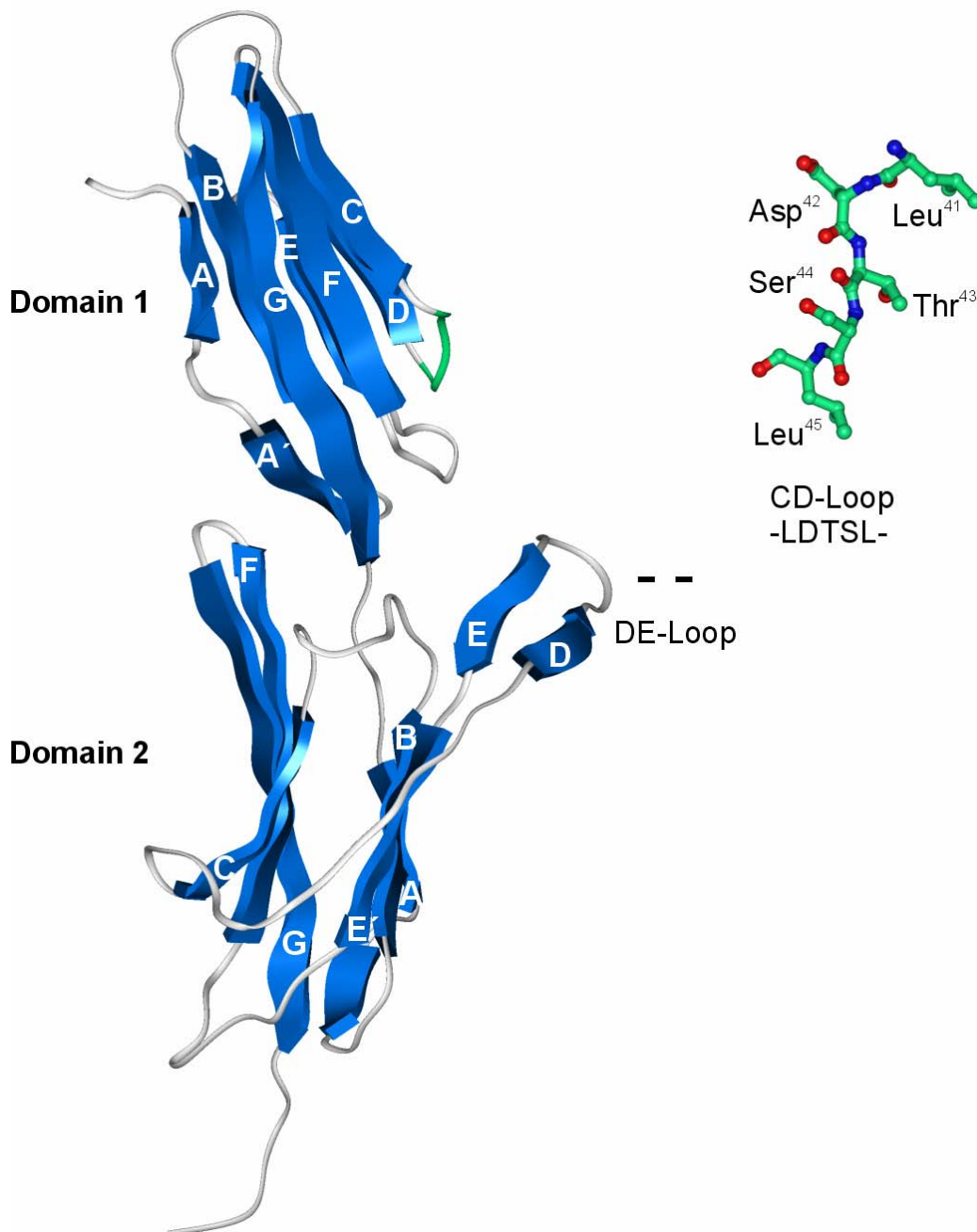


Figure 2-4: X-ray crystal structures of the two N-terminal Ig domains of MAdCAM-1.⁷⁴

The differential expression profiles of the $\alpha 4$ integrins and their various ligands imply that it may be desirable to block one receptor but not the other. MAdCAM binds $\alpha 4\beta 7$ specifically while VCAM has comparable affinity for both $\alpha 4\beta 1$ and $\alpha 4\beta 7$. This

behavior suggests that there may be therapeutically relevant differences between the proteins that will ultimately impact the selection of clinical candidates. For example, antagonist that bind α 4 β 1 selectively would be expected to block migration of α 4 β 1 positive leukocytes to tissues exposing high levels of VCAM while an α 4 β 7 specific antagonist would most likely impact migration of leukocytes to the gastrointestinal tract where only MAdCAM expression has been linked to human disease.⁷¹

The role of the aspartic acid in all ligands of integrins becomes clear due to the recent X-ray structure of α v β 3 without⁷⁷ and with⁷⁸ the peptide ligand cilengitide *cyclo*[-RGDfMeVal-].⁷⁹ The mechanism of the ligand recognition and signaling transduction has been discussed recently.^{80,81}

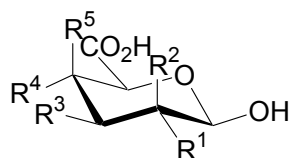
3 Carbohydrates and Sugar Amino Acids in Drug-Design

Among the major classes of biomolecules carbohydrates allow almost unlimited structural variations. The molecular diversity of carbohydrates offers a valuable tool for drug discovery in the areas of biologically important oligosaccharides, glycoconjugates and molecular scaffolds by investigating their structural and functional impact. The modifications such as those of the naturally occurring *O*-/*N*-glycosidic bonds remains of interest to increase the enzymatic stability, as well as to facilitate the assembly of large, diverse oligomer carbohydrate or peptidomimetic libraries by solid phase techniques.

The high density of functional groups per unit mass and the choice of stereochemical linkages at the anomeric carbon has always challenged synthetic chemists towards a multitude of approaches to this rich class of compounds. Monosaccharides also provide rigid molecular systems (privileged structures) which can be used as molecular templates to display pharmacophoric groups in well defined spatial orientations. In order to generate chemically diverse carbohydrate building blocks more suitable for use in combinatorial organic synthesis, at least one amine and one carboxylic acid functional group was incorporated into the sugar ring forming what we call a sugar amino acid (SAA).

3.1 Naturally occurring sugar amino acid (SAA)

Sugar amino acids can be found in nature largely as construction elements.^{3,82} The most prominent and abundant example is sialic acid often located peripherally on glycoproteins. This family of natural SAAs consists of *N*- and *O*-acyl derivatives of neuraminic acid **1** (Figure 3-1). The main substituents on nitrogen are the *N*-acetyl and *N*-glycosyl groups. Glycosaminuronic acids, **2-5**, are usually found in form of derivatives, such as 2-acetamido-2-deoxy-glucuronic acid, found in bacterial cell walls⁸³ and 2-acetamido-2-deoxygalacturonic acid as one component of bacterial Vi antigen of *Escherichia coli*.⁸⁴ Derivatives of glucosaminuronic acid were also detected in the cancomycin family of antibiotics similar to vancomycin.⁸⁵



Glycosaminuronic acids		R ¹	R ²	R ³	R ⁴	R ⁵
glucosaminuronic acid	2	NH ₂	H	OH	OH	H
galactosaminuronic acid	3	NH ₂	H	OH	H	OH
mannosaminuronic acid	4	H	NH ₂	OH	OH	H
4-amino-4-deoxy-glucuronic acid	5	OH	H	OH	NH ₂	H

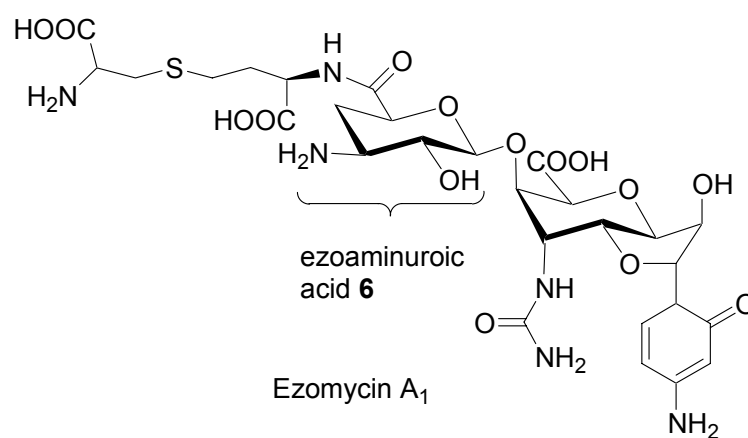
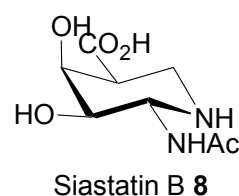
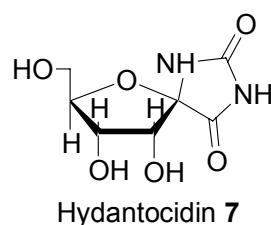
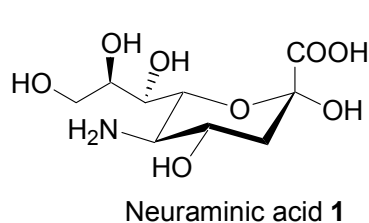


Figure 3-1: Naturally occurring SAA.

Interestingly, natural SAAs can be found in nucleoside antibiotics.⁸⁶ Two different 3-amino-3-deoxy uronic acids, derivatives of 3-amino-3-deoxy-D-gulopyranuronic acid and 3-amino-3,4-dideoxy-D-xylohexo-pyranuronic acid, were found in ezomycin A.^{86,87} 4-Amino-4-deoxy-glucuronic acid **5**, can be found in gougerotin,⁸⁸⁻⁹² an antibiotic from *Streptomyces* bacteria, as the carbohydrate residue of the nucleoside.

The naturally occurring furanoid SAA (+)-hydantocidin **7** (Figure 3-1), which represent a spirohydanthion derivative,⁹³⁻⁹⁵ exhibits herbicidal activity.

Siastatin B **8** (Figure 3-1) is among the class of SAAs, in which the nitrogen is located within the pyranose ring structure. This inhibitor for both β -glucuronidase and *N*-acetylneuraminidase was isolated from a *Streptomyces* culture.⁹⁶

3.2 Carbohydrate-based peptidomimetics

3.2.1 Turn mimetics and model peptides

SAAs can adopt rigid turn or helical structures and thus may allow one to mimic helices or sheets. They can be used as substitutes for single amino acids or as dipeptide isosteres. If used as replacement of hydrophobic residues, the sugar can also be functionalized with hydrophobic side chains (e.g. they may be benzylated), however, if hydrophilic residues are replaced, or if solubility should be improved the sugar hydroxyl groups are unprotected or functionalized with hydrophilic residues.

In 1994 the first example of pyranoid SAA as a new type of peptidomimetic was reported by our laboratories: the *Glucosyluronic acid methylamine* (Gum).⁴ The Gum building block was designed as a dipeptide isostere of the Gly-Ser sequence hold in a "flexible" β -turn conformation.⁴ This concept was later extended to the SAA construction kit as versatile tool to manipulate peptide conformations.⁹⁷

Fleet and co-workers developed tetrahydrofuran-based amino acids as dipeptide isosteres and described the potential for secondary structure predisposition of the correspondent oligomeric sequences.⁹⁸⁻¹⁰⁵

In recent work, we introduced oligomeric sequences containing furanoid SAAs alternating with β - and γ -amino acids and showed their propensity to form helical structures.¹⁰⁶

3.2.2 Biologically active peptides containing SAA

The conformational and biological influence of a range of pyranose-based building blocks on peptide chains has been investigated in our laboratory by replacing the original dipeptide sequences in a linear Leu-enkephalin analogue, in cyclic

somatostatin analogues and in cyclic α v-selective RGD peptides.^{4,97,107,108} SAAs were used also to improve pharmacokinetics,^{107,109} to introduce a radioactive label for imaging¹¹⁰ or to glycosylate a peptide.¹¹¹

3.3 SAA oligomers as carbohydrate mimetics

The development of SAA oligomers as biopolymer to mimic oligo- and polysaccharide structures *via* amide bond linkages is one of the ongoing application of these building blocks.^{112,113} In fact, the assembly of synthetic polysaccharide libraries in solution or on solid-phase is difficult in spite of the recent progresses using chemical and enzymatic techniques.^{114,115} Taking advantage of the well-established chemistry of peptides many homooligomers from SAAs and hybrid sequences containing natural amino acids (AAs), carbohydrates and SAAs have been synthesized. These resultant oligomers represent useful drug candidates, since they may overcome the problems associated with oligosaccharide and peptide libraries like the susceptibility towards glycosidases due to the altered peptide backbone, and their resistance to many proteases due to their resemblance to carbohydrates.

3.3.1 Linear oligomers

The first oligomers were synthesized in solution by Fuchs and Lehmann, although they did only characterize the individual products by mass spectroscopy.^{10,11,116} The first dimers were synthesized from D-glucosaminuronic acid and D-mannosaminuronic acid by coupling with DCC by Tsuchida *et al.* in 1976.¹¹⁷

More recently oligomers were synthesized both in solution¹¹⁸⁻¹²⁰ and on solid phase,^{121,122} and have been proposed to mimic oligosaccharide¹² and oligonucleotide (so called GNA, Glucopyranosyl Nucleic Amide) (Figure 3-2)^{13,14} backbone structures *via* amide bond linkages.

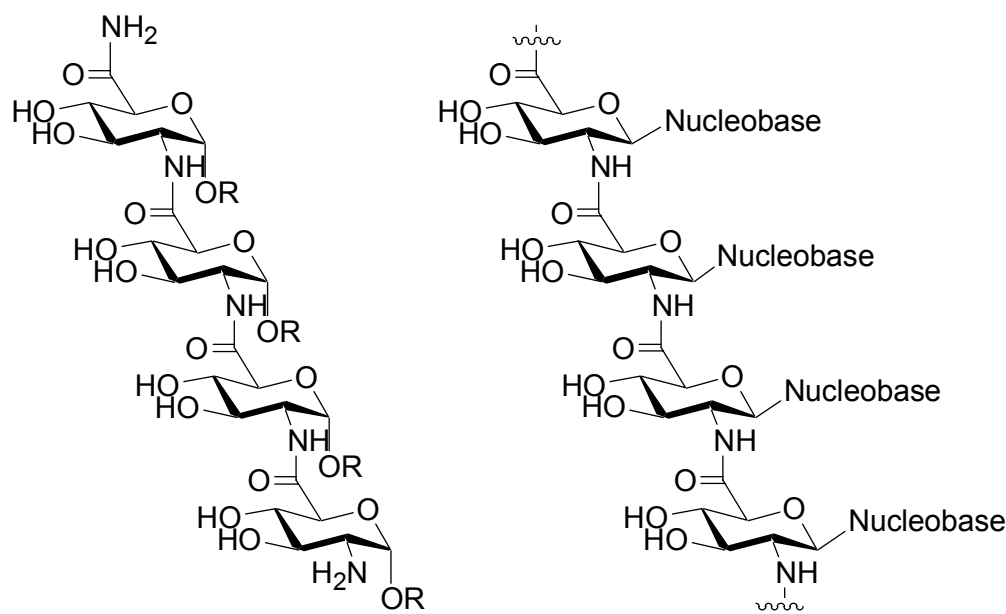


Figure 3-2: Oligomers from SAA: $R = Me$,⁸ $R = Bn$,¹²¹ and with nucleobases.^{13,14}

3.3.2 Cyclic oligomers

Mixed cyclic oligomers containing SAAs and amino acids have been proposed by van Boom *et al.*¹²³ as potential molecules for host guest chemistry. The parallel solid-phase synthesis of cyclic sugar amino acid/amino acid hybrid molecules containing furanoid SAAs was carried out by van Boom *et al.* using Boc *N*-protection strategy and BOP/DIPEA as coupling reagents. The first amino acid was anchored on an oxime resin in order to employ acid catalyzed cyclization and cleavage from the resin.

Oligomers containing Gum residues alternating with amino acids have also been developed in our group.¹²⁴ However cyclic homooligomers from SAA have not been described before our contributions.^{15,16}

We introduce here cyclic homooligomers of SAAs as novel cyclodextrin-like artificial receptors. This idea was based upon the assumption that a cyclic array of carbohydrate moieties and amino acid functional groups may lead to exquisite specificity of recognition and catalysis.

3.4 Carbohydrate and SAA as scaffolds

Carbohydrates represent an attractive source of readily available, stereochemically defined scaffolds as they contain well-defined and readily convertible substituents with a rigid pyran ring or the more flexible furan ring.^{22,125-127} The functional pharmacophoric groups can thus be presented in a distinct arrangement.

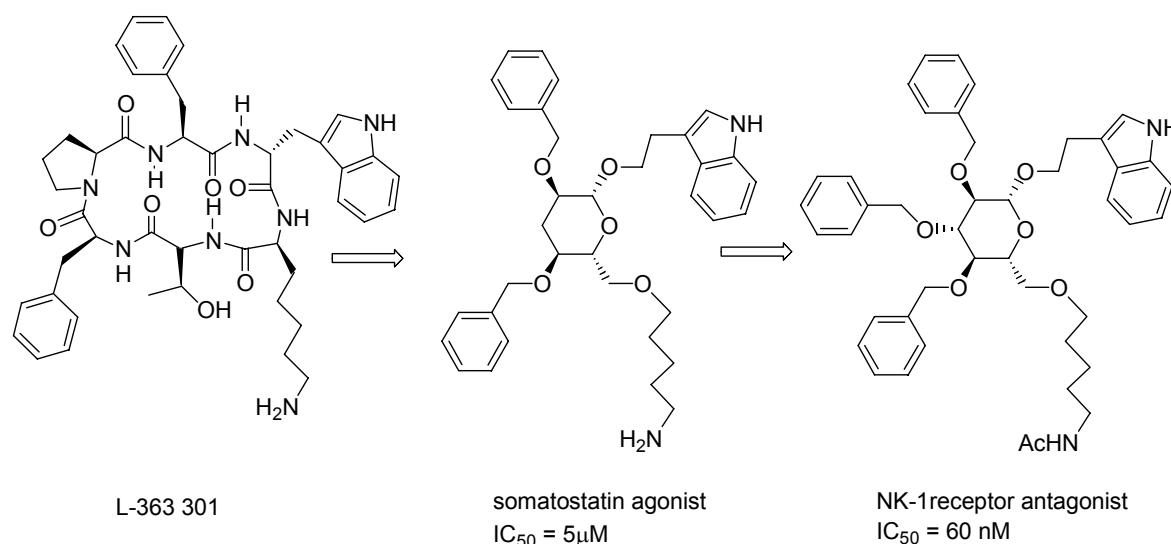


Figure 3-3: Glucose-based scaffold for the cyclic hexapeptide somatostatin agonist.

The genesis of carbohydrate privileged structures was first described by Hirschmann and co-workers.¹²⁸ A low affinity somatostatin agonist was discovered which contained a deoxyglucose nucleus carrying the key amino acid side chains of a cyclic hexapeptide agonist (Figure 3-3).²² Successively, a NK-1 receptor antagonist was identified by modification of the deoxyglucose-based somatostatin agonist.^{26,129}

The tetrasubstituted xylofuranose **9** was synthesized by Papageorgiou *et al.*²⁷ as a potential nonpeptide mimic of somatostatin (Figure 3-4). The scaffold was designed based on molecular dynamics simulations and on the data from Hirschmann *et al.*²² The biological activity of the mixture of the α and β anomers in a ratio of 2:3 revealed a promising IC₅₀ = 16 μ M. They did show a similar conformational behavior as the Hirschmann scaffolds.

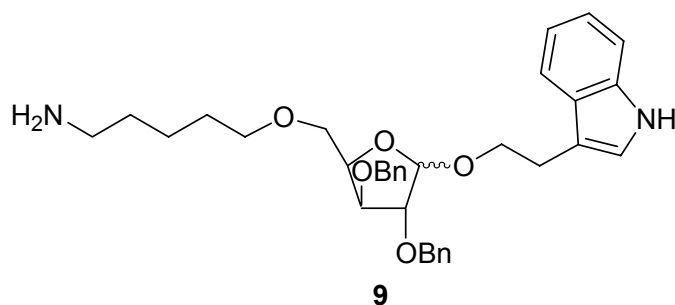


Figure 3-4: Somatostatin scaffold based on xylose by Papageorgiou *et al.*²⁷

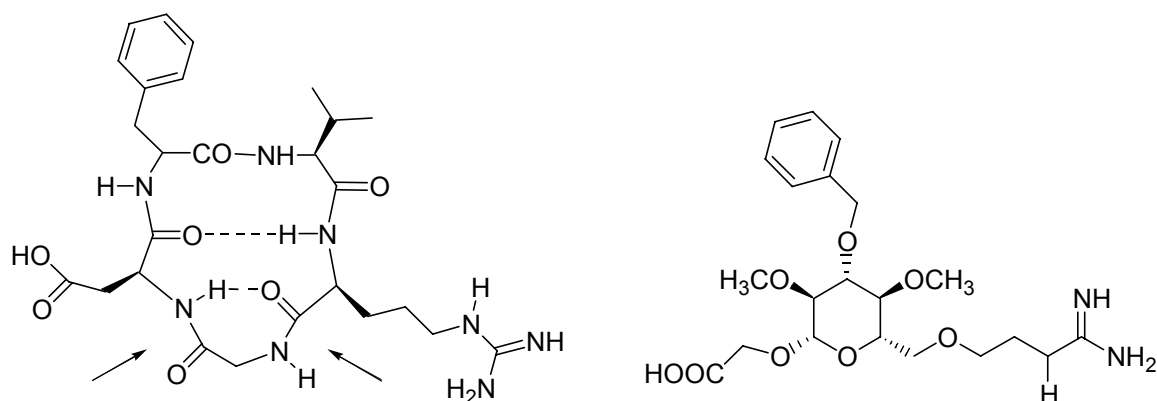


Figure 3-5: Scaffold based on glucose by Nicolaou *et al.*¹³⁰ and the cyclic pentapeptide with the bioactive RGD sequence and the essential two amide bonds.

A number of carbohydrate-based structures have been designed and synthesized by Nicolaou *et al.*¹³⁰ as potential mimics of the potent peptidic antagonist of $\alpha v \beta 3$ and $\alpha v \beta 5$, cyclic pentapeptide RGDfV (Figure 3-5).¹³¹⁻¹³⁵ The biological activity of the derivatives was rather low, which indicates that for this receptor the two amide bonds in the lower part of the cyclic peptide are indeed essential for activity.¹³⁶

A focused combinatorial library of mimetics of the RGD sequence based on sugar scaffolds have been rationally constructed by Moitessier *et al.* with a particular emphasis on the stereoselectivity of the library (Figure 3-6).^{137,138} In this case a modest biological activity was observed for the $\alpha IIb \beta 3$ antagonists (as low as $IC_{50} = 20 \mu M$).¹³⁷ For the $\alpha v \beta 3$ antagonists only percent of inhibition of cell adhesion on vitronectin substratum was reported.¹³⁸

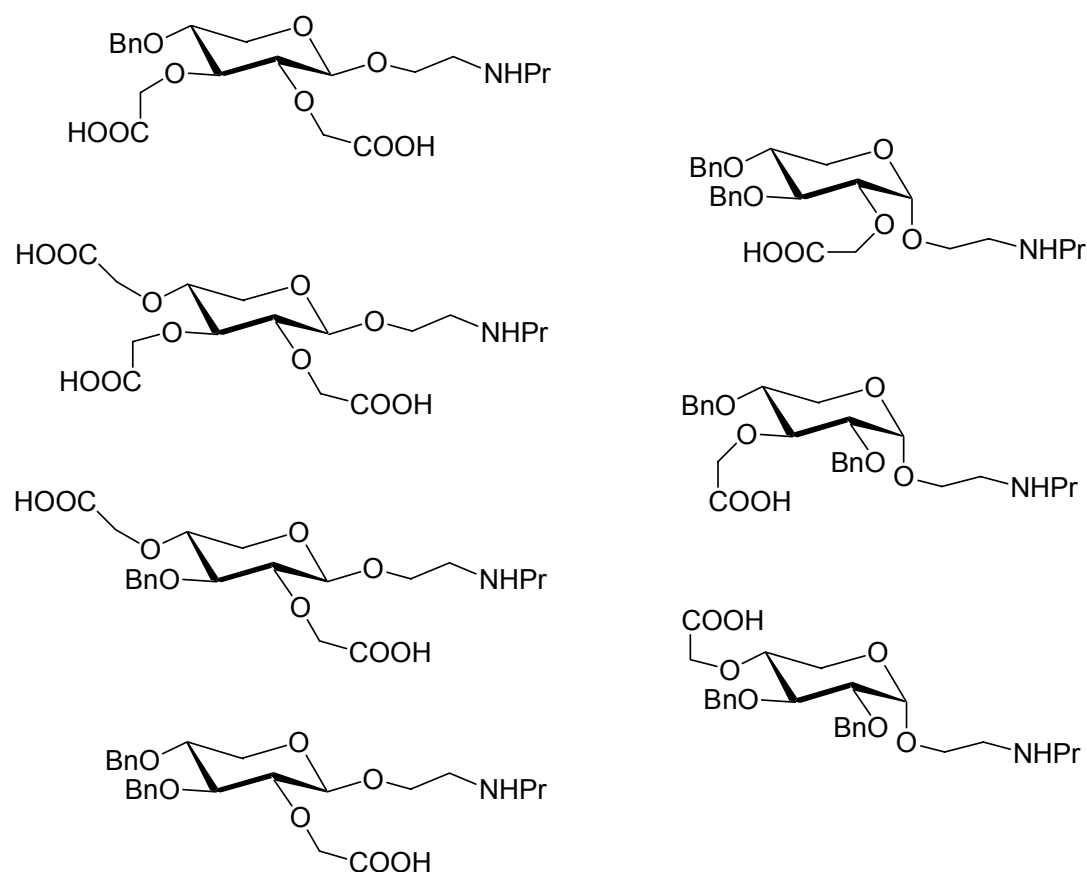


Figure 3-6: $\alpha\text{IIb}\beta\text{3}$ (left)¹³⁷ and $\alpha\text{v}\beta\text{3}$ (right)¹³⁸ antagonists based on xylose.

In search of nonpeptidic endothelin antagonists, Diguarher *et al.* synthesized a series of derivatives, such as compound **10**, based on the highly active endothelin antagonist BQ123 (Figure 3-7).¹³⁹ Although the side chain orientations of these compounds were close to those of the cyclic peptide, these derivatives did not show any significant binding to the endothelin receptors. This also indicates that some of the amide linkages in the peptidic backbone are essential for receptor binding.

Inspired by the work of Hirschmann and Nicolaou, Armstrong and co-workers prepared a D-glucose scaffold of hapalosin (Figure 3-8), a cyclic depsipeptide which inhibits the P-glycoprotein, P-gp.¹⁴⁰ This transmembrane protein effects the removal of a broad spectrum of structurally diverse compounds from the cell and therefore may play an important role in the phenomena of multiple drug resistance, which is a major problem in cancer therapy. Unfortunately, like many other scaffold mimetics, this compound did not produce any activity, although these derivatives also contribute to the setting of the framework of structure-activity relationships.

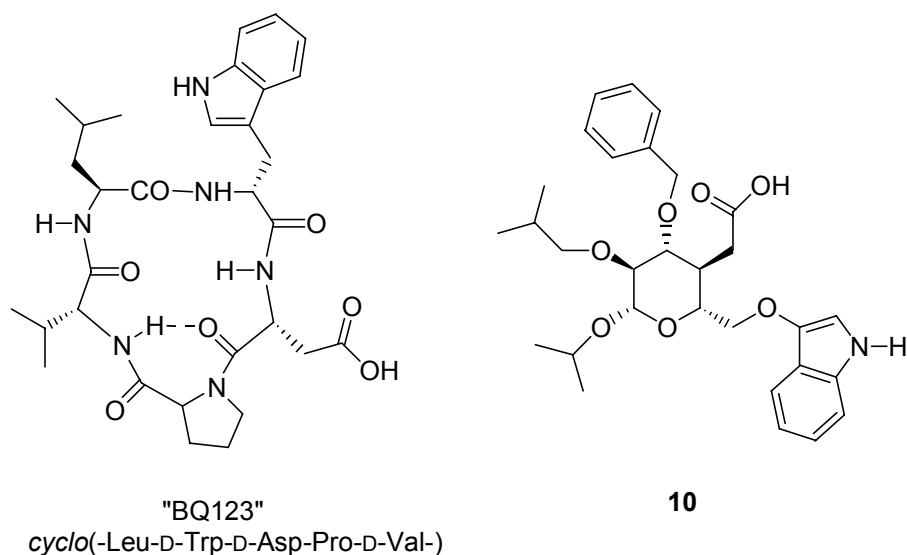


Figure 3-7: Glucose scaffold based on the cyclic pentapeptide endothelin antagonist BQ 123.¹³⁹

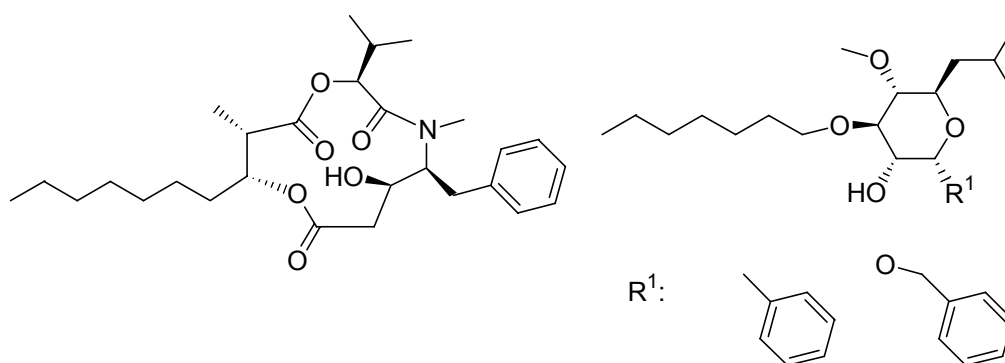


Figure 3-8: Glucose (and allose) scaffolds based on hepalosin by Armstrong *et al.*¹⁴⁰

Kunz *et al.* were able to synthesize large substance libraries of carbohydrates based on solid-phase chemistry, which allowed the defined functionalization of hydroxyl groups (Figure 3-9).¹²⁶ Although no biological activities were given, this approach represents a promising access to new lead structures. A similar diversity has been described by Wong *et al.*¹⁴⁰ More complex oligosaccharides structures can be synthesized using for example the Ugi reaction as utilized by Lockhoff.¹⁴¹

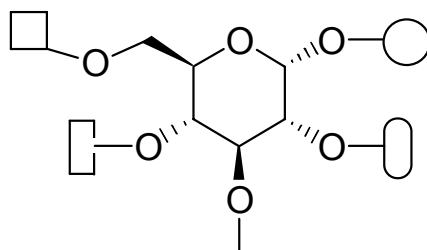


Figure 3-9: Combinatorial synthesis with carbohydrate scaffolds.¹²⁶

Sugar amino acids in particular are ideal peptidomimetic scaffolds, as they may function as structural pharmacophores depending on their substituents in addition to the imperative amino and carboxyl function.⁴ Smith III *et al.* reported the design of an inhibitor of mammalian ribonucleotide reductase (mRR) **12** based on the bound conformation of the heptapeptide AcNH-FTLDADF-OH using a pyranose SAA scaffold (Figure 3-10).¹⁴² This SAA was employed to mimic a β -turn present in the peptidic precursor and to carry, *via* ether linkage, the pharmacophores, Leu and Asp side chains, present in the *i*+1 and *i*+2 positions of the turn, respectively. The tetrahydropyran-based mimetic **12** was found to inhibit mRR, though considerably less well than N-AcFTLDADF (K_i of 400-500 μ M for **12** vs. K_i of 15-20 μ M for **11**).

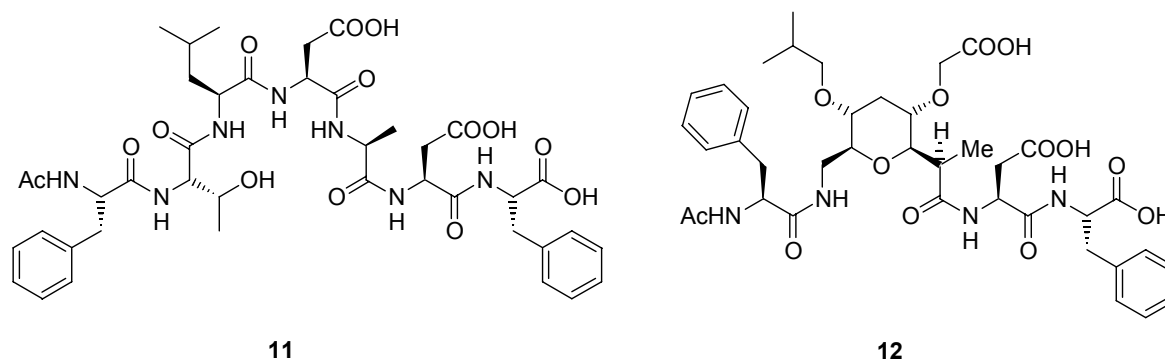


Figure 3-10: Carbohydrate-derived inhibitor **12** of mammalian ribonucleotide reductase.¹⁴²

To investigate the potential of carbohydrates for the design and synthesis of universal pharmacophore mapping libraries, two monosaccharide scaffolds **13** and **14** were prepared by Sofia *et al.* (Figure 3-11).⁶ Three sites of diversification were incorporated

to provide the minimal requirements for pharmacophoric chiral molecular recognition: the carboxylic acid moiety, a Fmoc-protected amine, and a hydroxyl group.

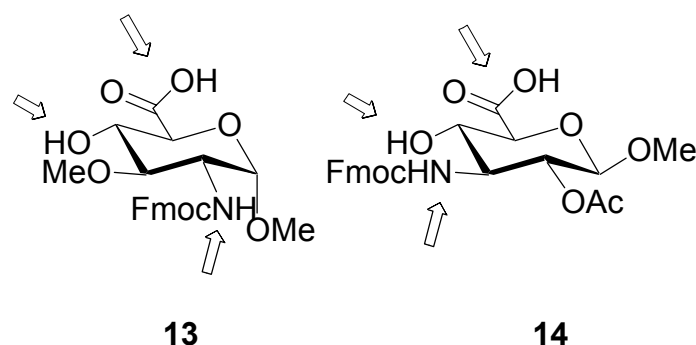


Figure 3-11: Carbohydrate-based scaffolds for pharmacophore mapping.⁶

Recently, we published the design, synthesis and biological evaluation of β -D-mannose based nonpeptidic mimetics of the vascular cell adhesion molecule-1 (VCAM-1), and of the mucosal addressin cell adhesion molecule-1 (MAdCAM-1) which are the natural ligands of $\alpha_4\beta_1$ and $\alpha_4\beta_7$ integrin receptors.²⁹

Our strategy for generating small molecule inhibitors of $\alpha_4\beta_7$ and $\alpha_4\beta_1$ integrins takes advantage of structural data available for VCAM and MAdCAM in order to design, *via* spatial screening, rigid peptides that mimic specific structures and interactions of essential binding epitopes within the native proteins. Based on the bioactive conformation of these constrained peptides a scaffold is identified carrying the pharmacophoric side chains and displaying them in the same orientation as in the peptidic inhibitors (Figure 3-12). Another methodology we developed for making the transition from a peptide inhibitor to a small molecule antagonist involves the replacement of backbone amide bonds or other backbone fragments of a peptide inhibitor with equivalent hydrophobic atoms or linkers and β -turn mimetics.^{143,144} We used this approach (combinatorial libraries) and the scaffold approach interactively to develop small α_4 -integrin antagonists (Figure 3-13).

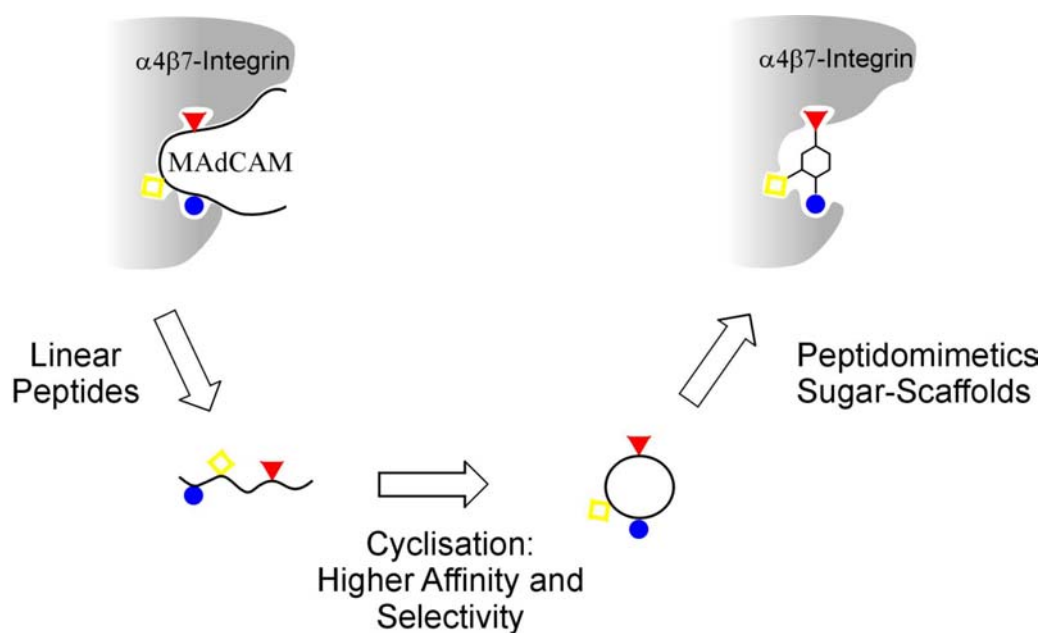


Figure 3-12: Design of $\alpha 4\beta 7$ -integrin antagonists.

The X-ray structures shown previously combined with mutagenesis data which identified the aforementioned I³⁹D⁴⁰S⁴¹ or L⁴¹D⁴²T⁴³ tripeptide binding epitopes within VCAM and MAdCAM respectively, made these ligands suitable candidates for attempting proteomimetic inhibitor design. Based upon these data, using the “spatial screening” procedure cyclic hexapeptides selective inhibitors of $\alpha 4\beta 7$ /MAdCAM mediated leukocyte adhesion were developed.²⁸ The bioactive conformation of these constrained peptides consists of two facing β -turns with the D-proline at the $i + 1$ position of a β II'-turn and the aspartic acid at the $i + 1$ position of a β I- and/or β II-type. The known conformation of our lead peptides recommended the replacement of the peptidic backbone by a sugar scaffold holding in a β -turn the pharmacophoric LDT side chains required for receptor binding. Prerequisite for a successful design of such scaffold mimetics is that the amide backbone is not strongly involved in receptor binding and that all essential groups are maintained in their active conformation.

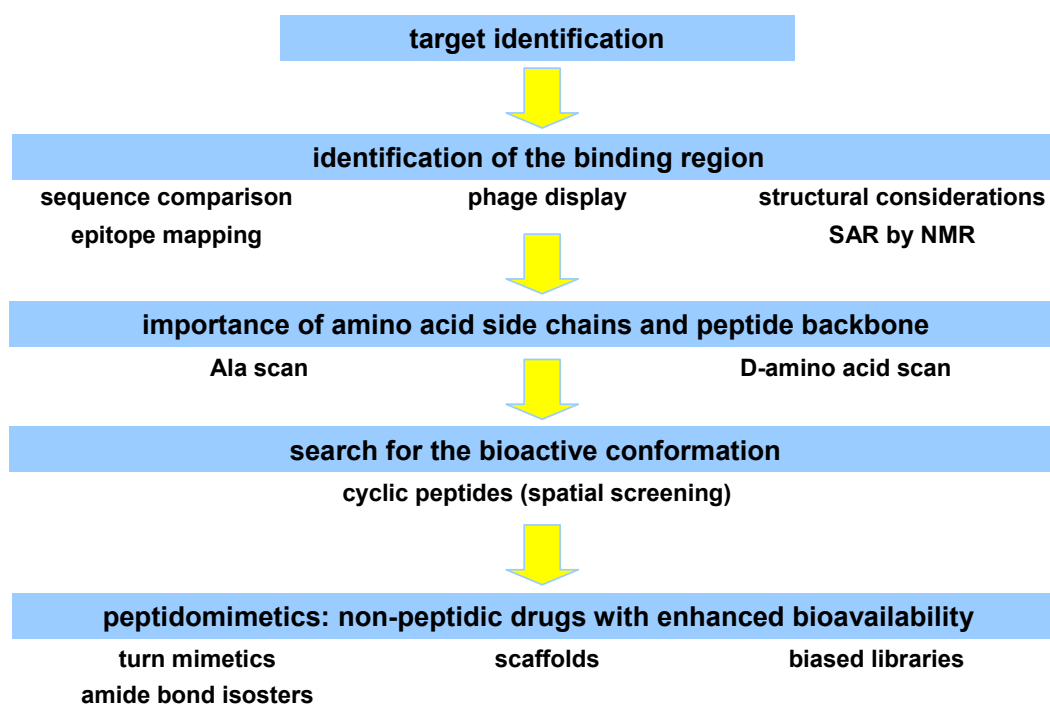


Figure 3-13: *Interactive approach to develop small bioactive molecules.*

Molecular modeling studies suggested β -D-mannopyranose as a proper scaffold to carry the pharmacophoric LDT sequence of our peptidic lead structures. The relative orientation of the LDT mimetics attached to a β -D-mannose core at positions 6, 1 and 2 (all up) resembles the orientation of the side chains of the leucine, aspartic acid and threonine, respectively in the peptide (Figure 3-14). A small biased library of peptidomimetics with β -D-mannose as rigid core was synthesized base upon this model. Unfortunately, the designed peptidomimetic did not show any activity towards the α 4 β 7/MAdCAM interaction. However, one analogue showed inhibitory activity of α 4 β 1/VCAM mediated leukocyte adhesion.²⁹ This lead structure was used here to broaden the original library of substituted monosaccharides.¹⁴⁵

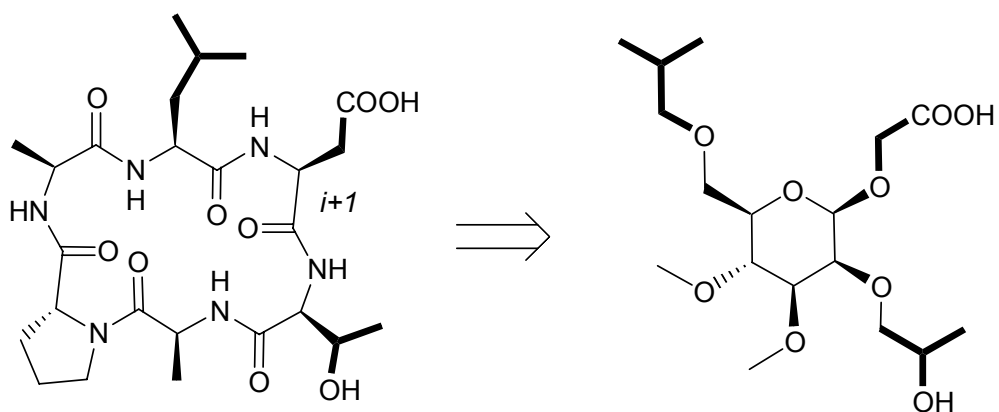


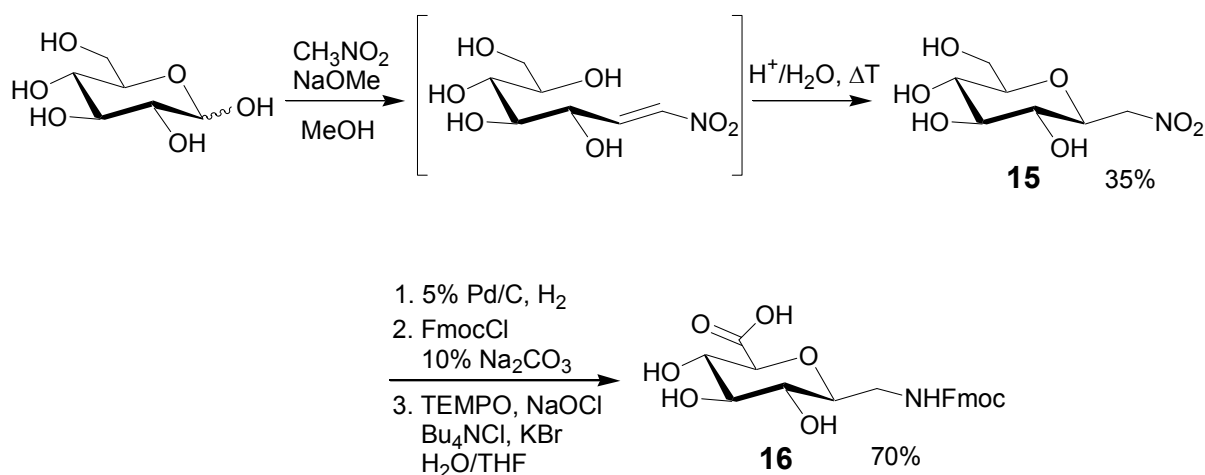
Figure 3-14: Comparison between our lead peptide and the mannose-based peptidomimetic.

4 Cyclic Homo-Oligomers from Sugar Amino Acids: Synthesis, Conformational Analysis and Significance

4.1 Synthesis in solution and on solid phase of the oligomers containing Gum

4.1.1 Synthesis of the Gum building block

The Fmoc-Gum-OH building block was derived in only 4 steps from very inexpensive α,β -D-glucose as reported in the literature (Scheme 4-1).⁴ The CH_2NH_2 equivalent is introduced as CH_3NO_2 *via* nucleophilic aldol reaction. The linear condensation product is cyclized by acid catalyzed intramolecular ring closure to yield β -D-glucopyranosylnitromethane, which because of its polarity is isolated using basic ion exchange resin. The nitro compound is reduced with hydrogen, using 10% Pd/C under pressure and subsequent protection with Fmoc-Cl. The synthesis was improved by selective oxidation of the primary hydroxyl group to carboxylic acid using the one-step oxyammonium (TEMPO)¹⁴⁶⁻¹⁴⁹ mediated reaction with sodium hypochlorite in $\text{H}_2\text{O}/\text{THF}$ solution.³

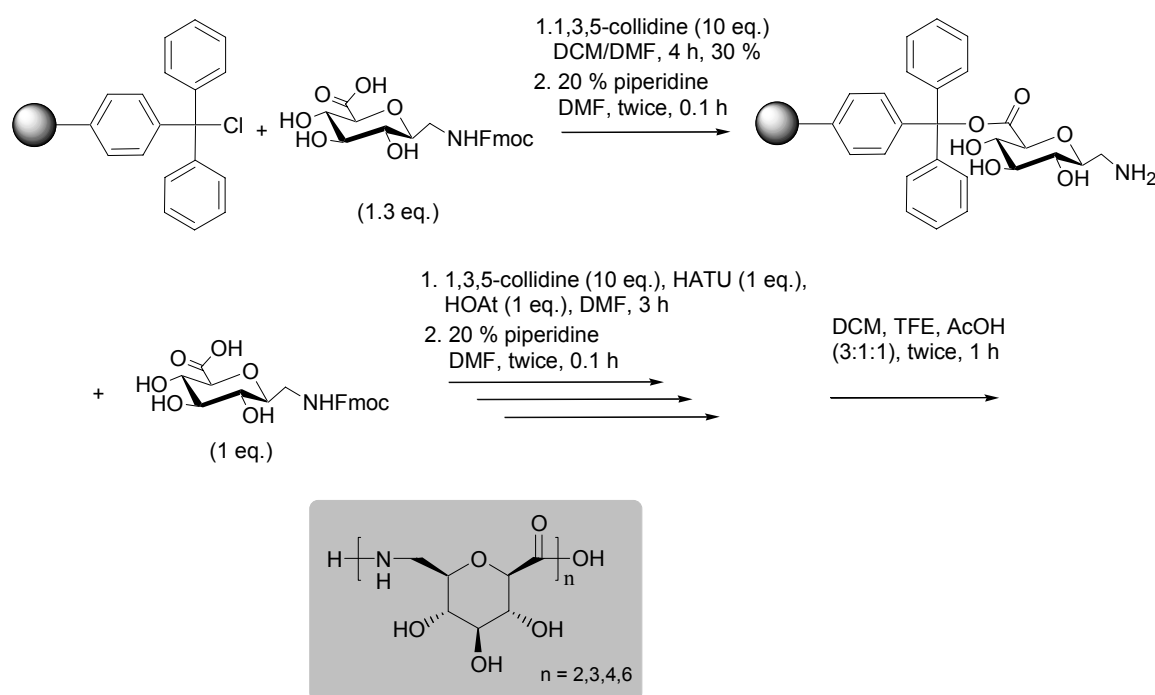


Scheme 4-1: Synthesis of the Fmoc-Gum-OH building block.

4.1.2 Solid phase synthesis of the linear sequences

The synthesis of the linear sequences $\text{H}-[\text{Gum}]_n-\text{OH}$ ($n = 2,3,4,6$) was performed using standard solid phase peptide techniques with tritylchloropolystyrene (TCP) resin applying Fmoc strategy (Scheme 4-2). Our protocol did not require the orthogonal

protection of the hydroxyl groups and consequently, the final tedious step of deprotecting the oligomeric sequences. The first Fmoc protected sugar amino acid was anchored to the tritylchlorid resin with 1,3,5-collidine as base in dimethylformamide (DMF) as solvent. The use of diisopropylethylamine (DIPEA), as stronger base, was avoided since it led to epimerization at the carbon adjacent to the carboxyl moiety and consequent flipping of the pyranose ring. Stepwise extensions of the sequence, i.e. Fmoc-deprotection with 20 vol % piperidine in DMF and subsequent coupling with Fmoc-Gum-OH under the influence of *N*-hydroxy-9-azabenzotriazole (HOAt), 2-(1H-9-azabenzotriazole-1-yl)-1,1,3,3-tetramethyluronium hexafluorophosphate (HATU), and 1,3,5-collidine in DMF, followed by final Fmoc-deprotection step afforded the immobilized dimer, trimer, tetramer and hexamer. Due to the steric hindrance of the carboxyl group, the coupling of Gum needed very efficient coupling reagents.



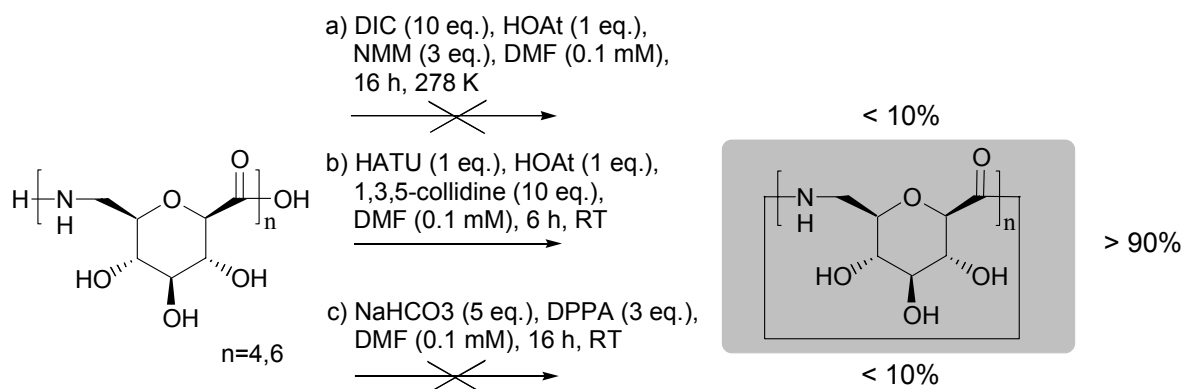
Scheme 4-2: Synthesis on solid-phase of the linear oligomers containing Gum.

The linear oligomers were cleaved from the resin using a mixture of dichloromethane (DCM), trifluoroethanol (TFE) and acetic acid (AcOH) 3:1:1. A crucial step in the solid phase synthesis of such hydrophilic compounds turned out to be the right choice of the solvent for cleaning the oligomers from the solid support. Several treatments of the resin with DMF or DMSO afforded the target oligomers in 40-50% yields after

purification using reversed phase high-performance liquid chromatography (RP-HPLC).

4.1.3 Cyclization methods

End-to-end cyclization was carried out under high dilution (0.1 mM) in DMF using HATU/HOAt system and 1,3,5-collidine (Scheme 4-3).¹⁵⁰⁻¹⁵³ Purification by RP-HPLC led to compounds which were > 98 % pure. The yields during cyclization were > 90 % for $n = 4,6$ while lower yields were achieved for the shorter sequences (35 % for $n = 2$ and 60 % for $n = 3$). During cyclization of the dimeric sequence we also observed the formation of the cyclic tetramer as byproduct which was easily separated by RP-HPLC. All compounds were characterized by ESI mass and NMR spectroscopy. The need of very strong C-terminal activation, the short coupling time and the high yields achieved during cyclization indicate a folded conformation in solution of the linear precursors bearing the two ends close to each other.



Scheme 4-3: Cyclization in solution of the linear oligomers containing Gum.

This method combines strong C-terminal activation with a good suppression of epimerization and has been successfully used in the cyclization of difficult sequences. The cyclization reaction itself proceeds fast and is usually completed within one hour. Attempts to apply milder cyclization conditions *via in situ* activation using diphenyl phosphorazidate (DPPA) with sodium bicarbonate as solid base¹⁵⁴⁻¹⁵⁷ led only to very low yields of the cyclic products. This method, a modification of the azide methods, is relatively reliable and offers a mild activation with good protection against

racemization, although longer reaction times have to be considered with this mild coupling method (usually one to three days). Bases such as triethylamine or Hünigs base, diisopropylethylamine, can also be used. Solid inorganic salts such as NaHCO_3 (or K_2HPO_4) are favored, because of their insolubility in DMF and the great excess of base that can be used without risking racemization. The cyclization reaction itself presumably does occur on the surface of the solid base.

Cyclization *via* the carbodiimide method using N,N' -diisopropylcarbodiimide (DIC), HOAt and *N*-methylmorpholine (NMM) at 278 K,^{152,158} was also unsuccessful. This method usually works also with other carbodiimides such as DCCI or EDCI. The addition of the acylating catalyst DMAP is also described. This relatively old method causes very strong *C*-terminal activation.

4.2 Conformational analysis by NMR

Since our target is the mimicking of water soluble biopolymers all spectra are acquired in aqueous solution.

4.2.1 Chemical shifts

The spectra of the linear oligomers show severe overlap of the resonances: only the *N*- and *C*-terminal residues are assigned. After cyclization the system collapses in a unique set of resonances for the Gum moieties which are easily assigned using DQF-COSY, ^{13}C -HSQC and ^{13}C -HMBC. A comparison between the linear tetrameric sequence and the corresponding cyclic derivative is shown in Figure 4-1.

In general, cyclic trimer, tetramer and hexamer show a pattern of the chemical shifts symmetrical on the NMR time scale, which does not change as the ring size increases. Interestingly, a more detailed analysis of the cyclic trimer in water shows a shift difference between the nonequivalent methylene protons as a function of temperature. Specifically, these resonances show a difference of 0.06 ppm at 293 K and completely overlap at lower temperature (273 K).

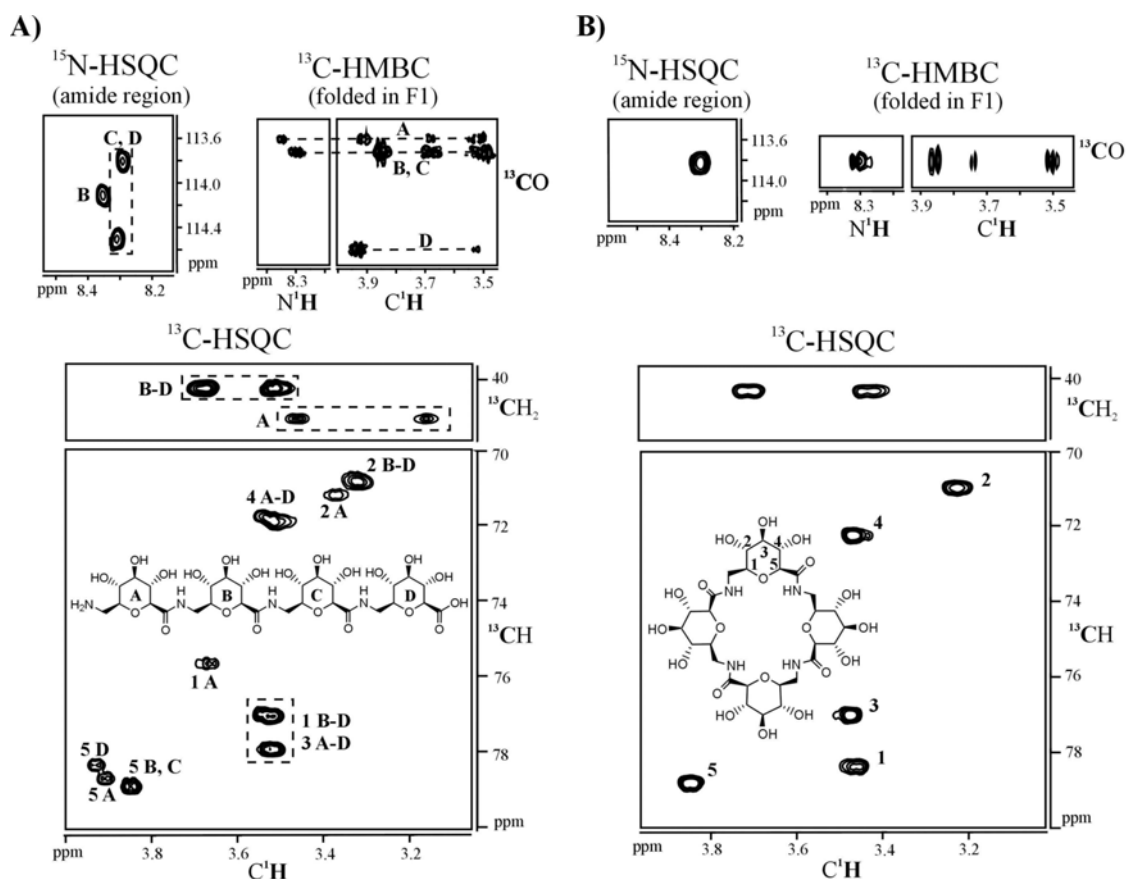


Figure 4-1: Comparison of the ^1H , ^{13}C and ^{15}N spectral regions exhibited in water solution at 293 K by the linear (A) and cyclic tetramer (B).

The cyclic tetramer and hexamer show no relevant shift difference as the temperature increases. A difference of 0.22-0.23 and 0.20-0.21 ppm, respectively is observed. The cyclic dimer is the only compound showing slow exchange in solution, on the NMR time scale, between three different conformers. Two are populated for less than 10% (spin systems not assigned) and interconvert at high temperatures as confirmed by exchange ROESY crosspeaks which can easily be discriminated by the positive sign with the diagonal. This exchange peak is only present in the ROESY spectrum at 293 K but not at lower temperatures ($T = 273$ K). The third conformation, which is the most populated, shows a symmetrical pattern of the resonances as for the other cycles. However, these do not resemble the one determined for the longer sequences. Once more, an invariable chemical shift difference between the nonequivalent methylene protons of 0.37-0.38 ppm is measured at low and high temperature.

4.2.2 Coupling constants

The 1D- ^1H spectra of all the compounds show large vicinal $^3\text{J}(\text{H-H})$ coupling constants (9-10 Hz) between the ring protons of the sugar moiety. This implies that no epimerization has occurred at the H^5 during the coupling step and that the pyranose ring is hold in the predicted $^4\text{C}_1$ chair conformation also after cyclization. The Gum sugar amino acid ' ϕ ' angle $\underline{\text{CO-N-CH}_2\text{-C}^1}$ was determined directly from $^3\text{J}(\text{CH}_2\text{-NH})$ coupling constants by means of the Karplus equation. Interestingly, for the most populated conformer, the amide proton of the cyclic dimer shows a large coupling ($^3\text{J} = 9.8$ Hz) with one of the methylene protons (lower field), which restricts the ' ϕ ' angle to ± 100.6 and ± 139.4 . The same methylene proton exhibits also a large coupling with H^1 ($^3\text{J} \cong 10$ Hz) indicating their reciprocal (preferred) anti orientation (-*sc* or *ap* rotamers in Figure 4-2). The cyclic trimer exhibits for the methylene proton at lower field a large coupling with H^1 ($^3\text{J} \cong 10$ Hz) indicating the same rotamer populations around the $\underline{\text{CH}_2\text{-C}^1}$ bond as for the cyclic dimer. For all the other compounds, an estimation of the ^3J between the methylene proton at lower field and H^1 led to values smaller than the line width of the peak ($^3\text{J} \leq 2$ Hz). In all the spectra the methylene proton at higher field exhibits spectral overlap. Moreover, the cyclic trimer and longer sequences reveal equivalent coupling constants between the NH group and both CH_2 protons ($^3\text{J} \cong 6$ Hz).

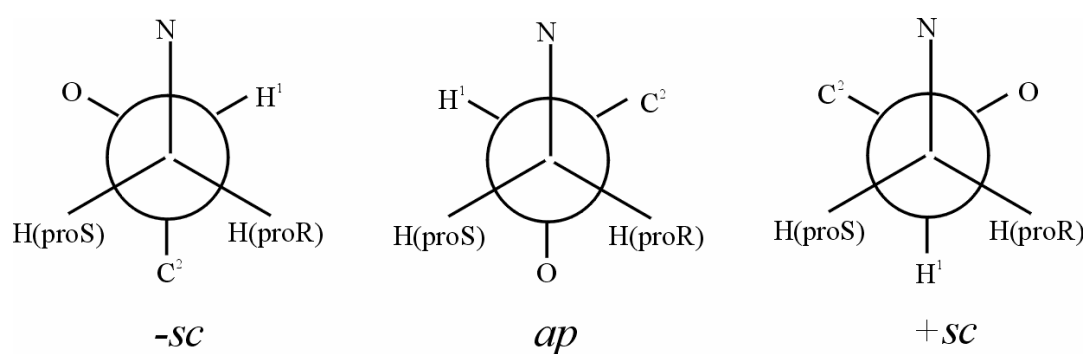


Figure 4-2: Rotamers around the $\underline{\text{CH}_2\text{-C}^1}$ bond. The assignment $\pm sc$ (\pm synclinal) and *ap* (antiperiplanar) is based upon the Klyne and Prelog nomenclature.

4.2.3 ROE data

Only the cyclic derivatives were investigated in detail. Due to the symmetry of the spectra it is not possible *a priori* to discriminate between intra- and inter-residue ROEs. Therefore we checked in our models systematically all possible combinations and considered only the unambiguous ROE connectivities. In this regard, the ‘finger print’ region is very informative. All the compounds show strong ROEs between the H⁵ and the amide proton (2.5-2.9 Å). Since the corresponding intra-residue connectivity would not cover such a short distance (3.9-4.6 Å) we assigned the ROE as sequential H⁵(i)-NH(i+1) which supports the trans configuration of the amide bonds. This is also confirmed by the symmetry of the chemical resonances which would imply a cis conformation for all the amide bonds in the linear precursors too. With the exception of the cyclic dimer, all the longer sequences show ROEs between the NH groups and H², H⁴ which are positioned on the opposite side of the sugar ring with respect to H⁵. The intensity of these ROEs increases with increasing ring sizes.

4.3 Molecular modeling

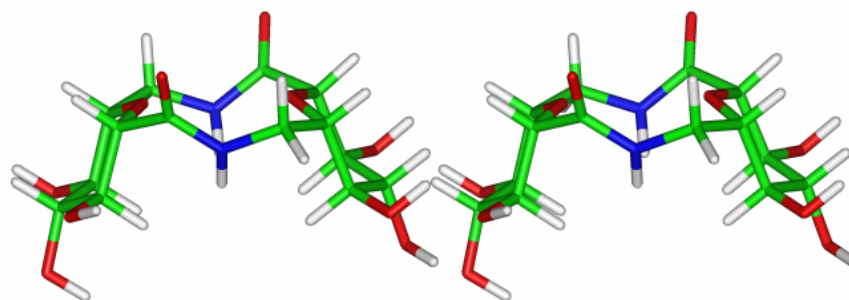
Molecular dynamic simulations were carried out on the cyclic oligomers in order to search for the whole conformational space accessible in solution (see experimental section). Molecular modeling studies run on the cyclic dimer show that indeed the predominant conformation possesses a two-fold symmetry as confirmed by NMR by the magnetic equivalence of ¹H, ¹³C and ¹⁵N nuclei.

Taking into consideration the trans configuration of the amide bonds and the ⁴C₁ conformation of the pyranose ring, two low energy structures were found (Figure 4-3) which differ in the relative orientation (*syn* or *anti*) of the C-H⁵ and C=O bonds. However, only one was in agreement with our experimental data.

The *anti* conformation was confirmed by the H⁵(i)-NH(i+1) connectivity (2.3 Å measured and 2.4 Å calculated from the correspondent ROE), the ‘ ϕ ’ dihedral angle (101.2 measured and 100.6 calculated from the Karplus equation) and the anti orientation of one of the methylene proton with respect to H¹ (*-sc* rotamer in Figure 4-2) as suggested by the ³J(CH₂-H¹) value. The *syn* conformation was discarded due to

the long $H^5(i)$ - $NH(i+1)$ distance (3.6 Å) and the gauche position of both methylene protons relative to H^1 (+*sc* rotamer in Figure 4-2).

A) all-*syn*



B) all-*anti*

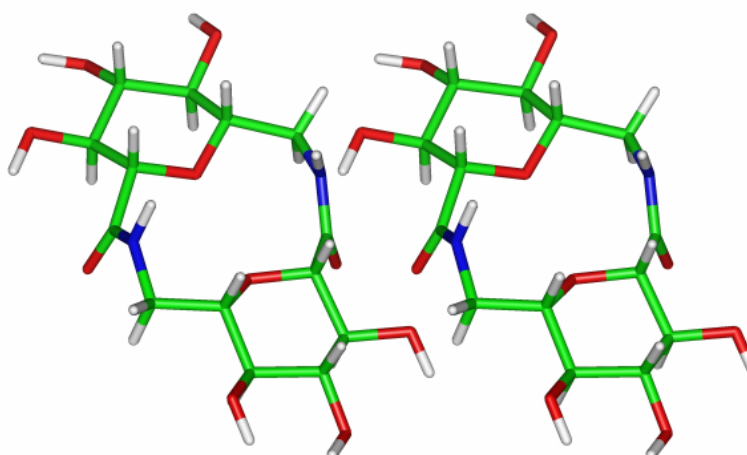


Figure 4-3: Stereoviews of the *syn* and *anti* conformations of the cyclic dimer.

Stereo specific assignments of the non equivalent methylene protons was deduced by means of our model together with $^3J(\text{CH}_2\text{-NH})$ and $^3J(\text{CH}_2\text{-H}^1)$ coupling constants which identify the proton at lower field having the largest coupling constants with both NH and H^1 as proS (Figure 4-2). This is in agreement with the known deshielding property of the carbonyl group in *syn* position to the proS proton considering the projection around CO-N-CH_2 . The strain of the ring excludes the population of the *ap* rotamer which would bring the proR proton in *anti* position to H^1 .

The *syn* and *anti* conformations of the Gum residue as described for the cyclic dimer, were also encountered during molecular simulations run on the other cyclic

compounds. The relative population of these structures can be estimated by the ROE analysis. As shown in Figure 4-4 and Table 4-1 proton-proton connectivities involving the amide group are unique for the *syn* and *anti* structures, due to the opposite orientations of the amide group with respect to the pyranose ring. In fact, the NH bond is oriented to the H^{2,4} side (*syn*) or to the H^{1,5} side (*anti*). Hence, these characteristic ROEs are taken to evaluate the *syn:anti* populations as a function of chain length.

Based upon these results, the cyclic trimer has a strong tendency to occupy the *anti* conformation. Indeed, the structure reported in Figure 4-5B bearing all the Gum in *anti* is the most populated in aqueous solution. C₃ symmetry is achieved with an all-up and all-down arrangement of the carbonyl and the NH groups with respect to the macrocyclic ring. Once more, the *-sc* rotamer about the $\underline{\text{C}}\text{H}_2\text{-C}^1$ bond is confirmed by the large $^3\text{J}(\text{CH}_2\text{-H}^1)$ coupling with one of the methylene proton (proS) which rules out the possibility of a structure bearing all the Gum in *syn* since this would require a *+sc* rotamer (Figure 4-5A).

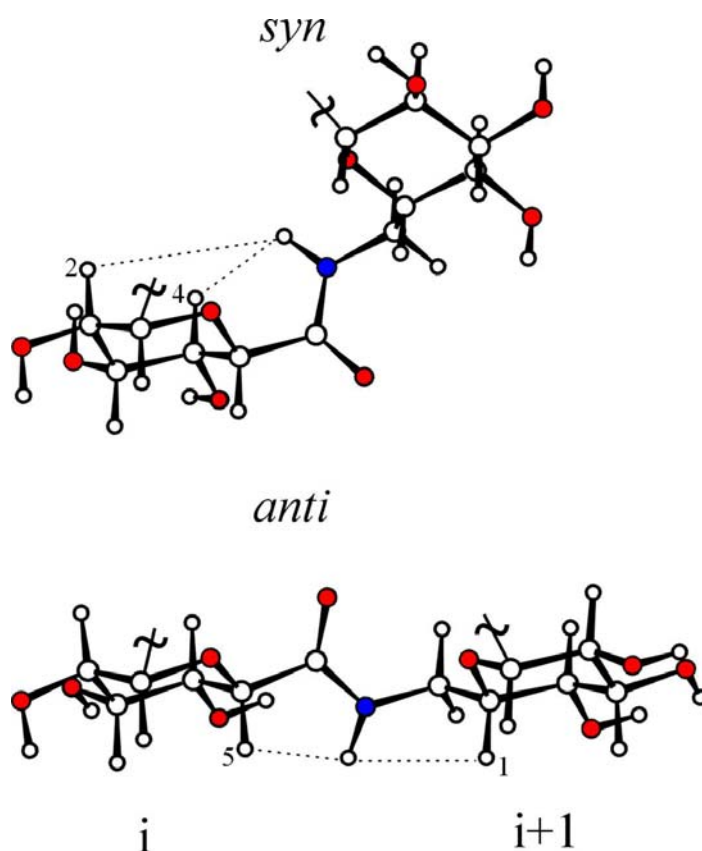


Figure 4-4: Proton-proton connectivities relevant for the conformational analysis. Hydrogen and carbon atoms are displayed as empty circles, nitrogens are filled in black and oxygens in gray.

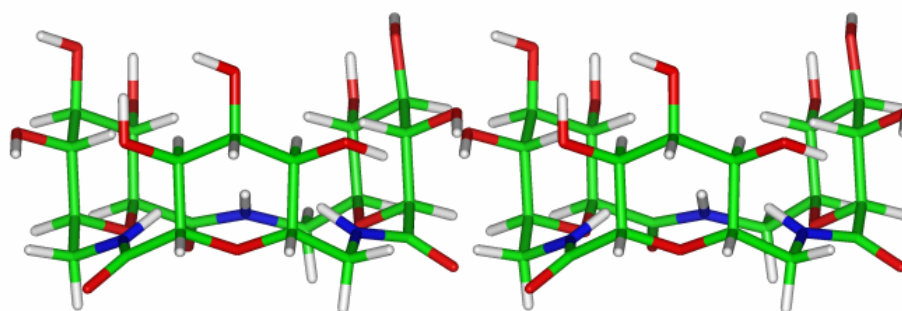
Table 4-1: Comparison between proton-proton distances (in Å) characteristic of the *syn* and *anti* conformations and ROE data.

	<i>sin</i>	<i>anti</i>	ROE		
			n=3	n=4	n=6
H ⁵ (i)-NH(i+1)	3.5-3.6	2.2-2.4	2.8	2.9	2.9
H ⁴ (i)-NH(i+1)	2.1-2.8	4.0-4.5	3.6	n.d. ^b	n.d.
H ² (i)-NH(i+1)	3.8-4.0	4.5-4.9 ^a	4.5	4.0	4.2

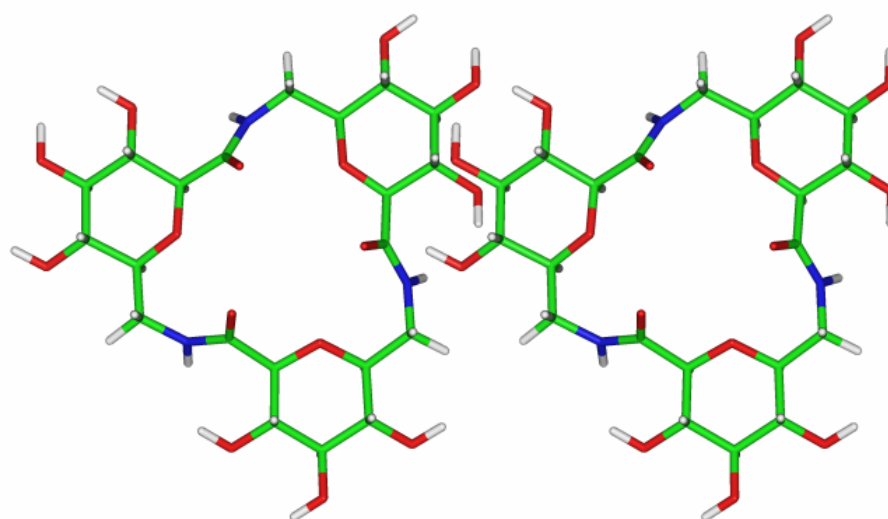
^a Intraresidue connectivity

^b n.d.=not determined due to spectral overlap

A) *all-syn*



B) *all-anti*

**Figure 4-5:** Stereoviews of the *all-syn* and *all-anti* conformations of the cyclic trimer.

4.4 Cyclodextrin-like complexation behavior of the cyclic hexamer

As underlined in the introduction, we focused on the potentials of cyclic arrangements comprising carbohydrate moieties and amide groups as molecular carriers with enhanced solubility and improved complexation behavior. This concept has also been recently considered by and co-workers using cyclic sugar amino acid/amino acid hybrid molecules.¹²³

Cyclodextrins (CD) have been extensively studied as water soluble receptors due to their ability to include a variety of guest molecules in their hydrophobic cavities.²¹ Furthermore, modified cyclodextrins with different functional groups showed additional specific interactions between host and guest molecules.¹⁵⁹

On the basis of these results, the study of cyclic homo-oligomers containing SAAs as cyclodextrin mimetics was advisable. Furthermore, NMR and molecular modeling studies in water solution revealed a strong similarity between the conformation of the cyclic oligomers bearing all the Gum in *syn* and cyclodextrins which contain a relatively hydrophobic central cavity and hydrophilic outer surface.

4.4.1 Chemical shifts

Complexation behavior of the cyclic hexamer was investigated by NMR spectrometric titration with two guest molecules, p-nitrophenol and benzoic acid. We recorded ¹H-NMR spectra at different host/guest ratio keeping constant the host concentration and observed variation of the chemical shift of specific protons of the cyclic hexamer as reported in Figure 4-6.

This clearly identifies a fast-exchange regime, with respect to the NMR time scale, between the 'free' and the 'bound' states. The difference in chemical shift experienced by the H⁵ and one of the methylene protons of the SAA is probably due to the ring-current effect of the aromatic ring of the guest molecule in the proximity of the cyclic oligomer.¹⁶⁰⁻¹⁶⁵

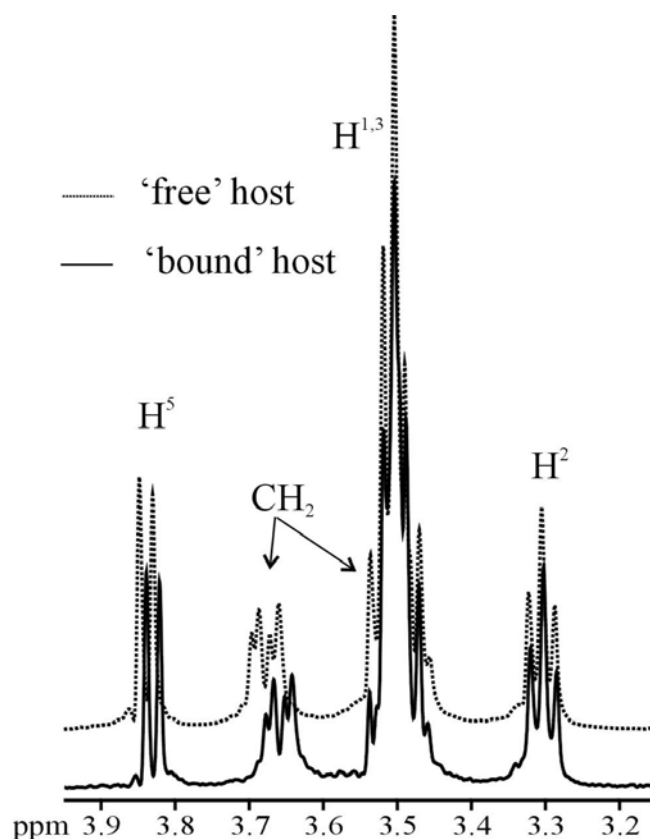


Figure 4-6: Comparison of the ^1H -1D spectra of the cyclic hexamer (host) in solution and in the presence of *p*-nitrophenol (guest) at a host/guest ratio of 4.

4.4.2 Relaxation studies

The longitudinal relaxation time (T_1)¹⁶⁵⁻¹⁶⁸ of the guest molecules was additionally used to identify host-guest binding. Complexation by the cyclic hexamer caused an increase in the correlation time of the guest molecules and this in turn led to a decrease in the T_1 (Figure 4-7).

The pulse sequence to measure T_1 is the inversion recovery reported in Figure 4-8, where the spin system is first inverted with a 180 degree pulse. It is then allowed to evolve during a variable delay and finally detected the magnetization is detected with a 90 degree observation pulse and acquired. The relaxation delay must be at least $5 \cdot T_1$.

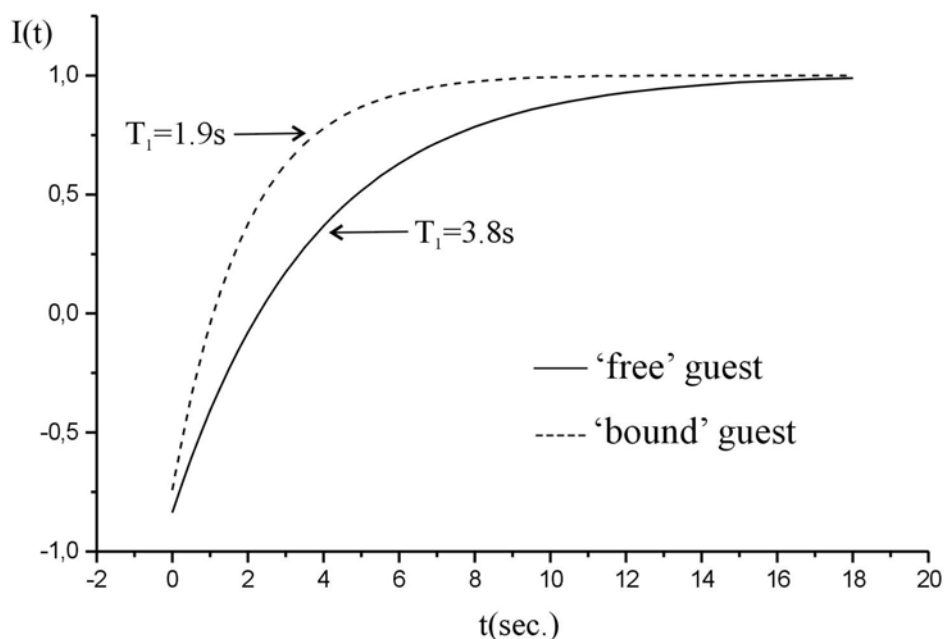


Figure 4-7: Comparison of the ^1H longitudinal relaxation times (T_1) of the benzoic acid (guest) in solution and in the presence of the cyclic hexamer (host) at 1:1 ratio.

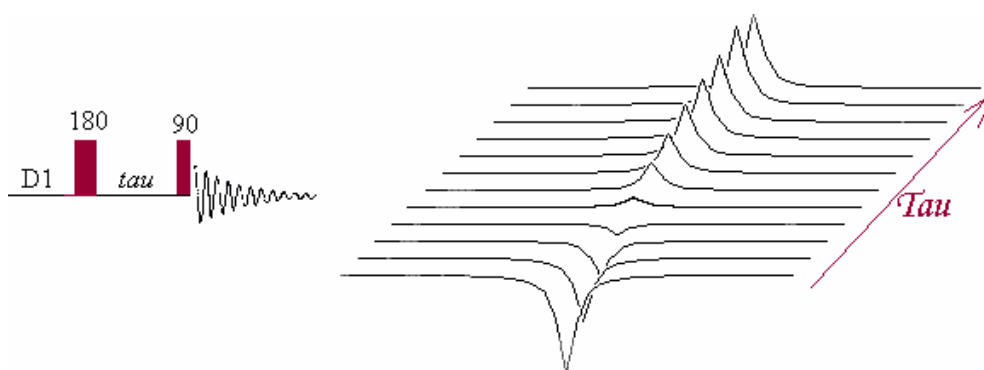


Figure 4-8: T_1 relaxation time measurement with inversion recovery.

4.4.3 Diffusion experiments

Finally, the formation of a host-guest complex was studied by measurements of the diffusion rate D .¹⁶⁹ By comparing the intensities of the signals of protons versus the intensity of the magnetic field gradient we obtained the mean values reported in Table 4-2. The change in value of D of the benzoic acid in aqueous solution and in the presence of the cyclic hexamer supports the idea of the formation of an inclusion complex. In fact, the diffusion of a compound is proportional to the molecular size,

and in the case of a host-guest complex, the diffusion behavior of a low molecular weight guest molecule decreases in proportion to the molecular size of the host molecule and to the binding affinity. Similar behavior was found for cyclodextrins and their ligands.^{169,170} Although the exact way of binding has not been defined yet, these results evidently identify this class of molecules as cyclodextrin-like artificial receptors.

Table 4-2: Diffusion coefficients (D) of benzoic acid (guest) and the cyclic hexamer (host) for a 1:1 ratio.

$D_{\text{free-guest}}$ (cm^2s^{-1}) $\times 10^6$	D_{host} (cm^2s^{-1}) $\times 10^6$	$D_{\text{bound-guest}}$ (cm^2s^{-1}) $\times 10^6$
7.4	2.7	5.7

The sequence to measure diffusion is very similar to the spin echo pulse sequence (CPMG), except that two gradient pulses are applied: one before the refocusing 180° pulse, and one after the 180° pulse (Figure 4-9). These two gradient pulses are identical in amplitude G and width d . They are separated by a time Δ and are placed symmetrically about the 180° pulse. The function of the first gradient pulse is to dephase magnetization according to its position in the NMR tube. During the subsequent Δ period, the spins are left to evolve and diffuse. Their chemical shift is refocused by applying the usual 180° pulse. At the end of the Δ period, the spins that have diffused to a new location in the NMR tube will not get refocused by the second gradient and will therefore attenuate the signal. These gradient pulses have no effect on stationary spins.

In that experiment, the echo time is left constant while the gradient strength G is varied (usually along the z -axis). The loss of magnetization can be plotted against the gradient strength to extract the diffusion coefficient D .

The relationship between the signal amplitude $I(\mathbf{g})$ obtained in the presence of a gradient amplitude Gz in the z direction and the diffusion coefficient Dz in the same direction is given by the following equation where $I(\mathbf{0})$ is the signal at zero gradient:

$$I(\text{grad})/I(0) = \exp[-(Gz * \gamma * d)^2 Dz (\text{DELTA} - d/3)]$$

where γ is the gyromagnetic constant of the nuclei, d is the length of the gradient pulse and **DELTA** is the interval between the two gradients.

Convection within the sample is a serious problem affecting NMR diffusion measurements and DOSY experiments, in particular at elevated temperatures. Convection currents are caused by small temperature gradients in the sample and cause additional signal decay that could be mistaken for faster diffusion. To overcome convection artifacts in stimulated-echo (STE) diffusion experiments we used a double-stimulated-echo (DSTE) sequence which refocuses all the constant-velocity effects (flow and convection).¹⁷¹

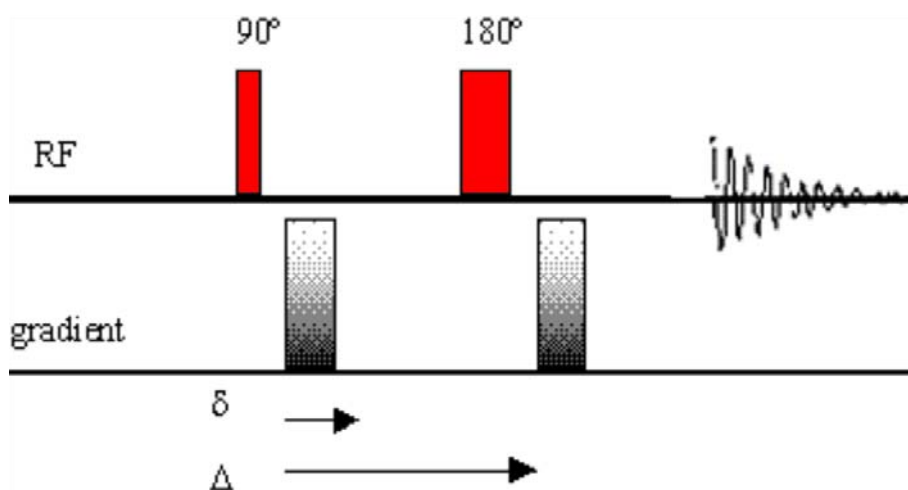


Figure 4-9: Stimulated-echo 1D-¹H diffusion experiment.

5 Synthesis and SAR of Mannose-Based Peptidomimetics Blocking Selectively Integrin $\alpha 4\beta 7$ Binding to MAdCAM-1

5.1 Design and synthesis of the mannose-based peptidomimetics

A biased library of mannose peptidomimetics was developed based upon the structure of an inhibitor of the VCAM/ $\alpha 4\beta 1$ interaction ($IC_{50} \cong 3.7$ mM), previously discovered in our laboratory. In our strategy, we maintained the original mannose core and the Leu and Asp pharmacophores at 6 and 1-positions of the sugar ring, respectively (Figure 5-1). For SAR studies, a spatial screening of the Asp pharmacophore was carried out by synthesizing and comparing the biological effects of the β and α -anomers. The Ser side chain, which is known to be not relevant for activity, was replaced at position 2 by the Phe side chain. In fact, a remarkable number of different research groups have discovered phenylalanine-based $\alpha 4$ antagonists.¹⁷²⁻¹⁷⁷ The phenanthrene-9,10-diacetals (PDA) group was attached to the mannose core as hydrophobic source at 3 and 4-positions. The mannose scaffold was rigidified by a trans ring fusion between a dioxane ring and the pyranoside at 3 and 4-positions. The Leu mimetic was introduced either *via* ether linkage or *via* carbon-carbon bonding, in order to examine the effects on activity of changes in polarity and in the conformational space available for this pharmacophore. At last, the metabolic stability of the mannose derivatives was improved by introducing the Asp side chain at the anomeric position through a C-glycosidic linkage.

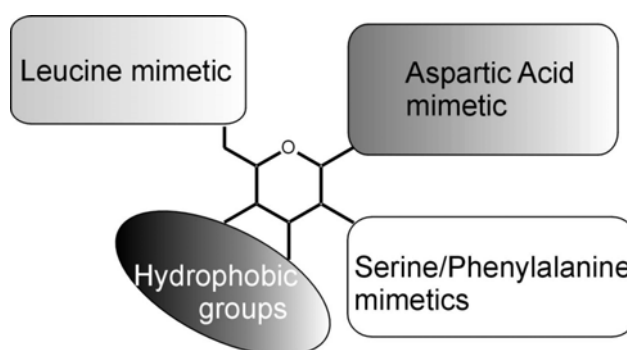
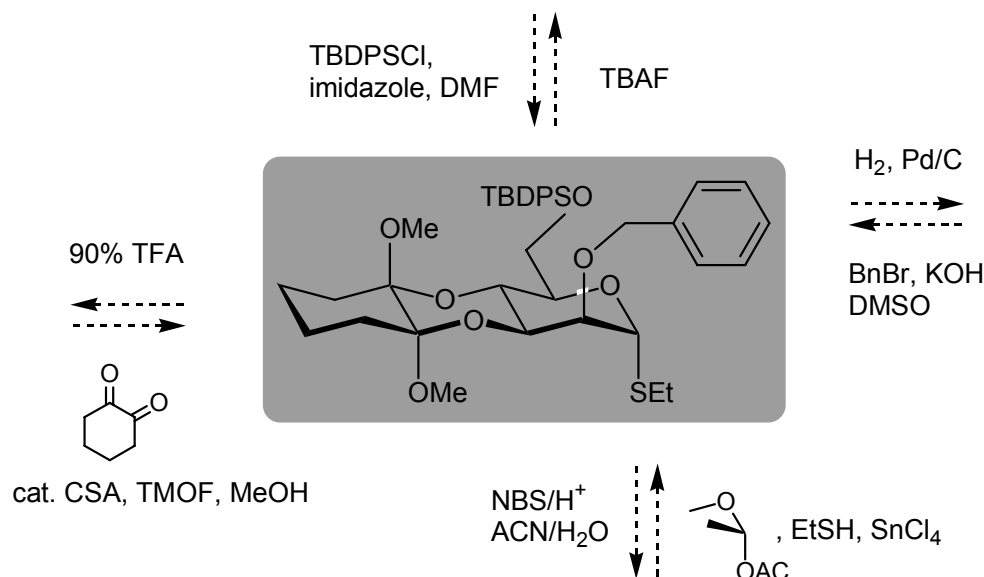


Figure 5-1: Development of a biased library of mannose derivatives.

5.1.1 Synthesis of an orthogonal protected mannose derivative

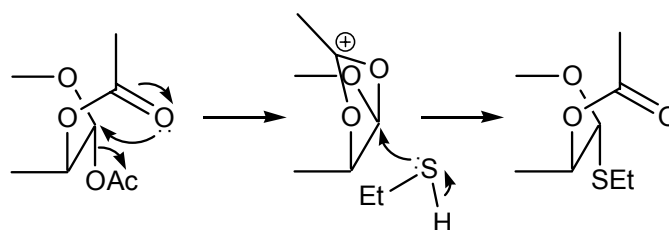
The synthetic protocol of the desired functionalized mannopyranosides required an orthogonal set of protecting groups.



Scheme 5-1: *Orthogonal protected mannose derivative.*¹⁷⁸

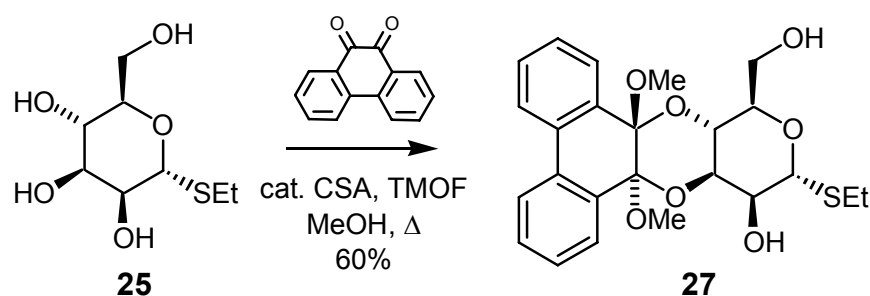
The fully protected mannose derivative we used is reported in Scheme 5-1. The orthogonal protecting groups were successively cleaved, as specified, and replaced by pharmacophoric side chains.

Ethyl 1-thio- α -D-mannopyranoside **25** was stereoselectively prepared from commercially available penta-O-acetyl- α -D-manno-pyranoside and ethanethiol in the presence of a Lewis acid as catalyst, and subsequent ester hydrolysis. In fact, reaction of penta-O-acetyl- α -D-manno-pyranoside with alcohols or thiols tends to proceed by intramolecular heterolysis of C¹-X bond assisted by a neighboring acyloxy group (Scheme 5-2).



Scheme 5-2: *Neighboring effect of an acyloxy group at C².*

We used the concept of 1,2-diacetals as regio-selective protecting groups for diequatorial 1,2-diol units in carbohydrates. In particular, acid catalyzed reaction of ethyl 1-thio- α -D-mannopyranoside **25** with cyclohexane-1,2-diones results in selective protection of diequatorial 3,4 diol functionalities as a cyclohexane-1,2-diacetal (CDA).



Scheme 5-3: Preparation of phenanthrene-9,10-diacetals (PDA) protected ethyl-1-thio- α -D-mannoside.

The resulting CDA protected derivatives can be readily functionalized to give rapid access to numerous key building blocks for oligosaccharide and natural product synthesis.¹⁷⁹ In a similar fashion, ethyl 1-thio- α -D-mannopyranoside could also be protected as phenanthrene-9,10-diacetals (PDA) under the same reaction conditions (Scheme 5-3).

The selectivity arises from the combination of two effects. Firstly, protection of the 3,4-diequatorial diol is favored over the 2,3-*cis* diol as this leads to the sterically less demanding *trans* ring fusion between the dioxane ring and the pyranoside. Secondly, only one diastereoisomer of this compound is produced as the configuration of the acetal centers is controlled by the anomeric effect.

Rapid selective protection of the 2-position of CDA mannoside **26** could, surprisingly, be achieved by benzylation with benzyl bromide using KOH in DMSO, yielding to the 2-benzyl ether **28** in 75-85%. Ley and coworkers achieved the same result using sodium hydride in DMF.¹⁷⁸ The regioselectivity was unambiguously assigned from the multiplicity of the hydroxyl proton in the ¹H NMR and by the observation of a long range ¹³C-¹H correlation between the benzylic protons and C² of the sugar ring in the HMBC spectrum. This reversal of selectivity (secondary versus primary hydroxyl

group) is not easily explained, however, it should be noted that benzylation involves formation of the oxyanion prior to reaction. The pK_a of the two hydroxyl groups will affect the population of each oxyanion in solution and their reactivity. The oxyanion at the 2-position is probably more basic and hence more reactive although it will be present in a lower equilibrium concentration. This would account for the observed reactivity profile. Direct protection of the 2-position of PDA mannoside **27** did not work but it was achieved in two steps: regioselective protection of the primary alcohol with *tert*-butyl diphenyl silyl chloride (TBDPSCI) and subsequent benzylation.

5.1.2 Ether formation with alkyl halides: The Williamson reaction

To introduce the Ser and Leu side chains as well as the benzyl and methyl groups we used the Williamson reaction,¹⁸⁰ which is still the best general method for the preparation of unsymmetrical ethers. The normal method involves treatment of the halide with alkoxide or aroxide ion prepared from an alcohol or phenol, but it is also possible to mix the halide and alcohol or phenol directly with the base. We used solid KOH in DMSO (Scheme 5-4).¹⁸¹ In the case of secondary halides an excess of halide was needed because of elimination which occurred as side reaction. Many other functional groups can be present in the molecule without interference.



Scheme 5-4: *The Williamson ether formation.*

5.1.3 β *O*-Glycosides: The Koenigs-Knorr method

The Asp side chain was introduced *via O*-glycosidation. Attempts towards the synthesis of β -mannose linkages have been well reviewed recently by Gridley and Osborn.¹⁸² The difficulties in constructing these ubiquitous linkages can be summarized:

1. The anomeric effect¹⁸³ in pyranosides can be seen as the propensity of an electronegative substituent to adopt an axial orientation. This tendency is caused by interaction between the axial lone pairs of electrons on the ring oxygen atom and the antibonding σ^* -orbitals of the C-X bond. This leads to shortening of the bond connecting the ring oxygen atom to the anomeric center and lengthening of the C-X bond in the case of anomers having the X group axial, relative to the respective bond lengths in the equatorial anomer (Figure 5-2a). Furthermore, there is a cooperative electrostatic factor acting against formation of the equatorial isomer (Figure 5-2b). In the latter, repulsion between the negative end of the C^1-X_e dipole and the unshared electrons of the ring oxygen atom is greater than for the C^1-X_a dipole.
2. The location of an axial acyl protecting group at C^2 in mannose that can participate in the glycosidation reaction (neighboring group participation), leads predominately to the α -mannosides (Scheme 5-2); this is opposite to glucose for which the equatorial acyl group participates to give predominately the β -glucoside product.

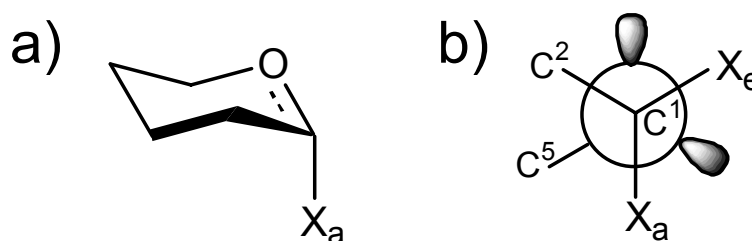
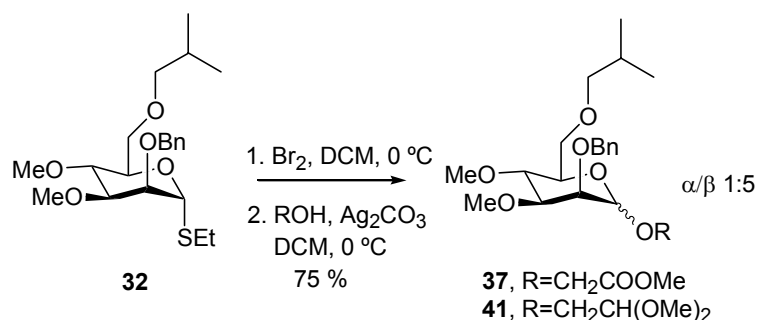


Figure 5-2: *The anomeric effect. a) Bonding factor and b) electrostatic factor.*

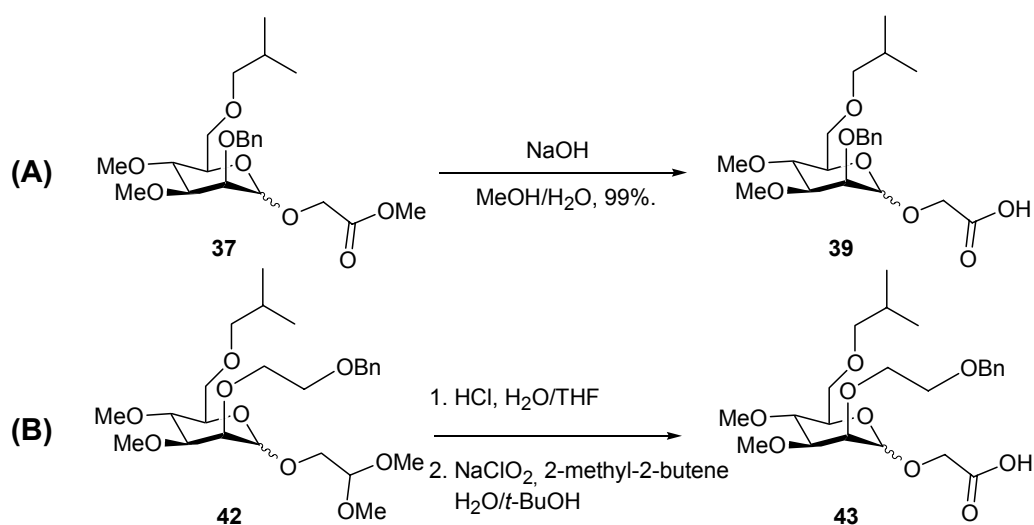
The methodology we used to overcome these problems is a modified Koenigs-Knorr coupling using insoluble silver salt promoters to block the α -face of mannosyl halides and direct glycosidation to give β -mannosides (Scheme 5-5).¹⁸⁴ The β -anomeric configuration was verified by interproton distances between protons at positions 1, 3 and 5 derived from NOESY spectra, and by ^{13}C NMR spectroscopy, based on the general rules^{185,186} governing the stereochemical dependence of the 1J ($\text{C}^{13}\text{-H}^1$) coupling constants in hexopyranoses, which for the β -anomer was < 160 Hz, while

that for the α -anomer was > 170 Hz. The two anomers were separated *via* flash column chromatography or *via* HPLC, when necessary.



Scheme 5-5: Formation of the *O*-glycosidic linkage via the Koenigs-Knorr reaction.

As glycosyl donor we used predominantly mannosyl bromide, which was prepared *via* direct activation of the S-Et group in ethyl 1-thio- α -D-mannoside with bromine in dichloromethane. In the case of less reactive *S*-glycosides, as for α -D-manno-Non-pyranoside, ethyl-6,7,8,9-tetra-deoxy-2-*O*-benzyl-3,4-di-*O*-methyl-8-methyl-1-thio **54** and α -D-manno-Oct-pyranoside, ethyl-6,7,8-tri-deoxy-2-*O*-benzyl-3,4-di-*O*-methyl-7-methyl-1-thio **55**, we achieved the desired halide in two steps: hydrolysis of the S-Et group with NBS/ H^+ and subsequent reaction with thionyl chloride leading to the mannosyl chloride almost quantitatively.



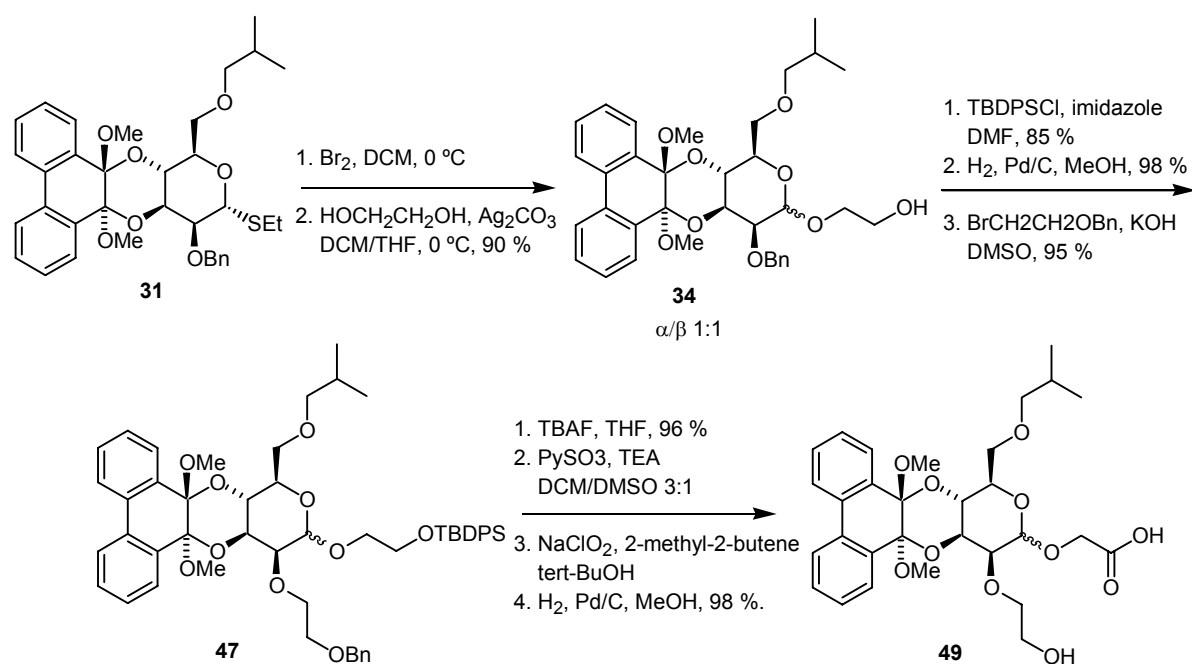
Scheme 5-6: Formation of the Asp mimetic starting from the methyl ester (A) or dimethyl acetal (B).

The Asp side chain (glycosyl acceptor) was masqueraded as methyl ester or acetal protected aldehyde (ROH in Scheme 5-5).

The latter strategy was chosen to avoid the problematic C^α acidity of the carboxylic acid derivatives which might result in undesired byproducts during ether formation. After cleavage of the acetal the free aldehyde was immediately oxidized to the corresponding carboxylic acid using sodium chlorite and 2-methyl-2-butene as scavenger for the hypochlorite which is produced during the oxidation (Scheme 5-6B).¹⁸⁷

For compounds in which the benzyl group was kept at position 2 as Phe mimetic, the carboxyl group of the Asp side chain was protected during the Koenigs-Knorr reaction only as methyl ester. The ester was easily hydrolyzed at the end using NaOH in H₂O/MeOH solution (Scheme 5-6A).

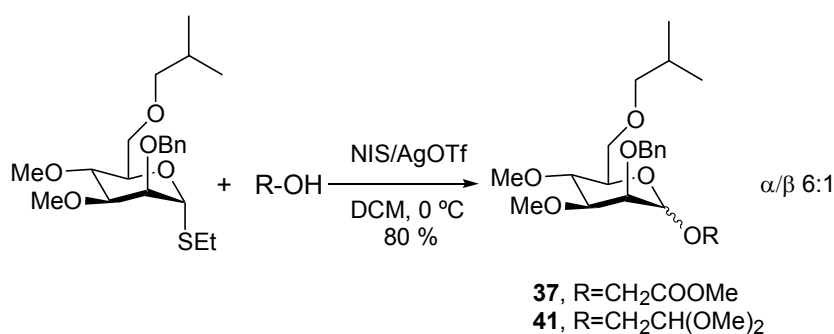
For the PDA protected sugar, the Asp side chain was introduced as primary alcohol *via* Koenigs-Knorr reaction using ethylene glycol as glycosyl acceptor leading to an α/β ratio of 1:1 (Scheme 5-7). The alcohol functionality was at the end oxidized to carboxylic acid in a two steps reaction. In fact, hydrolysis of the dimethyl acetal, required by the previous protocol, caused in this case byproducts due to a concurrent aldol condensation.



Scheme 5-7: Synthesis of the PDA-containing mannopyranosides.

5.1.4 α *O*-Glycosides: Thioglycoside methodology

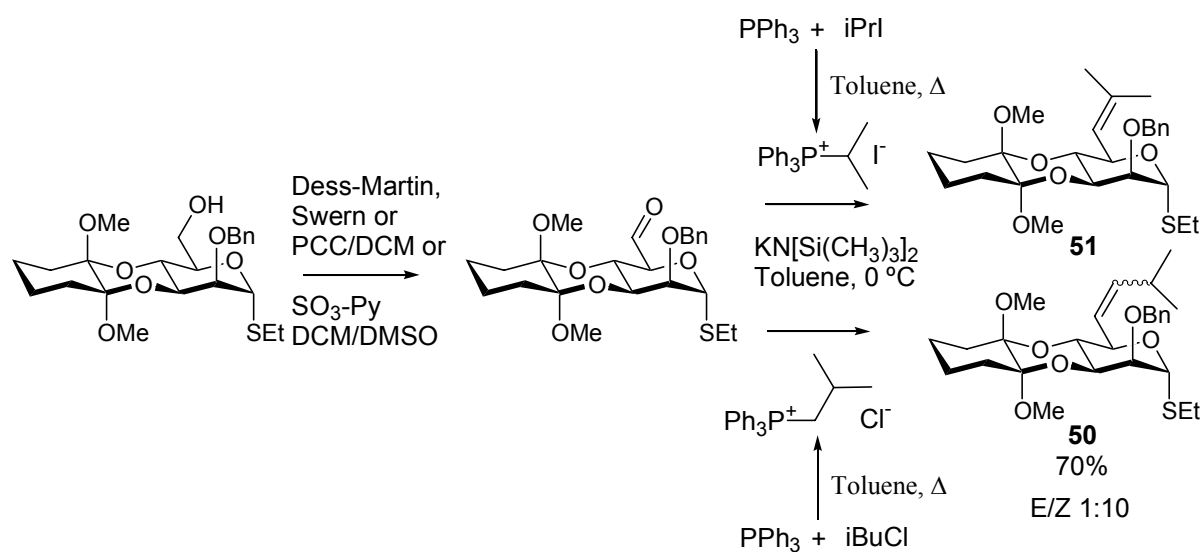
Such methodology employs a thioglycoside donor (e.g., having an alkylthio aglycon) which is *O*-glycosidically directly condensed with an alcohol acceptor in the presence of a thiophilic agent, where the latter is generated by a promoter system and transforms the aglycon into a good leaving group. In this case a selectivity towards the most favorable α -anomer was expected. In fact, α -mannosides are thermodynamically and kinetically favored, and are the major product when the oxonium ion is an intermediate in the glycosidation reaction. There are numerous promoter systems for thioglycoside activation, of which sulfenylhalides/silver trifluoromethanesulfonate, such as PhSCl/AgOTf and MeSBr/AgOTf, or *N*-iodosuccinimide (NIS) combined with either trifluoromethanesulfonic acid (TfOH) or silver trifluoromethanesulfonate appear to be the most commonly used. We chose the latter system to get the α -mannose glycosides (Scheme 5-8).



Scheme 5-8: *The thioglycoside methodology.*

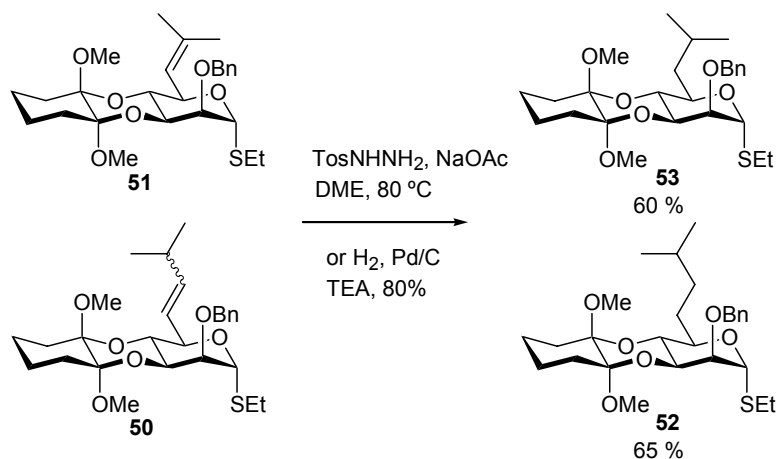
5.1.5 Wittig olefination of sugar aldehyde

The Leu side chain was introduced also *via* carbon-carbon bonding by Wittig olefination of sugar aldehyde at 6-position. The primary alcohol was oxidized to aldehyde according to known procedures either using DMSO as oxidizing reagent and sulfur trioxide pyridine complex as alcohol activating reagent or using the Dess-Martin reagent. As reported in Scheme 5-9, the *in situ* prepared ylide was then reacted with the crude aldehyde in cold toluene.



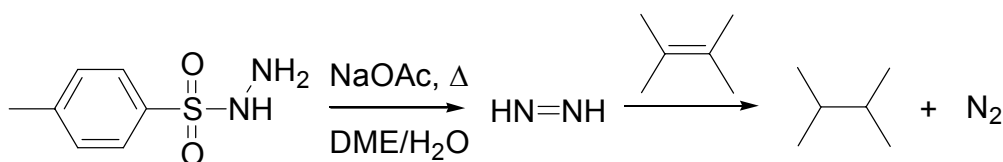
Scheme 5-9: Wittig olefination of sugar aldehyde.

The resulting double bond was successively reduced by *para*-toluenesulfonylhydrazide in dimethoxyethane (Scheme 5-10)



Scheme 5-10: Reduction of double bonds in the presence of the benzyl protecting group.

The actual reducing species is diimide $\text{NH}=\text{NH}$, which is formed *in situ* from tosylhydrazide (toluene-4-sulfonyl hydrazide) by NaOAc (Scheme 5-11). The addition is stereospecifically *syn* and, like catalytic hydrogenation, generally takes place from the less-hindered side of a double bond.



Scheme 5-11: Generation of diimide in situ and syn addition to double bonds.

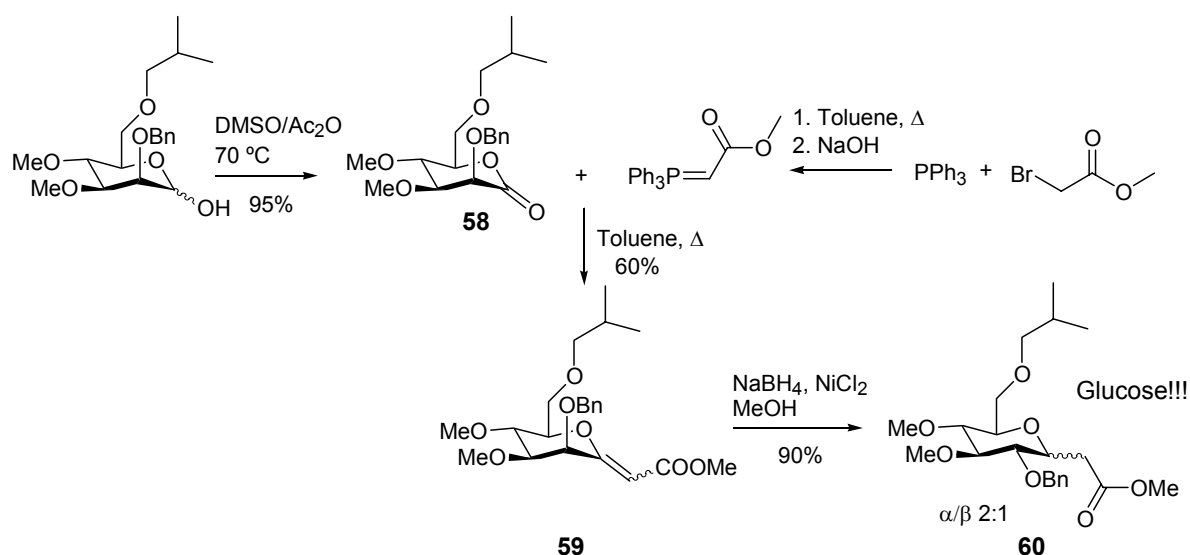
Another method we used to selectively reduce a double bond in the presence of a benzyl group was Pd/C catalyzed hydrogenation with a nitrogen-containing base or amine as poison.

5.1.6 C-glycosides: Wittig olefination of sugar lactones or Reformatzky-type reaction

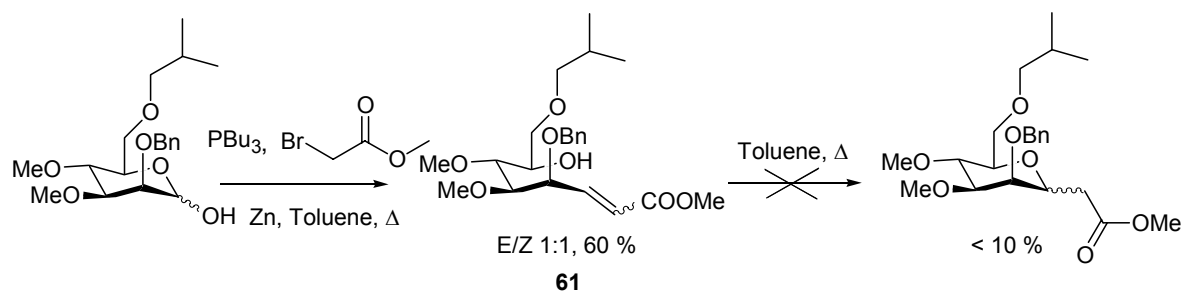
Direct olefination at the anomeric center of sugars is an interesting way to introduce a carbon chain, which can be in turn chemically manipulated. In fact, 1-exomethylene sugars (*exo*-glycals) have been intensively applied for the preparation of C-glycosides after reduction of the double bond. D-Manno-Oct-2-enonic acid, 3,7-anhydro-4-*O*-benzyl-2-deoxy-8-*O*-isobutyl-5,6-di-*O*-methyl, methyl ester **59** was synthesized according to Wittig olefination of sugar lactones by the methoxycarbonylmethylene-(triphenyl)-phosphorane.¹⁸⁸

As reported in Scheme 5-12, heating a toluene solution of the lactone, previously formed by oxidation of the free mannose with acetic anhydride in DMSO, and the stabilized phosphorane at 140 °C in a sealed vessel gave the expected olefin **59**. Selective reduction of the 1-exomethylene group proceeded using sodium borohydride and catalytic NiCl₂. In fact, both LiAlH₄ and as well as NaH, reduce ordinary alkenes and alkynes when complexed with transition metal salts.^{189,190} Due to the acidity of the allylic proton at 2 position of the pyranose ring, during reduction of the double bond we got complete conversion from mannose to glucose derivative **60**.

Another widely used method to obtain carbon-carbon bonding at the anomeric position of carbohydrates is a two step procedure involving the formation of an unsaturated, open-chain intermediate, followed by a cyclization leading to the expected C-glycosyl compound.



Scheme 5-12: Generation of C-pyranoside via Wittig olefination of sugar lactones.



Scheme 5-13: Generation of C-pyranoside via Reformatsky-type reaction.

Fréchou *et al.* developed a one-pot reaction of this procedure *via* a Reformatsky-type reaction, heating the free aldose in refluxing benzene with tributylphosphine, zinc dust, and methyl bromoacetate.¹⁹¹ In the case of our mannose derivative, the final cyclization of the unsaturated intermediate did not occur spontaneously (Scheme 5-13). After heating a toluene solution of **61** for 1 day in the presence of triethylamine only traces of the desired product was obtained.

5.2 Structure Activity Relationship for the Biased Mannose-Based Library

The inhibition of 38-β7 (α4β1⁻, α4β7⁺) cell adhesion to MAdCAM-1 in the presence 1 mg/mL of the sugar derivatives described here is reported in Table 5-1. In addition to biological activity, selectivity is a major goal in drug development. To verify selectivity, the ability of these compounds to inhibit specific interactions of integrins

with their cognate ligands, binding of the structurally related integrin $\alpha4\beta1$ to VCAM-1 was investigated. Adhesion mediated by $\alpha4\beta1$ integrin was tested using Jurkat ($\alpha4\beta1^+$, $\alpha4\beta7^-$) lymphoma cells.

When comparing the potencies of different compounds, however, it is important to consider that the measured IC_{50} values are highly dependent upon reagent concentrations and assay conditions. Therefore, only a comparison between the relative potencies of antagonists measured in the same assay is informative. To be able to compare the potencies of our antagonists with literature known active compounds (Figure 5-3), the activity of **62**, proposed by Shroff *et al.*¹⁹² as potent $\alpha4\beta7$ antagonist (Ref. $\alpha4\beta7$), and **63**, which was derived by Wang *et al.* from the crystal structure of VCAM (Ref. $\alpha4\beta1$),⁷⁵ were measured under the same conditions and the IC_{50} curves are reported in Figure 5-4 and Figure 5-6, respectively.

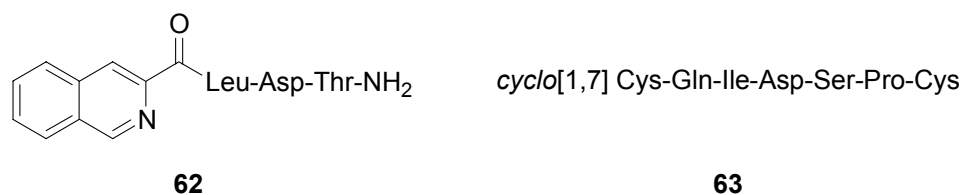
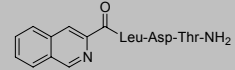
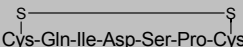
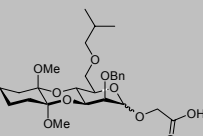
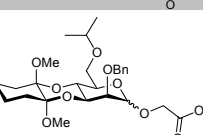
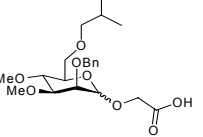
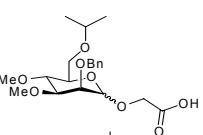
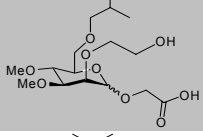
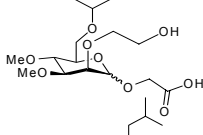
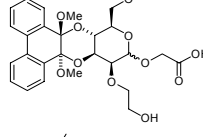
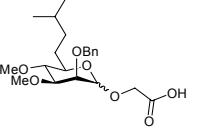
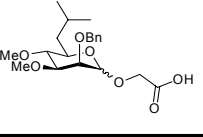
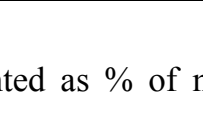




Figure 5-3: Structures of the $\alpha4\beta7$ reference **62** (Ref. $\alpha4\beta7$)¹⁹² and $\alpha4\beta1$ reference **63** (Ref. $\alpha4\beta1$).⁷⁵

Compound **35- β** showed inhibitory activity towards the $\alpha4\beta7$ /MAdCAM interaction with an IC_{50} of 420 μ M (Figure 5-5). This result is comparable with the activity of the literature known tripeptide $\alpha4\beta7$ antagonist **62**, showing in our assay an IC_{50} of 280 μ M. In a previous report,¹⁹² the IC_{50} of Ref. $\alpha4\beta7$ was found to be 3 μ M.

Furthermore, the tripeptide Ref. $\alpha4\beta7$ did not show any selectivity with respect to $\alpha4\beta1$ binding to VCAM-1 (Table 5-1). Considering that the two receptors share a common $\alpha4$ chain, it is not surprising that many of the potent $\alpha4\beta7$ /MAdCAM antagonists are inhibitors of $\alpha4\beta1$ as well. In contrast, the $\alpha4\beta1$ /VCAM-1 interaction was not affected significantly by compound **35- β** demonstrating its high selectivity for integrin $\alpha4\beta7$ (Table 5-1).

Table 5-1: 38- β 7 cell adhesion to MAdCAM-1 and Jurkat lymphoma cell adhesion to VCAM-1 with 1 mg/mL of the inhibitor.

		38- β 7 (α 4 β 7) MAdCAM-1 adhesion [%] ^a	Jurkat (α 4 β 1) VCAM-1 adhesion [%]
Ref. ^b	α 4 β 7 	10	10
Ref. ^c	α 4 β 1 	n.d.	52
35-	β 	15	77
	α 	90	89
36-	β 	76	100
	α 	100	100
39-	β 	100	86
	α 	100	100
40-	β 	100	86
	α 	100	92
44-	β ^d 	100	60
	α 	100	100
46-	β 	100	100
	α 	100	98
49-	β	80	82
	α	76	81
56-	β	100	100
	α	100	97
57-	β	100	100
	α	100	100

^a Cell adhesion is presented as % of medium control in the presence of 1 mg/mL antagonist; ^b 192, ^c 75, ^d 29

Because our compound **35- β** blocks selectively the $\alpha 4\beta 7$ /MAdCAM interaction, it would most likely impact *in vivo* migration of leukocytes to the gastrointestinal tract, where only MAdCAM expression has been linked to human disease (colitis),⁷¹ without interfering with $\alpha 4\beta 1$ /VCAM-1 immune functions.

These present studies also reconfirmed the β orientation of the Asp side chain to be necessary for activity. In fact, the α -anomer **35- α** did not show any inhibitory activity. Besides, the original chain length for the Leu pharmacophore present in **44- β** turned out to be a winning solution also for blocking $\alpha 4\beta 7$ binding to MAdCAM. For instance, $\alpha 4\beta 7$ activity of **35- β** is almost completely lost as the iBu group is replaced by the iPr group as for **36- β** (Table 5-1).

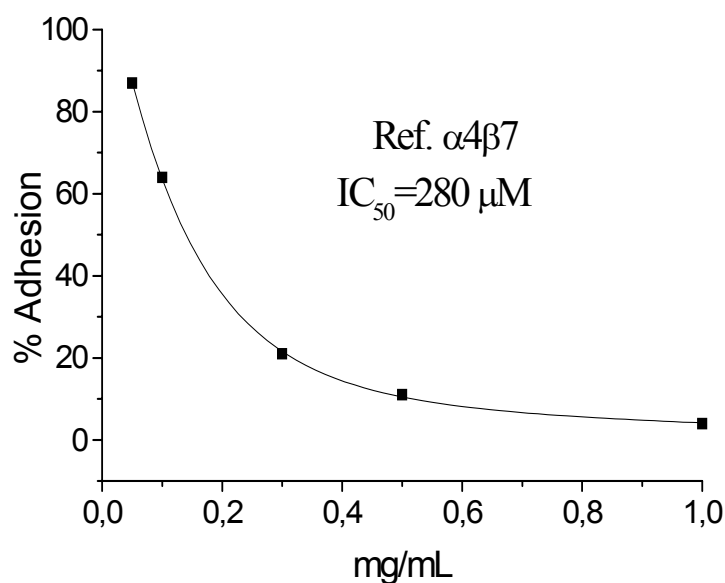


Figure 5-4: $38-\beta 7$ cell adhesion to immobilized MAdCAM-1 as function of the concentration of $\alpha 4\beta 7$ reference 62.¹⁹²

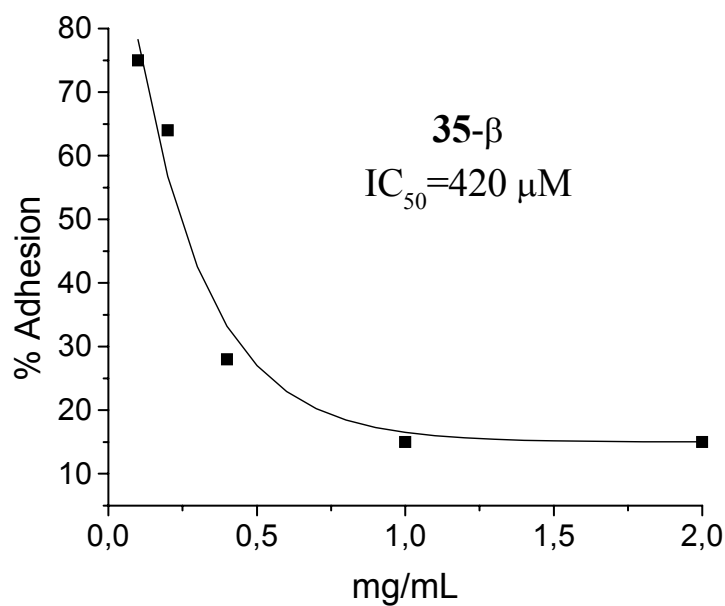


Figure 5-5: 38- β 7 cell adhesion to immobilized MAdCAM-1 as function of the concentration of our antagonist 35- β .

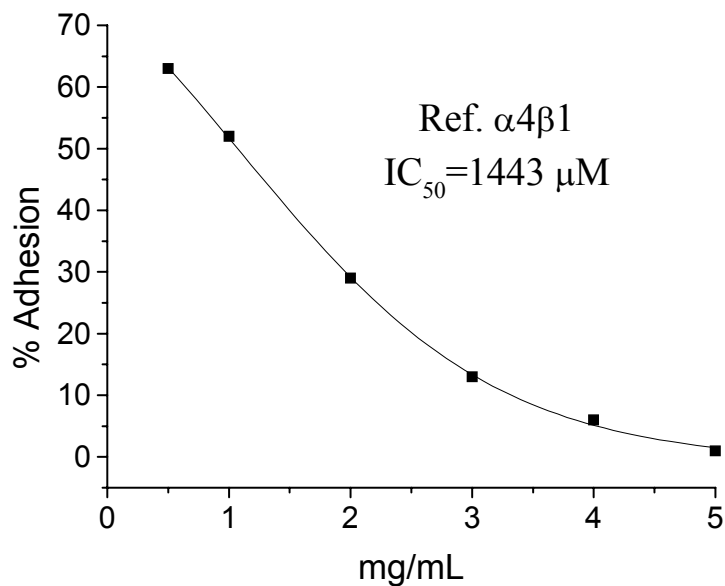


Figure 5-6: Jurkat lymphoma cell adhesion to immobilized VCAM-1 as function of the concentration of $\alpha 4\beta 1$ reference 63.⁷⁵

5.3 Structure activity relationship

Conformational analysis was carried out for the sugar inhibitor **35- β** based upon NMR data and molecular modeling. The NOESY spectrum acquired in CD_3CN is reported in Figure 5-7. Long range connectivities involving aromatic protons of the Phe pharmacophore and protons of the Leu side chain indicated hydrophobic interactions between these residues. These proximities were observed also in a more polar solution (D_2O/CD_3CN 1:1).

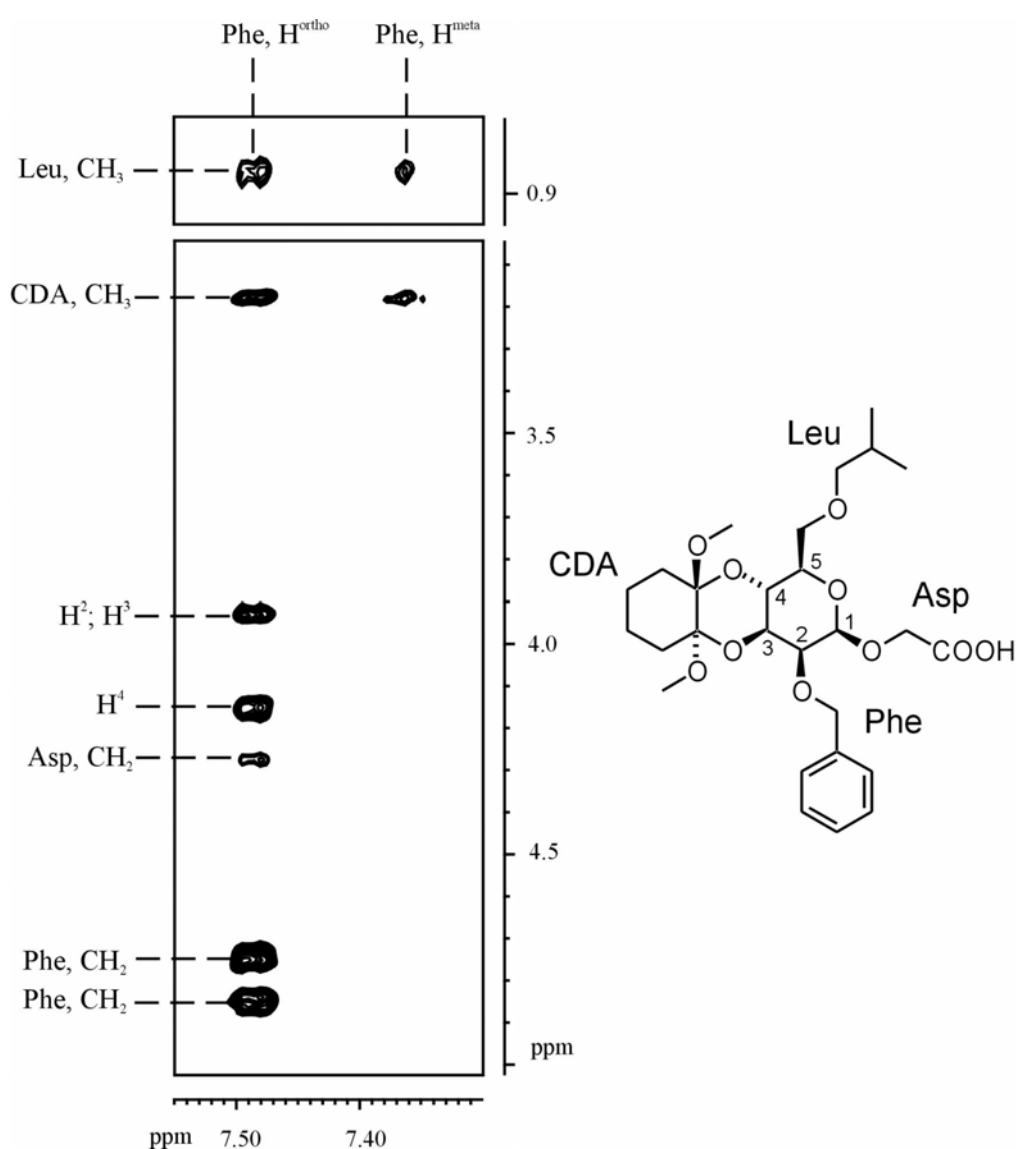


Figure 5-7: NOESY spectrum acquired at 275 K in CD_3CN for the sugar inhibitor **35- β** . Long chain connectivities involving the aromatic protons of Phe are labeled.

A simulating annealing protocol generated 50 structures which were classified in 5 families based upon the orientation of the Asp, Phe and Leu pharmacophores. Representative structures for each family were superimposed in Figure 5-8. During the whole simulation, the sugar core remained rigid. The 5 structures were classified based upon the NOE deviations, which of course have to be considered as average values due to the mobility of the side chains. However, the structure forming an hydrophobic pocket between the aromatic ring of Phe and the Leu side chain, which can be clearly seen in the side-view of Figure 5-8, is in agreement with the NOE data and it is by far the most populated conformation during simulated annealing.

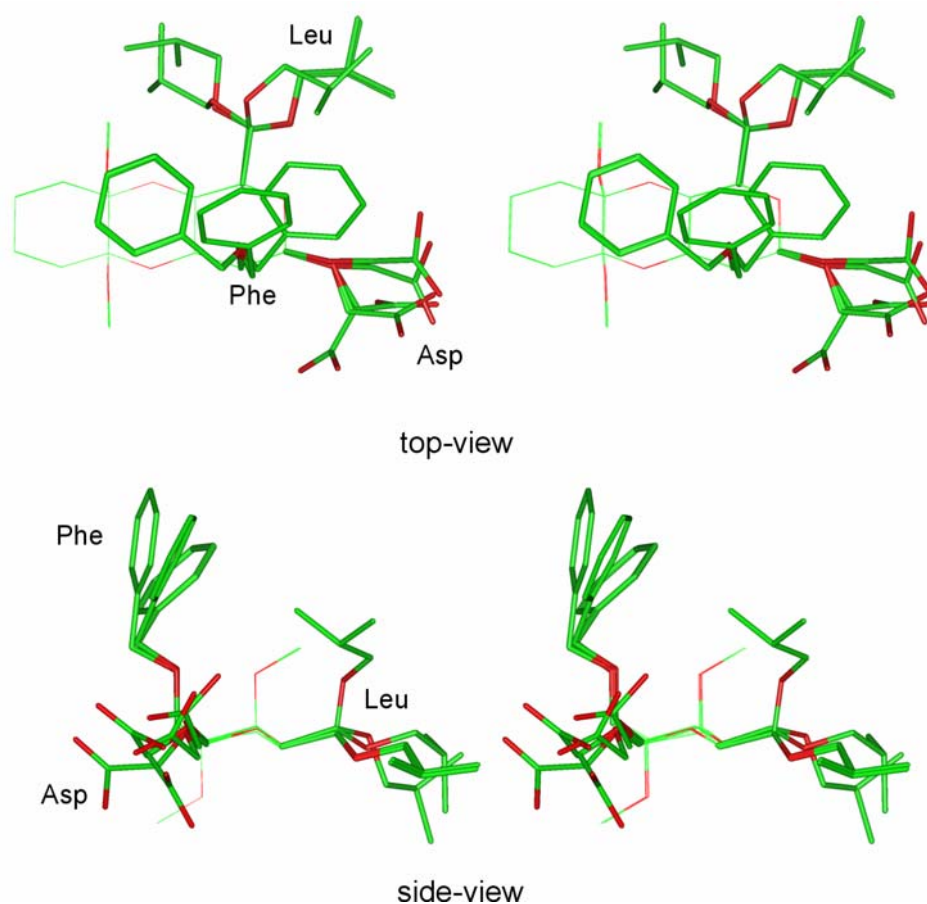


Figure 5-8: Stereo view of the superposition of representative structures of $35\text{-}\beta$ for each of the 5 cluster determined by molecular modeling.

Several possible mechanisms could explain the selectivity of antagonist $35\text{-}\beta$ for $\alpha4\beta7$. Either $35\text{-}\beta$ lacks a critical $\alpha4\beta1$ binding interaction, like the Ser side chain in $44\text{-}\beta$. This could also explain the negative effect on activity of the replacement of the

ethylene glycol moiety at 2-position of the original $\alpha 4\beta 1$ antagonist **44**- β by the benzyl group as for **39**- β . Otherwise the relatively bulky CDA group sterically hinders binding to $\alpha 4\beta 1$ but not to $\alpha 4\beta 7$. In fact, the incorporation of the PDA group, as source of aromaticity, at 3 and 4-positions of **44**- β causes in **49**- β a decrease of $\alpha 4\beta 1$ activity as well. Besides, changes in antagonist conformation, due to the constraints introduced by the CDA group, can have a marked effect on binding affinity. An additional possibility exists that the activity and selectivity of **35**- β may be dictated by the hydrophobic pocket created by the Leu and Phe interactions as confirmed by NMR spectroscopy and molecular modeling.

The sugar-based $\alpha 4\beta 7$ antagonist **35**- β , which was derived from structural requirements in the natural ligand MAdCAM-1 and in active and selective peptides, can be considered as a new lead structure for rational combinatorial development of anti-inflammatory drugs (Figure 5-9).

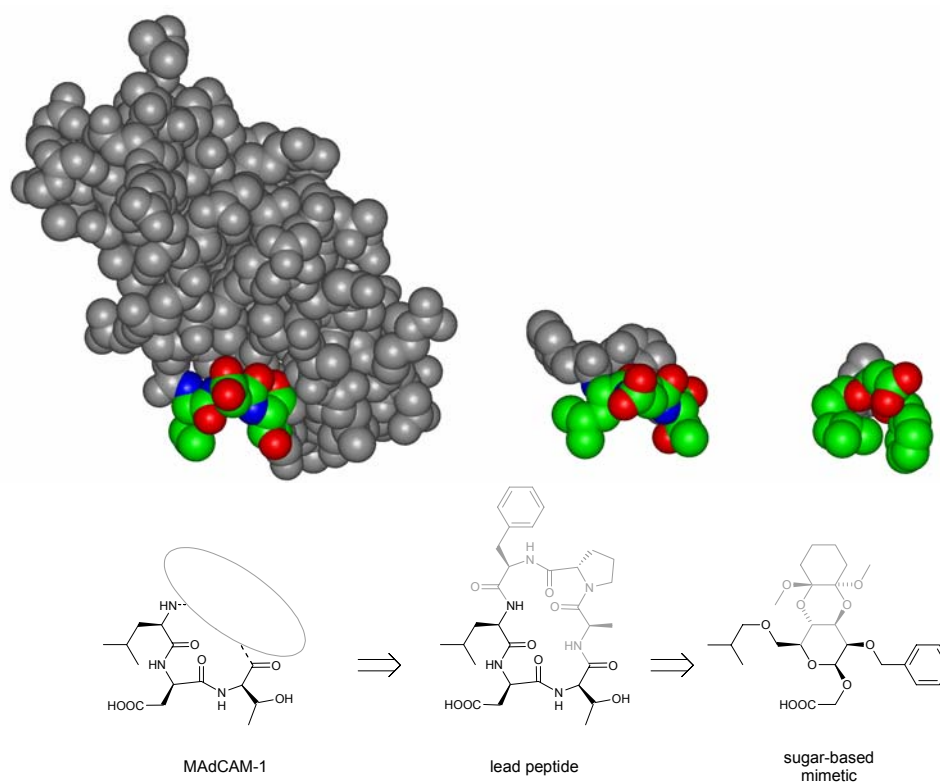
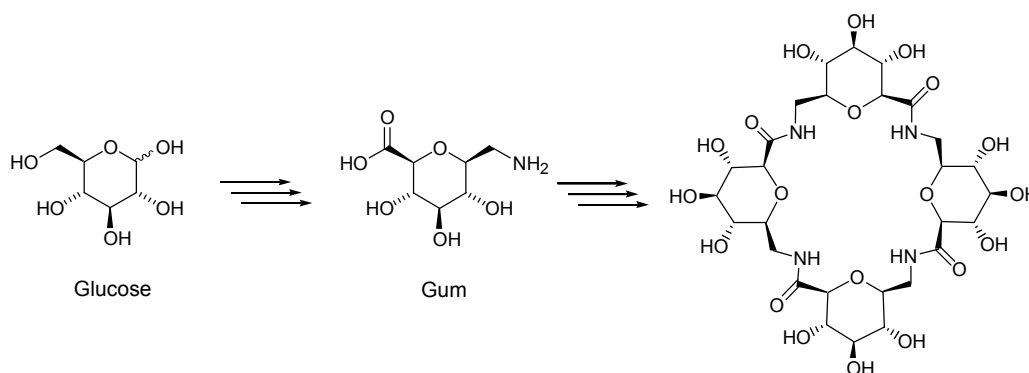


Figure 5-9: From proteins to sugar-based small molecules: development of an $\alpha 4\beta 7$ antagonist.

6 Summary

In this work we presented the straightforward synthesis of water soluble materials possessing functional groups with well-defined secondary structure. Our approach involves the use of *Glucosyluronic acid methylamine* (Gum) as repetitive unit. The design and synthesis of this sugar amino acid was previously reported by our laboratories.⁴ By exploiting standard solid and solution phase coupling procedures, linear and cyclic homo-oligomers containing *Glucosyluronic acid methylamine* (Gum) were synthesized.¹⁶ We achieved high yield and very short coupling time for the oligomerization and cyclization of sequences encompassing 2,3,4 and 6 Gum units. To the best of our knowledge, the synthesis of cyclic oligomers containing only SAAs as repetitive units have not been reported before our contributions.^{15,16} Furthermore, our synthetic protocol did not require any orthogonal protection of the hydroxyl groups which speeded up the synthesis of the building block and the oligomerization. Conformational preferences in water solution for the cyclic analogues based upon ¹H-¹H vicinal scalar correlations, ROE data and molecular modeling as well as their applications as potential host molecules were discussed.



Two low energy structures were found for the Gum residue, which differ in the relative orientation (*syn* or *anti*) of the C-H⁵ and C=O bonds. The molecular structure of the cyclic oligomers in the all-*syn* conformation generates a hydrophilic exterior surface and a nonpolar interior cavity which resemble the cyclodextrin molecular shape. However, the all-*anti* conformation leads to a flat structure. Here the characteristic sequence of alternating ether and amide linkages arranged in a symmetrical array, is clearly reminiscent of macrocyclic chelating agents. Through ROE analysis the *syn* and *anti* population for the Gum residue was estimated.

Benzoic acid and *p*-nitrophenol were chosen as model guest molecules to study the formation of cyclodextrin-like inclusion complexes. The complexation behavior of the cyclic hexamer was proved from three different points of view: chemical shifts, longitudinal relaxations (T_1) and diffusion coefficients. All of them showed different values for host and guest molecules measured independently and in the presence of each other. Specifically, the decrease in T_1 and diffusion value of the guest molecules in the presence of the cyclic hexamer is reminiscent of the host-guest chemistry.

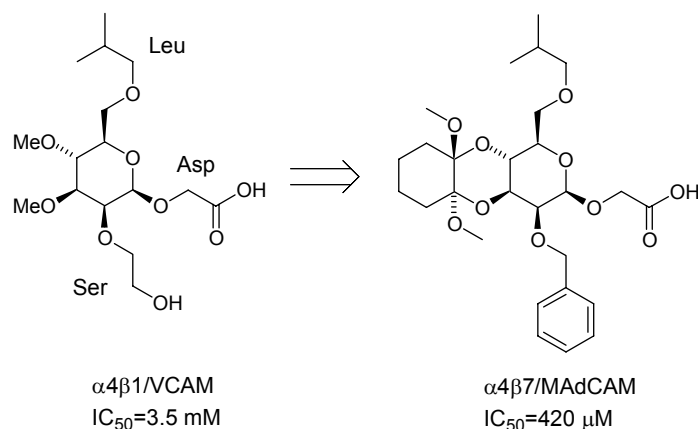
There are considerable implications of linking sugar moieties in natural carbohydrates through amide bonds. Specifically, we can take advantage of a very well established peptide solid phase chemistry which can bring to peptide-carbohydrate chimeras and to the extension to combinatorial chemistry. Cyclodextrins, in their native state, are rigid molecules and offer limited utility in term of size, shape, and availability of chemically useful functionalities. Our synthetic protocol offers an attractive alternative towards the existing methods for selective modifications of cyclodextrins.¹⁵⁹ The synthesis and characterization of cyclic peptides containing sugar amino acids and natural amino acids is an ongoing project in our laboratory.¹²⁴ The replacement of the glycosidic linkage by the amide group allows also a more detailed structure elucidation *via* NMR through the NH-CH dipolar relaxation. The amide bond might itself participate in the binding as chelating group. The results of this study are encouraging from the perspective of preparing easily accessible materials for drug delivery. The possibility of choosing different ring-sizes and consequently the number of chelating groups has led to the idea that this class of cyclic oligomers might represent versatile tools for ligand binding and molecular recognition.

Interfering protein-protein interaction by small non-peptidic molecules is one of the great challenges in medicinal chemistry. Based on a D-mannose core we developed in a rational combinatorial approach a selective inhibitor of the $\alpha 4\beta 7$ /MAdCAM interaction.

The biased library of mannose peptidomimetics originated from an inhibitor of the $\alpha 4\beta 1$ /VCAM interaction previously developed in our laboratory. In our strategy, we maintained the original mannose core and the Leu and Asp pharmacophores at 6 and 1-positions of the sugar ring, respectively, occurring in the binding motif of $\alpha 4$ natural

ligands. A spatial screening for the Asp pharmacophore was carried out by measuring the activity for both, α and β , anomers.

The Ser side chain at position 2 was replaced by the Phe side chain. Aromatic residues were introduced at 3 and 4-positions to increase hydrophobicity of the mannose peptidomimetics. The mannose scaffold was rigidified by a trans ring fusion between a dioxane ring and the pyranoside at 3 and 4-positions. The length, polarity and conformational space available to the Leu side chain was modified by carbon-carbon linkage. At last, the metabolic stability of the mannose derivatives was improved by introducing the Asp side chain at the anomeric position through a C-glycosidic linkage.



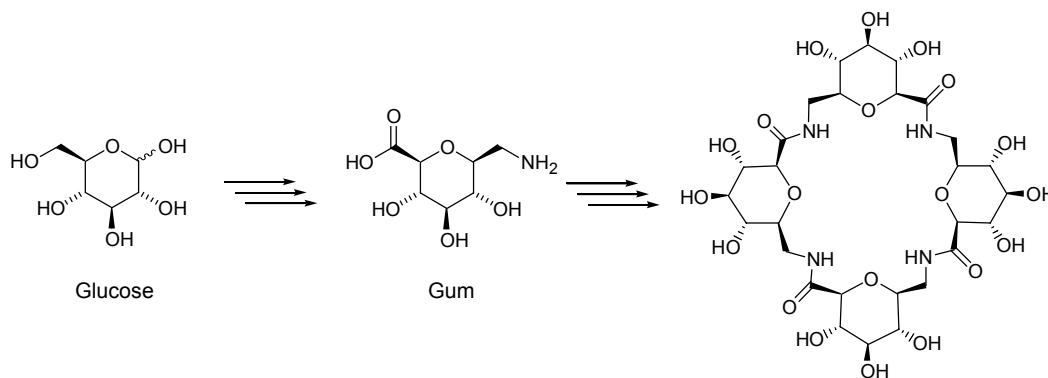
SAR studies reconfirmed the β orientation of the Asp side chain to be necessary for activity. The basis for affinity and selectivity towards the $\alpha 4\beta 7/\text{MAdCAM}$ interaction is likely to be the hydrophobic pocket formed by the Leu and Phe pharmacophores together with the conformational restraints introduced by the cyclohexane-1,2-diacetal group (CDA) at 3 and 4 positions. Besides, the mannose-based antagonist mimics the conformation in solution of $\alpha 4\beta 7$ selective cyclic peptides, previously developed in our group. Furthermore, antagonist **35**- β exhibits a $-1 < \log P > 5$ ($\log P = 3.35$) which is one requirement for orally availability according to Lipinski *et al.*¹⁹³ In conclusion, this class of peptidomimetics overcomes the limitations of peptidic drugs, generally associated with mediocre absorption and poor metabolic stability amongst other factors, and represents a promising candidate for drug development.

7 Zusammenfassung

Das erste Ziel dieser Arbeit war das Design und die Synthese von cyclischen, homooligomeren Zuckeraminosäuren (SAAs, Sugar Amino Acids) als Cyclodextrinmimetika.

Als monomere Einheit für die Synthese von homooligomeren Zuckeraminosäuren diente Glucuronsäuremethylamin (Gum). Ausgehend von α,β -D-Glucose wurde Gum in vier Schritten dargestellt. Die Methylaminfunktion des Gum-Bausteins wurde über eine nukleophile Aldolreaktion der Glucose mit Nitromethan, anschließender intramolekularer Michaeladdition und darauffolgender Reduktion der Nitrogruppe eingeführt. Anschließend wurde durch selektive TEMPO-Oxidation die primäre Hydroxylgruppe an Position 6 der Glucose zu dem entsprechenden Carboxylat funktionalisiert.

Die Oligomerisierung des Gum-Bausteins konnte an fester Phase nach der Fmoc-Strategie verwirklicht werden. Sowohl die Kupplung der einzelnen Monomeren als auch die Cyclisierung wurden ohne Schutzgruppen für die freien Hydroxylfunktionen der SAAs unter HATU/HOAt Aktivierung durchgeführt. Nach diesem Verfahren gelang die Synthese der cyclischen di-, tri-, tetra- und hexameren SAAs.

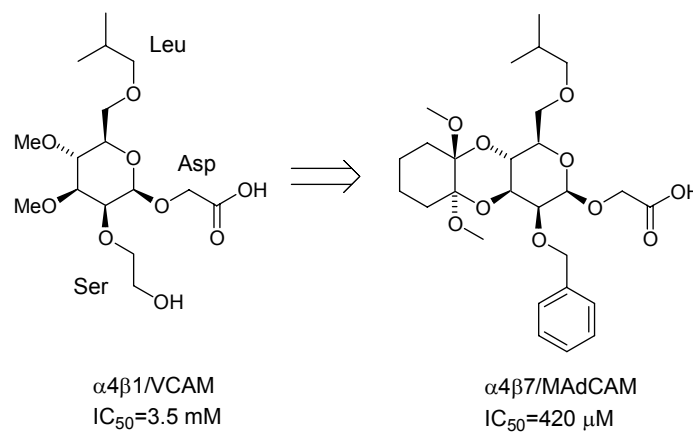


Die cyclischen Gum-Oligomere wurden auf der Basis von NMR-spektroskopischen Untersuchungen und Modellierungstudien als Mimetika für Cyclodextrine vorgeschlagen. Die Fähigkeit der cyclischen, homooligomeren Zuckeraminosäuren Wirt-Gast-Verbindungen zu bilden wurde mit Hilfe von NMR-spektroskopischen Methoden demonstriert.

Die Synthese von nicht-peptidischen $\alpha 4$ -Integrinantagonisten auf der Basis von Monosacchariden bildete den zweiten Schwerpunkt dieser Arbeit.

Die $\alpha 4$ -Integrine, $\alpha 4\beta 1$ und $\alpha 4\beta 7$, spielen zusammen mit ihren endogenen Liganden Fibronectin, VCAM-1 und MAdCAM-1 bei einer Vielzahl pathologischer Vorgänge wie chronischen Entzündungen und Autoimmunerkrankungen eine entscheidende Rolle. $\alpha 4$ -Integrine erkennen in ihren Liganden die Aminosäuresequenzen Leu-Asp-Thr (LDT), Leu-Asp-Val (LDV) und Ile-Asp-Ser (IDS).

Basierend auf einem β -D-Mannosegerüst wurde in dieser Arbeit in einem rational-kombinatorischen Ansatz ein selektiver Antagonist der $\alpha 4\beta 7$ /MAdCAM-1 Wechselwirkung entwickelt.



Dabei wurde ausgehend von einem in unserer Gruppe erst kürzlich publizierten Inhibitor der VCAM/ $\alpha 4\beta 1$ Wechselwirkung eine Bibliothek von Mannosiden synthetisiert. Bei dem Design dieser Bibliothek wurde das ursprüngliche Gerüst sowie das Leucin- als auch Aspartatpharmakophor an den Positionen 6 bzw. 1 des Zuckers beibehalten. Ein räumliches Screening des Aspartatpharmakophors wurde durch Vergleich der Aktivität der α - und β -Anomeren durchgeführt. Die Serinfunktion an Position 2, von der bekannt ist, dass sie nicht relevant für Aktivität ist, wurde durch eine Phenylalaninseitenkette ersetzt. In den Positionen 3 und 4 wurden aromatische Reste eingeführt um die Hydrophobizität der Peptidomimetika zu erhöhen. Zusätzlich wurde die Flexibilität des Mannosegerüst durch eine *trans*-Ringfusion zwischen einem Dioxanring und dem Pyranosid an Position 3 und 4 eingeschränkt. Über eine C-C Bindung wurde die Länge, die Polarität und der konformationelle Raum der Leucinseitenkette an Position 6 modifiziert. Darüber hinaus wurde die metabolische

Stabilität der Mannosederivate durch Einführung der Aspartatseitenkette am anomeren Zentrum über eine C-glycosidische Bindung erhöht.

In SAR-Studien konnte bestätigt werden, dass die β -Orientierung des anomeren Zentrums für die Aktivität der Peptidomimetika essentiell ist. Es zeigte sich, dass die Ursache für die Affinität und Selektivität gegenüber der $\alpha 4\beta 7$ /MAdCAM-1 Wechselwirkung eine hydrophobe Tasche ist, die durch das Leucinmimetikum an Position 6 und die Phenylalaninseitenkette an Position 2 zusammen mit der konformationellen Versteifung des Mannosegerüst durch die Einführung des Cyclohexan-1,2-diacetals (CDA) an den Positionen 3 und 4 ausgebildet wird.

Aufgrund dieser Studien konnte ein aktiver und selektiver nicht-peptidischer $\alpha 4\beta 7$ Inhibitor identifiziert werden, der das Leu-Asp Motiv enthält, von dem bekannt ist, dass es eine entscheidende Rolle bei der Wechselwirkung von MAdCAM-1 und Fibronectin mit $\alpha 4\beta 7$ Integrinen spielt. Darüber hinaus mimiken die auf Mannose basierenden Peptidomimetika die Konformation eines aktiven, $\alpha 4\beta 7$ -selektiven cyclischen Peptids, das kürzlich in unserer Gruppe entwickelt wurde. Der log P des **35**- β Inhibitors liegt mit einem Wert von $\log P = 3.35$ zwischen $-1 < \log P > 5$ und erfüllt somit eine wesentlichen Anforderung der Lipinski-Regeln¹⁹³ für orale Bioverfügbarkeit. Diese Klasse von Peptidomimetika überwindet die bekannten Nachteile peptidischer Verbindungen in Bezug auf ihre Anwendung als Arzneimittel und ist daher sehr vielversprechend für die Wirkstoffentwicklung.

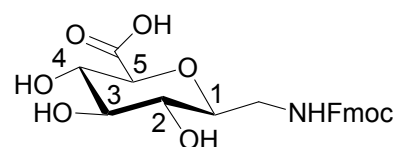
8 Experimental Section

8.1 General methods

All chemicals were used as supplied without further purification. All organic solvents were distilled before use. For solid-phase synthesis TCP resin was bought from PepChem Goldammer & Clausen (Tübingen, Germany), and HATU, HOAT from Perseptive Biosystems (Warrington, England). Pd/C was donated by Degussa (Frankfurt/M., Germany). RP-HPLC analysis and semiscale preparations were carried out on a Waters (high pressure pump 510, multiwavelength detector 490E, chromatography workstation Maxima 820), Beckman (high pressure pump 110B, gradient mixer, controller 420, UV detector Uvicord from Knauer), Amersham Pharmacia Biotech (Äkta Basic 10/100, autosampler A-900). RP-HPLC preparative separations were carried out on Beckman System Gold (high pressure pump modul 126, UV detector 166). C₁₈-columns were used. Solvents: A: H₂O + 0.1% CF₃COOH and B: CH₃CN + 0.1% CF₃COOH with UV detection at 220 and 254 nm. HPLC-ESI mass spectra were recorded on Finnigan NCQ-ESI with HPLC conjunction LCQ (HPLC-system Hewlett Packard HP 1100, Nucleosil 100 5C₁₈).

8.2 Synthesis of the oligomers containing Gum

8.2.1 Synthesis of the Fmoc-Gum-OH building block (16)



Anhydrous glucose (250 g, 1.39 mol) was dissolved in abs. DMSO (1 L) in a 10 L Erlenmeyer flask and abs. MeOH (500 mL) was added. Subsequently abs. nitromethane (500 mL) and a solution of sodium (62.5 g) in abs. MeOH (1750 mL) was added and the mixture was stirred for at least 24h at room temperature. (The mixture warms up in the beginning and solid material starts to precipitate.) *n*-Butanol (1250 mL) was added and the mixture was stirred for 1h at 0 °C. The solid material was filtered off with a sintered glass filter (G3, diameter 20 - 25cm) under slight suction and washed with 2-propanol (500 mL) and diethyl ether (500 mL). The residue

was dried by suction to give large quantities of a slightly yellow powder which contains the intermediate and non reacted glucose (all TLC were performed on silica gel 60, mobile phase CH₃CN/H₂O 4:1). The powder was dissolved in dest. water (1 L) and applied onto a column (10 x 30 cm) of cation exchange resin (1 kg, Amberlite IR-120, H⁺-form, thoroughly washed with MeOH and dest. H₂O before using!). The resin is eluted with dest. water (2.5 L). The red aqueous solution was concentrated under reduced pressure to 1 L and heated for 30 h at 90 °C. The cooled solution was given over a column (10 x 50 cm) with anion exchange resin (2 kg; Amberlite IRA-120, OH⁻-form, anion exchange resin was conditioned before use with 5 N NaOH (2 L) and washed thoroughly with dest. water). The column was as long eluted with dest. water (ca. 25 L dest. water) until no glucose was anymore detectable by TLC. The product was then eluted with water saturated with CO₂ (dry ice was constantly added onto the column) and the fractions with the product was collected (ca. 15 L, TLC control, don't be fooled by the color of the eluate). The water was removed under reduced pressure and the residue was five times coevaporated with toluene. The residue was recrystallized from MeOH (dissolved in minimum boiling MeOH and crystallize at 0 °C overnight). 72 g (23.2% yield, referring to the used glucose) crude product which contains 25% α-product (α- and β-product are not separable by preparative TLC, determination by ¹H NMR in D₂O). By two further recrystallization steps from MeOH three fractions of product were obtained: 31 g (10.0% yield, ca. 2% α-side product), 11 g (3.4% yield, ca. 25% α-product), 28 g (9.0% yield, ca. 50% α-product). In every crystallization step the amount of the α-side product is lowered by ca. 70% while about 25% to 40% of the material stays in the mother liquor.

β-D-Glucopyranosylnitromethane (16 g, 50 mmol, 2% α) was dissolved in a mixture of water (50 mL) and MeOH (100 mL). Pd/C catalyst (2.5 g, 5% Pd, 50% water, Degussa, Frankfurt) was added, and the solution was hydrogenated with H₂ (45 bar pressure) in a 0.5 L autoclave under stirring for 20 h at room temperature. (Hydrogenation at atmospheric pressure is also feasible, but takes app. 3 d). After the reaction was finished (TLC control) the catalyst was filtered off. Water (150 mL) was added to the filtrate and the MeOH was removed under reduced pressure. In the aqueous solution of β-D-glucopyranosylmethylamine, NaHCO₃ (15.04 g, 60mmol) was dissolved and THF (200 mL) was added. The solution was cooled to 0 °C and a

solution of Fmoc-Cl (14.3 g, 55 mmol) in THF (100 mL) was added and stirred for 30 min. at 0 °C. After completion of the reaction (TLC control), 24 g cation exchange resin (Amberlyst 15, H⁺-form, Fluka) was added and the solution stirred for 10 min. The cation exchange resin was filtered off and washed with ethanol. Water (200 mL) was added to the filtrate and all the organic solvents were removed under reduced pressure. The product was precipitated and the mixture was cooled to 4 °C. The product was filtered off, washed with a little amount of water and with n-hexane (200 mL) and dried in vacuum (19.60 g, 94%). The powder (25.4 mmol) and 2,2,6,6-tetra-methyl-1-piperidinyloxy (TEMPO) (50 mg) were suspended in water (500 mL). A small amount of THF and tetrabutylammonium bromide (TBAB) was added so that a clear solution was obtained. The solution was cooled to 0 °C and the pH was monitored with a pH meter during the reaction. An aqueous sodium hypochlorite solution (50 mL, 12%) was added dropwise under stirring so that the pH never exceeds 10. When all the NaOCl solution was added the pH 10 was adjusted by dropwise adding 1N NaOH. The reaction was finished when pH 10 was stable without any further addition of 1N NaOH (TLC-control). Then cation exchange resin (Amberlyst 15, H⁺-form, Fluka) was added until the pH was 1.5. The resin was filtered off and washed with water. The product was extracted from the filtrate seven times with ethyl acetate (50 mL). The combined organic phases were washed with saturated NaCl solution (50 mL) and twice with water (50 mL). The organic solution was not dried with inorganic salts. The ethyl acetate was removed under reduced pressure and the product was coevaporated with toluene. By treating the resulted syrup with diethyl ether the product crystallized. The colorless product was collected and washed with diethyl ether and n-pentane and dried in vacuum (8.71 g , 20.3 mmol, 81%).

¹H-NMR (500 MHz, DMSO-d₆, 300 K): δ = 7.88 (d, J = 7.3 Hz, 2H), 7.69 (d, J = 7.3 Hz, 2H), 7.40 (t, J = 7.6 Hz, 2H), 7.32 (t, J = 7.6 Hz, 2H), 4.29-4.19 (m, 3H), 3.52-3.44 (m, 2H), 3.26 (t, J = 9.4 Hz, 1H), 3.20-3.13 (m, 2H), 3.03-2.92 (m, 2H).

Assignment: δ = 7.88, 7.69, 7.40, 7.32 (Fmoc, arom.), 7.32 (NH), 4.25 (Fmoc, CH₂), 4.22 (Fmoc, CH), 3.49 (CH₂), 3.47 (H⁵), 3.26 (H⁴), 3.17 (H¹), 3.16 (H³), 2.99 (CH₂), 2.96 (H²).

^{13}C -NMR (125 MHz, DMSO- d_6 , 300 K): δ = 127.30, 126.80, 124.93, 119.82 (Fmoc, arom.), 79.03 (C^5), 78.70 (C^1), 77.32 (C^3), 71.65 (C^4), 71.32 (C^2), 65.48 (Fmoc, $\underline{\text{C}}\text{H}_2$), 46.42 (Fmoc, $\underline{\text{C}}\text{H}$), 42.07 ($\underline{\text{C}}\text{H}_2$).

ESI-MS: m/z : 430.0 [$\text{M}+\text{H}^+$], MW calcd. for $\text{C}_{22}\text{H}_{23}\text{NO}_8$: 429.4.

8.2.2 Oligomerization on solid phase

The Gum oligomer assembly *via* Fmoc chemistry was performed manually (0.25 mmol scale, 2.5 mL wash volumes) starting from TCP resin (1 mmol/g, 250 mg). The first Fmoc-Gum-OH (1.3 equiv.) was attached to the resin with 1,3,5-collidine (10 equiv.) in 2.5 mL DMF (1 \times 4 h), followed by washing with DMF (6 \times 1 min). Fmoc removal on resin was accomplished with 20 vol % piperidine/DMF (2 \times 10 min), followed by washing with DMF (6 \times 1 min). Successive Fmoc-Gum-OH building blocks (1 equiv.) were coupled with HATU (1 equiv.), HOAt (1 equiv.) reagents and 1,3,5-collidine (10 equiv.) (1 \times 3 h). Each coupling was followed by washing with DMF (6 \times 1 min) and Fmoc removal as described above. Cleavage from the resin was done using a mixture of DCM/TFE/AcOH (3:1:1, 2 \times 1 h). The solid support was washed with DMF or DMSO (6 \times 1 min) and the solvent vacuum distilled at 303-308 K. The white-yellowish residue was dissolved in water and purified *via* RP-HPLC (40-50 %).

8.2.3 Cyclization of the linear sequences

Method 1: Cyclization with DPPA. The linear oligomer was dissolved in DMF (0.1 mM) in the presence of DPPA (3 equiv.) and NaHCO_3 (5 equiv.) and the solution stirred at RT for 16 h. Successively, NaHCO_3 was filtered off, excess DPPA was hydrolyzed by addition of a few drops of H_2O and the solution was concentrated in vacuum. The residue, after RP-HPLC purification, was dissolved in *t*BuOH (or dioxane)/ H_2O and lyophilized (< 10 %).

Method 2: Cyclization with DIC/HOAt. The linear compound was dissolved in a mixture of DMF and DCM (1:1 v/v, 0.1 mM), treated with HOAt (1 equiv.), NMM (3 equiv.), and DIC (10 equiv.) at 273K and stirred at this temperature for 16 h. Excess DIC was hydrolyzed by addition of H₂O and the solution was concentrated. The residue, after RP-HPLC purification, was dissolved in *t*BuOH (or dioxane)/H₂O and lyophilized (< 10 %).

Method 3: Cyclization with HATU/HOAt. The linear oligomer was dissolved in DMF (0.1 mM), treated with HATU (1 equiv.), HOAt (1 equiv.) and 1,3,5-collidine (10 equiv.). The solution was stirred at RT for 6 h. The cyclization was monitored *via* analytical HPLC. Upon completion of the reaction, the solvent was removed. The residue, after RP-HPLC purification, was dissolved in *t*BuOH (or dioxane)/H₂O and lyophilized (35 % for n = 2, 60 % for n = 3 and > 90 % for n = 4,6).

8.2.4 Synthesis of H-[Gum]₂-OH (17)

The synthesis of the dimer was carried out as outlined in section 8.2.2.

¹H-NMR (500 MHz, H₂O/D₂O, 293 K): δ = 8.36 (t, J = 6 Hz, 1H), 7.83 (br s, 1H), 3.94-3.88 (m, 2H), 3.71-3.60 (m, 2H), 3.56-3.41 (m, 7H), 3.38-3.26 (m, 2H), 3.15 (br s, 1H).

ESI-MS: *m/z*: 397.2 [M+H⁺], MW calcd. for C₁₄H₂₄N₂O₁₁: 396.1.

8.2.5 Synthesis of *cyclo*[-Gum₂-] (18)

The linear dimer was cyclized as described in section 8.2.3 (Method 3).

¹H-NMR (500 MHz, H₂O/D₂O, 293 K): δ = 7.86 (d, J = 9.8 Hz, 2H), 3.97-3.84 (m, 4H), 3.80 (d, J = 9.5 Hz, 2H), 3.65 (t, J = 9.2 Hz, 2H), 3.58-3.46 (m, 6H).

Assignment: δ = 7.86 (NH), 3.93 (H⁴), 3.88 (CH₂, proS), 3.80 (H⁵), 3.65 (H³), 3.53 (H¹), 3.51 (H²), 3.50 (CH₂, proR).

^{13}C -NMR (125 MHz, $\text{H}_2\text{O}/\text{D}_2\text{O}$, 293 K): $\delta = 80.25$ (C^5), 78.08 (C^3), 77.87 (C^1), 73.81 (C^2), 69.75 (C^4), 43.29 ($\underline{\text{C}}\text{H}_2$).

ESI-MS: m/z : 379.2 [$\text{M}+\text{H}^+$], MW calcd. for $\text{C}_{14}\text{H}_{22}\text{N}_2\text{O}_{10}$: 378.1.

8.2.6 Synthesis of H-[Gum]₃-OH (19)

The synthesis of the trimer was carried out as outlined in section 8.2.2.

^1H -NMR (500 MHz, $\text{H}_2\text{O}/\text{D}_2\text{O}$, 293 K): $\delta = 8.36$ (t, $J = 6$ Hz, 1H), 8.31 (t, $J = 6$ Hz, 1H), 7.83 (br s, 1H), 3.94-3.88 (m, 2H), 3.84 (d, $J = 9.3$ Hz, 1H), 3.71-3.60 (m, 3H), 3.56-3.41 (m, 11H), 3.38-3.26 (m, 3H), 3.15 (br s, 1H).

ESI-MS: m/z : 586.4 [$\text{M}+\text{H}^+$], MW calcd. for $\text{C}_{21}\text{H}_{35}\text{N}_3\text{O}_{16}$: 585.5.

8.2.7 Synthesis of *cyclo*[-Gum₃-] (20)

The linear trimer was cyclized as described in section 8.2.3 (Method 3).

^1H -NMR (500 MHz, $\text{H}_2\text{O}/\text{D}_2\text{O}$, 293 K): $\delta = 8.17$ (t, $J = 6$ Hz, 3H), 3.84 (d, $J = 9.5$ Hz, 3H), 3.63 (m, 3H), 3.60-3.47 (m, 12H), 3.27 (t, $J = 9.0$ Hz, 3H).

Assignment: $\delta = 8.17$ ($\underline{\text{N}}\text{H}$), 3.84 (H^5), 3.63 ($\underline{\text{C}}\text{H}_2$), 3.57 ($\underline{\text{C}}\text{H}_2$), 3.56 (H^1), 3.54 (H^3), 3.49 (H^4), 3.26 (H^2).

^{13}C -NMR (125 MHz, $\text{H}_2\text{O}/\text{D}_2\text{O}$, 293 K): $\delta = 78.03$ (C^5), 77.60 (C^1), 77.05 (C^3), 72.53 (C^4), 71.00 (C^2), 39.95 ($\underline{\text{C}}\text{H}_2$).

ESI-MS: m/z : 568.3 [$\text{M}+\text{H}^+$], MW calcd. for $\text{C}_{21}\text{H}_{33}\text{N}_3\text{O}_{15}$: 567.2.

8.2.8 Synthesis of H-[Gum]₄-OH (21)

The synthesis of the tetramer was carried out as outlined in section 8.2.2.

$^1\text{H-NMR}$ (500 MHz, $\text{H}_2\text{O}/\text{D}_2\text{O}$, 293 K): $\delta = 8.36$ (t, $J = 6$ Hz, 1H), 8.34-8.26 (m, 2H), 7.83 (br s, 1H), 3.94-3.88 (m, 2H), 3.84 (d, $J = 9.3$ Hz, 2H), 3.71-3.60 (m, 4H), 3.56-3.41 (m, 15H), 3.38-3.26 (m, 4H), 3.15 (br s, 1H).

ESI-MS: m/z : 775.5 [$\text{M}+\text{H}^+$], MW calcd. for $\text{C}_{28}\text{H}_{46}\text{N}_4\text{O}_{21}$: 774.3.

8.2.9 Synthesis of *cyclo*[-Gum₄-] (22)

The linear tetramer was cyclized as described in section 8.2.3 (Method 3).

$^1\text{H-NMR}$ (500 MHz, $\text{H}_2\text{O}/\text{D}_2\text{O}$, 293 K): $\delta = 8.27$ (t, $J = 6$ Hz, 4H), 3.84 (d, $J = 9.4$ Hz, 4H), 3.72 (dd, $J = 13.2$ and 6 Hz, 4H), 3.56-3.44 (m, 16H), 3.31 (t, $J = 9.2$ Hz, 4H).

Assignment: $\delta = 8.27$ (NH), 3.84 (H^5), 3.72 (CH_2), 3.51 (H^1), 3.52 ($\text{H}^{3,4}$), 3.49 (CH_2), 3.31 (H^2).

$^{13}\text{C-NMR}$ (125 MHz, $\text{H}_2\text{O}/\text{D}_2\text{O}$, 293 K): $\delta = 78.84$ (C^5), 78.38 (C^1), 77.01 (C^3), 72.23 (C^4), 70.96 (C^2), 40.29 (CH_2).

ESI-MS: m/z : 757.4 [$\text{M}+\text{H}^+$], MW calcd. for $\text{C}_{28}\text{H}_{44}\text{N}_4\text{O}_{20}$: 756.3.

8.2.10 Synthesis of H-[Gum]₆-OH (23)

The synthesis of the hexamer was carried out as outlined in section 8.2.2.

$^1\text{H-NMR}$ (500 MHz, $\text{H}_2\text{O}/\text{D}_2\text{O}$, 293 K): $\delta = 8.36$ (t, $J = 6$ Hz, 1H), 8.34-8.26 (m, 4H), 7.83 (br s, 1H), 3.94-3.88 (m, 2H), 3.84 (d, $J = 9.3$ Hz, 4H), 3.71-3.60 (m, 6H), 3.56-3.41 (m, 23H), 3.38-3.26 (m, 6H), 3.15 (br s, 1H).

ESI-MS: m/z : 1153.8 [$\text{M}+\text{H}^+$], MW calcd. for $\text{C}_{42}\text{H}_{68}\text{N}_6\text{O}_{31}$: 1153.0.

8.2.11 Synthesis of cyclo[-Gum₆-] (24)

The linear hexamer was cyclized as described in section 8.2.3 (Method 3).

¹H-NMR (500 MHz, H₂O/D₂O, 293 K): δ = 8.30 (t, J = 6 Hz, 6H), 3.84 (d, J = 9.3 Hz, 6H), 3.68 (dd, J = 13.2 and 6 Hz, 6H), 3.56-3.44 (m, 24H), 3.30 (t, J = 9.2 Hz, 6H).

Assignment: δ = 8.30 (NH), 3.84 (H⁵), 3.68 (CH₂), 3.52 (H¹), 3.51 (H^{3,4}), 3.49 (CH₂), 3.30 (H²); ¹³C-NMR (125 MHz, H₂O/D₂O, 293 K): δ = 78.82 (C⁵), 78.11 (C¹), 77.08 (C³), 72.19 (C⁴), 70.90 (C²), 40.34 (CH₂).

ESI-MS: *m/z*: 1135.6 [M+H⁺], MW calcd. for C₄₂H₆₆N₆O₃₀: 1134.4.

8.3 Synthesis of individual mannose-based compounds

8.3.1 General procedure for Williamson ether synthesis

To DMSO (15 mL) powdered KOH was added (20 mmol per replaceable hydrogen of substrate). After stirring for 10 min, the substrate alcohol (1 mmol) was added, followed immediately by the alkyl halide (10 mmol per replaceable hydrogen of substrate). Stirring was continued until completion of the reaction, followed by TLC, after which the mixture was poured into water (20 mL) and extracted with diethylether or dichloromethane (3 x 20 mL). The combined organic extracts were washed with water (5 x 10 mL), dried with NaSO₄ and the solvents removed under reduced pressure. The residue was purified by flash column chromatography (gradient elution: hexane/EtOAc 9:1 to hexane/EtOAc 4:1) to give the title compounds in 70-95 %.

8.3.2 General procedure for the SET cleavage of ethyl-1-thio- α -D-mannopyranoside

The ethyl-1-thio- α -D-mannopyranoside substrate (4 mmol) was dissolved in 60 mL CH₃CN/H₂O 2:1 solution. At RT *N*-bromosuccinimide (8 mmol) and 1 mL conc. HCl were added. The solution was stirred for 3 hours until completion of the reaction, followed by TLC, after which CH₃CN was evaporated and the residue was extracted with dichloromethane (3 x 20 mL). The combined organic extracts were dried with Na₂SO₄, evaporated and the residue purified by flash column chromatography (gradient elution: hexane/EtOAc 5:1 to hexane/EtOAc 2:1) to give the title compounds in 90-95 %.

8.3.3 General procedure for the synthesis of mannosyl chloride

The α,β -D-mannopyranoside mixture (4 mmol) resulted in section 8.3.2 was dissolved at RT in pure thionyl chloride (10 mL) and stirred for about 2 hours. After this time the solution was evaporated and the residue was used immediately as glycosyl donor in a Koenigs-Knorr type reaction.

8.3.4 General procedure for the synthesis of mannosyl bromide

A solution of ethyl-1-thio- α -D-mannopyranoside substrate (1 mmol) in 10 mL of dried dichloromethane was treated with bromine (53 μ L, 164 mg, 1 mmol) at 0 °C for 10-15 min. The solution was then successively washed with ice-cold, 10 % aqueous NaHSO₃ and water, dried (Na₂SO₄), and concentrated. The residue was used immediately as glycosyl donor in a Koenigs-Knorr type reaction.

8.3.5 General procedure for α -O-glycosidic linkage formation

A solution of the ethyl-1-thio- α -D-mannopyranoside substrate (1 mmol) and alcohol (3 mmol), which were previously rotoevaporated with toluene and dried under vacuum, in dry dichloromethane (10 mL) containing freshly activated 4-Å molecular sieves (2 g) was treated with *N*-iodosuccinimide (1.2 mmol), followed by a solution of silver trifluoromethanesulfonate (1.2 mmol) in 1 mL of dry toluene. The reaction was essentially complete (as judged by TLC) after the addition of the triflate. The mixture was then diluted with CH₂Cl₂ and filtered. The filtrate was washed with 10 % aqueous sodium thiosulfate, saturated aqueous sodium bicarbonate, and brine. The solution was dried (Na₂SO₄) and concentrated to an oil that was flash chromatographed on silica gel (gradient elution: hexane/EtOAc 4:1 to hexane/EtOAc 1:1) to give the title compounds in 75-85 % yield as α/β mixture 6:1.

8.3.6 General procedure for β -O-glycosidic linkage formation

Solid Ag₂CO₃ (6 mmol) was added at 0 °C to a solution of mannosyl bromide or chloride (3 mmol), the specified glycosyl acceptor (10 mmol), 4-Å molecular sieves (2 g) and 10 mL of dichloromethane, previously stirred at RT for 1 hour. Stirring was continued overnight in the dark. Successively, the mixture was filtered through celite and concentrated. The residue was purified by flash column chromatography (gradient elution: hexane/EtOAc 5:1 to hexane/EtOAc 2:1) to give the title compounds in 70-75 % yield as α/β mixture 1:5.

8.3.7 General procedure for primary alcohol oxidation to aldehyde

A solution of 2,3,4 protected ethyl-1-thio- α -D-mannopyranoside (0.6 mmol) and Et₃N (380 μ L, 2.72 mmol) in CH₂Cl₂-DMSO (3:1, 12 mL) was cooled to 0 °C and treated with sulfur trioxide pyridine complex (344 mg, 2.16 mmol). After being stirred at 0 °C for 30 min, the mixture was diluted with CH₂Cl₂ (100 mL), washed with H₂O (2 x), and brine, dried (Na₂SO₄), and concentrated to give crude aldehyde, which was used in the following reaction without purification.

8.3.8 General procedure for the synthesis of the phosphonium salt

A solution of triphenylphosphine (10 mmol) and the alkyl halide (10 mmol) in dry toluene (20 mL) was heated under reflux for 24 hours. After this time the mixture was cooled with ice and filtrated. The white precipitate was washed with cold toluene, dried under vacuum and used immediately.

8.3.9 General procedure for Wittig olefination of sugar aldehyde

A mixture of the phosphonium salt (0.5 mmol) obtained in 8.3.8, activated 4-Å powdered molecular sieves (480 mg), and anhydrous toluene (5 mL) was cooled to –10 °C. To this suspension was added potassium bistrimethylsilylamide (1 mL of 0.5 M solution in toluene, 0.5 mmol) as base, followed by the aldehyde (0.5 mmol) obtained in 8.3.7 dissolved in anhydrous toluene (2 mL). The suspension was allowed to slowly warm to room temperature (about 3 hours), maintained for an additional 30 min at room temperature, and then filtered through celite. The solvent was evaporated and the residue dissolved in CH₂Cl₂. The organic layer was washed with water (10 mL), dried (Na₂SO₄) and concentrated. Flash chromatography (12:1 hexane/EtOAc) of the residue furnished the olefins in 65-70 % yield.

8.3.10 General procedure for CDA and PDA deprotection

20 mmol of 3,4 CDA or PDA-protected 1-thio-mannopyranoside were stirred at room temperature for 1 hour in 90 % TFA solution in CH₂Cl₂. At completion of the reaction,

the solvents were evaporated and the residue purified by flash chromatography (2:1 hexane/EtOAc) to give a colorless oil in 75-85 % yield.

8.3.11 Synthesis of methoxycarbonylmethylene-triphenylphosphorane

A solution of triphenylphosphine (10 mmol) and methyl bromoacetate (10 mmol) in dry toluene (20 mL) was heated under reflux for 1 hours. After this time the mixture was cooled with ice and filtrated. The white precipitate was washed with cold toluene, treated with 1 N NaOH in H₂O (15 mL) and extracted with EtOAc (3 x 10 mL). The organic extract was dried with Na₂SO₄ and concentrated. The residue was used immediately in the following reaction.

8.3.12 General procedure for alkene reduction with *para*-toluenesulfonylhydrazide

1 M aqueous sodium acetate (1.53 mL) was added in 6 portions during 3 hours to a warmed (85 °C), stirred solution of alkene substrate (0.5 mmol) and freshly recrystallized *para*-toluenesulfonylhydrazide (285 mg, 1.53 mmol) in dimethoxyethane (10 mL). After an additional 3 hours at 85 °C the mixture was diluted with H₂O (5 mL) and extracted with CH₂Cl₂ (2 x 30 mL). The organic phase was dried (Na₂SO₄) and concentrated. The residue was eluted from a column of silica gel with hexane/AcOAc 12:1 to give the reduced product in 60-65 % yield.

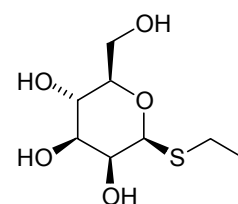
8.3.13 General procedure for selective hydrogenation of alkene in the presence of the benzyl group

A solution of the alkene substrate (0.5 mmol), 30 mg 10% Pd/C (ca. 50 % water) and ethylenediamine (0.25 mmol) in MeOH (10 mL) as poison was stirred at room temperature under hydrogen atmosphere (50 mbar) for 12 hours until completion of the reaction, monitored by TLC. The solution was then filtered through celite, the solvent evaporated and the residue used in the following reaction without purification (75-80 %).

8.3.14 General procedure for benzyl group cleavage

A solution of the benzyl protected alcohol (0.5 mmol), 60 mg 10% Pd/C (ca. 50 % water) in MeOH (15 mL) was stirred at room temperature under hydrogen atmosphere (balloon) for 1 hour until completion of the reaction, monitored by TLC. The solution was then filtered through celite, the solvent evaporated and the residue used in the following reaction without purification (90-98 %).

8.3.15 Synthesis of ethyl-1-thio- α -D-mannopyranoside (25)



100 g (280 mmol) 1,2,3,4,6-penta-*O*-acetyl- α -D-mannopyranoside were dissolved in 500 mL DCM. At 0 °C, 20.4 mL ethanethiol (280 mmol) and successively, 4.40 mL SnCl₄ (37.5 mmol) were added dropwise and the solution was stirred at RT overnight. To completion of the reaction, more ethanethiol (8.10 mL, 150 mmol) and SnCl₄ (1.80 mL, 3.10 mmol) were added. After the reaction was stirred for another 12 hours, much DCM was removed in vacuum. Extraction with 10% KF aqueous solution (2 x 25 mL) and sat. NaHCO₃ solution (2 x 25 mL), and purification *via* crystallization (hexane/EtOAc 1:1), resulted in colorless crystals (61.6 g, 160 mol, 64%). 35.0 g (89.2 mmol) ethyl 2,3,4,6-tetra-*O*-acetyl-1-thio- α -D-mannopyranoside were added slowly to a solution of 2.00 g Na (86.9 mmol) in 300 mL abs. methanol and the mixture was stirred for 2 hours. The strong basic solution was neutralized using cation exchange resin (DOWEX 50(H⁺)WX8), the resin was filtrated off and the solvents removed under reduced pressure. The residue was purified by flash column chromatography (gradient elution: CHCl₃/MeOH 4:1) to give the title compound ethyl-1-thio- α -D-mannopyranoside as a white solid after crystallization from the concentrated elution mixture (18.0 g, 86.1 mmol, 97 %).

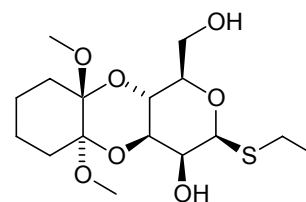
¹H-NMR (500 MHz, DMSO, 300 K): 5.12 (s, 1H), 4.91 (d, J = 4.27 Hz, 1H), 4.74 (d, J = 4.85 Hz, 1H), 4.62 (d, J = 5.52 Hz, 1H), 4.42 (d, J = 6.02 Hz, 1H), 3.68 – 3.59 (m, 3H), 3.36 – 3.48 (m, 3H), 2.63 – 2.47 (m), 1.20 (t, J = 7.36 Hz, 3H).

Assignment: 5.12 (H¹), 4.91 (HO-C²), 4.74 (HO-C⁴), 4.62 (HO-C³), 4.42 (HO-CH₂), 3.67 (H²), 3.64 (CH₂), 3.62 (H⁵), 3.46 (CH₂), 3.41 (H³), 3.40 (H⁴), 2.56 (SEt, CH₂), 1.20 (SEt, CH₃).

^{13}C -NMR (125 MHz, DMSO, 300 K): 83.29 (C^1), 73.66 (C^5), 71.01 (C^2), 70.73 (C^3), 66.49 (C^4), 60.34 ($\underline{\text{C}}\text{H}_2$), 23.27 (SEt, $\underline{\text{C}}\text{H}_2$), 14.21 (SEt, $\underline{\text{C}}\text{H}_3$).

ESI-MS: m/z : 247.2 [$\text{M}+\text{Na}^+$], MW calcd. for $\text{C}_8\text{H}_{16}\text{O}_5\text{S}$: 224.1.

8.3.16 Synthesis of ethyl-3,4-*O*-[1',2'-dimethoxycyclohexan-1',2'-diyl]-1-thio- α -D-mannopyranoside (26)



(±) Camphorsulfonic acid (1.5 g, 6.46 mmol) was added to a solution of ethyl-1-thio- α -D-mannopyranoside **25** (13.0 g, 58.0 mmol), cyclohexane-1,2-dione (7 g, 62.5 mmol) and trimethylorthoformate (20 mL, 182.5 mmol) in dry methanol (100ml) under an argon atmosphere. After the mixture was heated under reflux for 24 hours, more cyclohexane-1,2-dione (3 g, 26.8 mmol) and trimethylorthoformate (9.3 mL, 84.9 mmol) was added and then stirred under reflux for another 48 hours. At completeness of the reaction, followed by TLC, the reaction was neutralized with triethylamine (1.5 mL) and the solvents removed under reduced pressure. The residue was purified by flash column chromatography (gradient elution: hexane/EtOAc 9:1 to hexane/EtOAc 4:1) to give the title compound as a white solid (10.6 g, 29.1 mmol, 50 %).

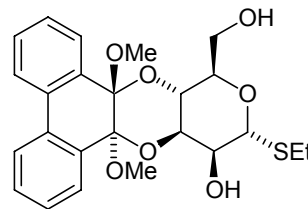
$^1\text{H-NMR}$ (500 MHz, CDCl_3 , 300 K): δ = 5.28 (s, 1H), 4.29 (t, J = 9.8 Hz, 1H), 4.15 - 4.10 (m, 2H), 4.01 (d, J = 3.5 Hz, 1H), 3.80 – 3.77 (m, 2H), 3.20 (s, 6H), 2.66 – 2.51 (m, 2H), 1.89 – 1.63 (m, 4H), 1.55 – 1.44 (m, 2H), 1.42 – 1.31 (m, 2H), 1.25 (t, 3H, J = 7.1 Hz).

Assignment: δ = 5.28 (H^1), 4.29 (H^4), 4.13 (H^5), 4.01 (H^2), 4.11 (H^3), 3.78 (CH_2), 3.19 (CDA, CH_3), 2.58 (SEt, CH_2), 1.73 (CDA, CH_2), 1.49 (CDA, CH_2), 1.35 (CDA, CH_2), 1.25 (SEt, CH_3).

$^{13}\text{C-NMR}$ (125 MHz, CDCl_3 , 300 K): δ = 84.40 (C^1), 71.44 (C^2), 70.77 (C^5), 69.31 (C^3), 64.04 (C^4), 61.25 (CH_2), 46.83 (CDA, CH_3), 26.90 (CDA, CH_2), 25.58 (SEt, CH_2), 21.22 (CDA, CH_2), 14.66 (SEt, CH_3).

ESI-MS: m/z : 387.2 [$\text{M}+\text{Na}^+$], MW calcd. for $\text{C}_{16}\text{H}_{28}\text{O}_7\text{S}$: 364.2.

8.3.17 Synthesis of ethyl-3,4-*O*-[9',10'-dimethoxyphenanthrene-9',10'-diyl]-1-thio- α -D-mannopyranoside (27)



(±) Camphorsulfonic acid (180 mg, 0.78 mmol) was added to a solution of ethyl-1-thio- α -D-mannopyranoside **25** (1.50 g, 6.69 mmol), phenanthrene-9,10-quinone (1.55 g, 7.45 mmol) and trimethylorthoformate (2.5 mL, 22.8 mmol) in dry methanol (20ml) under an argon atmosphere. After the mixture was heated under reflux for 24 hours, more phenanthrene-9,10-quinone (0.50 g, 2.40 mmol) and trimethylorthoformate (1 mL, 9.13 mmol) was added and then stirred under reflux for another 48 hours. At completeness of the reaction, followed by TLC, the reaction was neutralized with triethylamine (0.5 mL) and the solvents removed under reduced pressure. The residue was purified by flash column chromatography (gradient elution: hexane/EtOAc 9:1 to hexane/EtOAc 4:1) to give the title compound as a white solid (1.84 g, 4.01 mmol, 60 %).

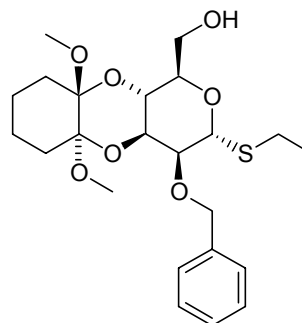
$^1\text{H-NMR}$ (500 MHz, CDCl_3 , 300 K): δ = 7.84 (d, J = 7.6 Hz, 2H), 7.65 (d, J = 7.6 Hz, 1H), 7.60 (d, J = 7.6 Hz, 1H), 7.47 (t, J = 7.6 Hz, 2H), 7.38 (t, J = 7.6 Hz, 1H), 7.36 (t, J = 7.6 Hz, 1H), 5.38 (s, 1H), 4.42 (t, J = 10.4 Hz, 1H), 4.28 (dd, J = 11.0 and 2.8 Hz, 1H), 4.23 – 4.18 (m, 1H), 4.19 (d, J = 2.8 Hz, 1H), 3.96 (d, J = 12.5 Hz, 1H), 3.90 (dd, J = 12.5 and 4.9 Hz, 1H), 2.85 (s, 3H), 2.83 (s, 3H), 2.78 – 2.64 (m, 2H), 1.32 (t, 3H).

Assignment: δ = 7.84 (PDA, $\text{H}^{4,5}$), 7.65 (PDA, H^1), 7.60 (PDA, H^8), 7.47 (PDA, $\text{H}^{3,6}$), 7.38 (PDA, H^2), 7.36 (PDA, H^7), 5.38 (H^1), 4.42 (H^4), 4.28 (H^3), 4.21 (H^5), 4.19 (H^2), 3.96 (CH_2), 3.90 (CH_2), 2.85 (PDA, CH_3), 2.83 (PDA, CH_3), 2.71 (SEt, CH_2), 1.32 (SEt, CH_3).

^{13}C -NMR (125 MHz, CDCl_3 , 300 K): δ = 128.53 (PDA, $\text{C}^{3,6}$), 127.56 (PDA, $\text{C}^{2,7}$), 125.75 (PDA, $\text{C}^{1,8}$), 124.64 (PDA, $\text{C}^{4,5}$), 85.81 (C^1), 72.40 (C^5), 71.58 (C^2), 70.42 (C^3), 64.84 (C^4), 60.98 ($\underline{\text{C}}\text{H}_2$), 48.77 (PDA, $\underline{\text{C}}\text{H}_3$), 25.13 (SEt, $\underline{\text{C}}\text{H}_2$), 14.71 (SEt, $\underline{\text{C}}\text{H}_3$).

ESI-MS: m/z : 483.2 [$\text{M}+\text{Na}^+$], MW calcd. for $\text{C}_{24}\text{H}_{28}\text{O}_7\text{S}$: 460.2.

8.3.18 Synthesis of ethyl-2-*O*-benzyl-3,4-*O*-[1',2'-dimethoxycyclohexan-1',2'-diyl]-1-thio- α -D-mannopyranoside (28)



Ethyl-3,4-*O*-[1',2'-dimethoxycyclohexan-1',2'-diyl]-1-thio- α -D-mannopyranoside **26** was benzylated at position 2 as outlined in 8.3.1 using benzyl bromide. Notice that no primary alcohol protection was needed.

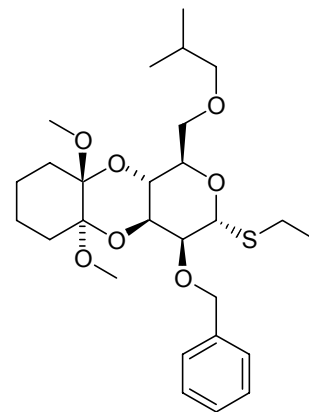
$^1\text{H-NMR}$ (500 MHz, CDCl_3 , 300 K): δ = 7.44 – 7.23 (m, 5H), 5.23 (s, 1H), 4.94 (d, J = 11.5 Hz, 1H), 4.61 (d, J = 11.5 Hz, 1H), 4.42 – 4.33 (m, 2H), 4.20 – 4.16 (dd, J_1 = 11.8 Hz, J_2 = <2 Hz, 1H), 4.14 - 4.09 (m, 1H), 3.84 – 3.76 (m, 3H), 3.22 (s, 3H), 3.21 (s, 3H), 2.63 – 2.49 (m, 2H), 1.84 – 1.64 (m, 4H), 1.55 – 1.46 (m, 2H), 1.44 – 1.30 (m, 2H), 1.21 (t, J = 7.3 Hz, 3H).

Assignment: δ = 7.41 (Bn, ϕ), 7.31 (Bn, ϕ), 7.25 (Bn, ϕ), 5.23 (H1), 4.93 (Bn, CH_2), 4.61 (Bn, CH_2), 4.38 (H^4), 4.18 (H^3), 4.11 (H^5), 3.82 (H^2), 3.79 (CH_2), 3.22, (CDA, CH_3), 3.21 (CDA, CH_3), 2.56 (SEt, CH_2), 1.77 (CDA, CH_2), 1.52 (CDA, CH_2), 1.38 (CDA, CH_2), 1.22 (SEt, CH_3).

$^{13}\text{C-NMR}$ (125 MHz, CDCl_3 , 300 K): δ = 128.19 (Bn, ϕ), 128.04 (Bn, ϕ), 127.53 (Bn, ϕ), 84.16 (C^1), 78.10 (C^2), 73.20 (Bn, CH_2), 71.21 (C^5), 70.27 (C^3), 64.89 (C^4), 61.67 (CH_2), 46.85 (CDA, CH_3), 27.04 (CDA, CH_2), 25.51 (SEt, CH_2), 21.40 (CDA, CH_2), 14.88 (SEt, CH_3).

ESI-MS: m/z = 477.3 [$\text{M}+\text{Na}^+$], MW calcd. for $\text{C}_{23}\text{H}_{34}\text{O}_7\text{S}$: 454.2.

8.3.19 Synthesis of ethyl-2-*O*-benzyl-3,4-*O*-[1',2'-dimethoxycyclohexan-1',2'-diyl]-6-*O*-isobutyl-1-thio- α -D-mannopyranoside (**29**)



Ethyl-2-*O*-benzyl-3,4-*O*-[1',2'-dimethoxycyclohexan-1',2'-diyl]-1-thio- α -D-mannopyranoside **28** was alkylated at position 6 as outlined in 8.3.1 using isobutyl bromide.

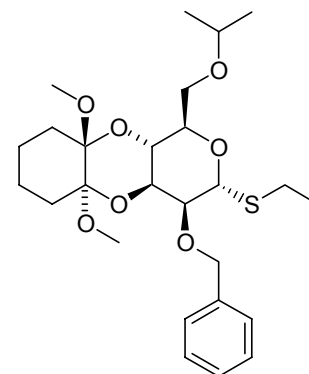
$^1\text{H-NMR}$ (500 MHz, CDCl_3 , 300 K): δ = 7.42 – 7.21 (m, 5H), 5.27 (s, 1H), 4.90 (d, J = 12.1 Hz, 1H), 4.62 (d, J = 12.1 Hz, 1H), 4.31 (dd, J_1 = J_2 = 10.1 Hz, 1H), 4.21 (m, 1H), 4.18 (dd, J_1 = 10.4 Hz, J_2 = 2.9 Hz, 1H), 3.78 (d, J = 3.4 Hz, 1H), 3.68 – 3.63 (m, 2H), 3.31-3.14 (m, 8H), 2.68 – 2.48 (m, 2H), 1.88 – 1.62 (m, 5H), 1.56 – 1.44 (m, 2H), 1.43 – 1.33 (m, 2H), 1.22 (t, J = 7.6 Hz, 3H), 0.85 (m, 6H).

Assignment: δ = 7.39 (Bn, ϕ), 7.27 (Bn, ϕ), 7.21 (Bn, ϕ), 5.27 (H^1), 4.87 (Bn, CH_2), 4.60 (Bn, CH_2), 4.28 (H^4), 4.19 (H^5), 4.17 (H^3), 3.76 (H^2), 3.62 (CH_2), 3.22 (Leu, CH_2), 3.18 (CDA, CH_3), 3.15 (Leu, CH_2), 2.56 (SEt, CH_2), 1.81 (Leu, CH), 1.71 (CDA, CH_2), 1.48 (CDA, CH_2), 1.36 (CDA, CH_2), 1.20 (SEt, CH_3), 0.87 (Leu, CH_3).

$^{13}\text{C-NMR}$ (125 MHz, CDCl_3 , 300 K): δ = 128.00 (Bn, ϕ), 127.74 (Bn, ϕ), 127.16 (Bn, ϕ), 83.36 (C^1), 78.42 (Leu, CH_2), 78.01 (C^2), 72.66 (Bn, CH_2), 71.06 (C^5), 70.33 (C^3), 69.21 (CH_2), 64.80 (C^4), 46.76 (CDA, CH_3), 28.51 (Leu, CH), 27.01 (CDA, CH_2), 25.14 (SEt, CH_2), 21.45 (CDA, CH_2), 19.27 (Leu, CH_3), 14.95 (SEt, CH_3)

ESI-MS: m/z = 533.6 [$\text{M}+\text{Na}^+$], MW calcd. for $\text{C}_{27}\text{H}_{42}\text{O}_7\text{S}$: 510.3.

8.3.20 Synthesis of ethyl-2-*O*-benzyl-3,4-*O*-[1',2'-dimethoxycyclohexan-1',2'-diyl]-6-*O*-isopropyl-1-thio- α -D-mannopyranoside (**30**)



Ethyl-2-*O*-benzyl-3,4-*O*-[1',2'-dimethoxycyclohexan-1',2'-diyl]-1-thio- α -D-mannopyranoside **28** was alkylated at position 6 as outlined in 8.3.1 using isopropyl iodide.

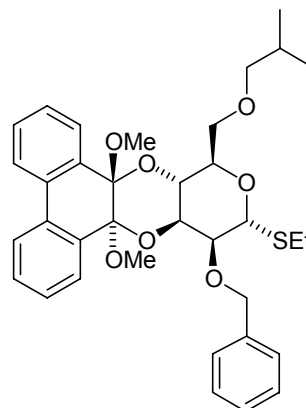
$^1\text{H-NMR}$ (500 MHz, CDCl_3 , 300 K): δ = 7.45, (d, J = 7.3 Hz, 2H), 7.34 (t, J = 7.3 Hz, 2H), 7.30 – 7.25 (m, 1H), 5.34 (s, 1H), 4.94 (d, J = 11.6 Hz, 1H), 4.67 (d, J = 11.6 Hz, 1H), 4.40 (t, J = 10.5 Hz, 1H), 4.24 – 4.18 (m, 2H), 3.82 (s, 1H), 3.74 – 3.61 (m, 3H), 3.26 (s, 3H), 3.25 (s, 3H), 2.70 – 2.54 (m, 2H), 1.89 – 1.68 (m, 4H), 1.59 – 1.50 (m, 2H), 1.48 – 1.36 (m, 2H), 1.26 (t, J = 7.3 Hz, 3H), 1.19 – 1.13 (m, 6H).

Assignment: δ = 7.45 (Bn, ϕ), 7.34 (Bn, ϕ), 7.28 (Bn, ϕ), 5.34 (H^1), 4.94 (Bn, $\underline{\text{CH}_2}$), 4.67 (Bn, $\underline{\text{CH}_2}$), 4.40 (H^4), 4.21 (H^5), 4.21 (H^3), 3.82 (H^2), 3.68 ($\underline{\text{CH}_2}$), 3.67 (iPr, $\underline{\text{CH}}$), 3.25 (CDA, $\underline{\text{CH}_3}$), 2.67 (SEt, $\underline{\text{CH}_2}$), 2.58 (SEt, $\underline{\text{CH}_2}$), 1.80 (CDA, $\underline{\text{CH}_2}$), 1.77 (CDA, $\underline{\text{CH}_2}$), 1.54 (CDA, $\underline{\text{CH}_2}$), 1.42 (CDA, $\underline{\text{CH}_2}$), 1.26 (SEt, $\underline{\text{CH}_3}$), 1.16 (iPr, $\underline{\text{CH}_3}$).

$^{13}\text{C-NMR}$ (125 MHz, CDCl_3 , 300 K): δ = 128.50 (Bn, ϕ), 128.20 (Bn, ϕ), 127.71 (Bn, ϕ), 84.03 (C^1), 78.45 (C^2), 73.02 (Bn, $\underline{\text{CH}_2}$), 72.31 (iPr, $\underline{\text{CH}}$), 71.78 (C^5), 70.80 (C^3), 66.65 ($\underline{\text{CH}_2}$), 65.21 (C^4), 47.19 (CDA, $\underline{\text{CH}_3}$), 27.49 (CDA, $\underline{\text{CH}_2}$), 25.60 (SEt, $\underline{\text{CH}_2}$), 22.47 (iPr, $\underline{\text{CH}_3}$), 21.78 (CDA, $\underline{\text{CH}_2}$), 14.46 (SEt, $\underline{\text{CH}_3}$)

ESI-MS: m/z = 519.3 [$\text{M}+\text{Na}^+$], MW calcd. for $\text{C}_{26}\text{H}_{40}\text{O}_7\text{S}$: 496.2.

8.3.21 Synthesis of ethyl-2-*O*-benzyl-3,4-*O*-[9',10'-dimethoxyphenanthrene-9',10'-diyl]-6-*O*-isobutyl-1-thio- α -D-mannopyranoside (**31**)



Ethyl-3,4-*O*-[9',10'-dimethoxyphenanthrene-9',10'-diyl]-1-thio- α -D-mannopyranoside **27** (13 mmol) and imidazole (39 mmol) were dissolved in 50 mL DMF and the solution was stirred at room temperature. Successively, *tert*-butyl diphenyl silyl chloride (TBDPSCl, 17 mmol) was added dropwise. Stirring was continued for 3 hours until completion of the reaction, followed by TLC. The solvent was evaporated under vacuum and the residue purified by flash column chromatography (gradient elution: hexane/EtOAc 9:1 to hexane/EtOAc 4:1) to give the title compound as a colorless oil (11.0 mmol, 85 %). The TBDPS-protected mannoside was then benzylated at position 2 following the general procedure 8.3.1 using benzyl bromide. Note that protection of the 2-position of PDA mannoside **27** could not be achieved by benzylation as for the CDA mannoside **26** without protection of the primary alcohol. TBDPS removal was carried out overnight under stirring in 20 mL THF using 2 eq. of tetrabutylammonium fluoride (TBAF) of a 1 M TBAF solution in THF. The solvent was evaporated and the residue purified by flash column chromatography (gradient elution: hexane/EtOAc 6:1 to hexane/EtOAc 4:1) (96 %). The 6 position was then alkylated following the general procedure 8.3.1 using isobutyl bromide.

$^1\text{H-NMR}$ (500 MHz, CD_3CN , 300 K): δ = 7.85 (d, J = 7.9 Hz, 2H), 7.65 – 7.59 (m, 2H), 7.53 – 7.46 (m, 4H), 7.43 – 7.31 (m, 5H), 5.48 (s, 1H), 4.95 (d, J = 11.9 Hz, 1H), 4.82 (d, J = 11.9 Hz, 1H), 4.49 (t, J = 10.8 Hz, 1H), 4.36 (dd, J = 10.4 and 3.0 Hz, 1H), 4.30 – 4.25 (m, 1H), 4.06 (s, 1H), 3.88 – 3.76 (m, 2H), 3.39 – 3.26 (m, 2H), 2.87 (s,

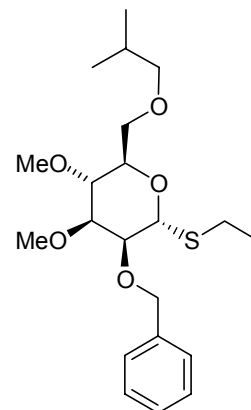
3H), 2.84 (s, 3H), 2.78 – 2.62 (m, 2H), 1.92 – 1.82 (m, 1H), 1.32 (t, $J = 7.6$ Hz, 3H), 0.92 (d, $J = 6.7$ Hz, 6H).

Assignment: $\delta = 7.85$ (PDA, $H^{4,5}$), 7.62 (PDA, $H^{1,8}$), 7.51 (Bn, ϕ), 7.48 (PDA, $H^{3,6}$), 7.40 (Bn, ϕ), 7.38 (PDA, $H^{2,7}$), 7.34 (Bn, ϕ), 5.48 (H^1), 4.95 (Bn, \underline{CH}_2), 4.82 (Bn, \underline{CH}_2), 4.49 (H^4), 4.36 (H^3), 4.28 (H^5), 4.06 (H^2), 3.86 (\underline{CH}_2), 3.80 (\underline{CH}_2), 3.36 (Leu, \underline{CH}_2), 3.29 (Leu, \underline{CH}_2), 2.87 (PDA, \underline{CH}_3), 2.84 (PDA, \underline{CH}_3), 2.72 (SEt, \underline{CH}_2), 2.67 (SEt, \underline{CH}_2), 1.87 (Leu, \underline{CH}), 1.31 (SEt, \underline{CH}_3), 0.92 (Leu, \underline{CH}_3).

^{13}C -NMR (125 MHz, CD_3CN , 300 K): $\delta = 129.40$ (PDA, $C^{3,6}$), 128.65 (Bn, ϕ), 128.30 (Bn, ϕ), 127.99 (Bn, ϕ), 127.49 (PDA, $C^{2,7}$), 125.68 (PDA, $C^{1,8}$), 124.64 (PDA, $C^{4,5}$), 83.65 (C^1), 78.55 (Leu, \underline{CH}_2), 78.30 (C^2), 72.80 (Bn, \underline{CH}_2), 71.28 (C^5), 70.92 (C^3), 69.40 (\underline{CH}_2), 65.21 (C^4), 48.80 (PDA, \underline{CH}_3), 48.74 (PDA, \underline{CH}_3), 28.78 (Leu, \underline{CH}), 25.38 (SEt, \underline{CH}_2), 18.97 (Leu, \underline{CH}_3), 14.70 (SEt, \underline{CH}_3).

ESI-MS: $m/z = 629.3$ [$\text{M} + \text{Na}^+$], MW calcd. for $\text{C}_{35}\text{H}_{42}\text{O}_7\text{S}$: 606.3.

8.3.22 Synthesis of ethyl-2-*O*-benzyl-6-*O*-isobutyl-3,4-di-*O*-methyl-1-thio- α -D-mannopyranoside (**32**)



CDA deprotection of ethyl-2-*O*-benzyl-3,4-*O*-[1',2'-dimethoxycyclohexan-1',2'-diyl]-6-*O*-isobutyl-1-thio- α -D-mannopyranoside **29** was carried out as outlined in 8.3.10. Subsequent methylation at 3 and 4 positions as described in section 8.3.1 using methyl iodide afforded **32** in 70 % yield. Activation of the S*Et* group in the presence of MeI caused the formation of methyl-mannopyranoside as byproduct. Before purification by flash column chromatography, the excess of toxic alkyl halide was destroyed with a 15 % solution of ammonium hydroxide.

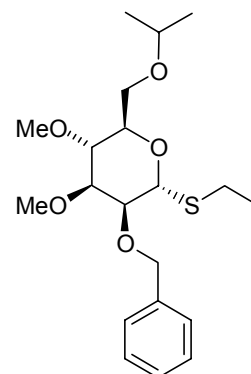
¹H-NMR (500 MHz, CDCl₃, 300 K): δ = 7.22 – 7.39 (m, 5H), 5.37 (d, J = <1.5 Hz, 1H), 4.70 (d, J = 12.3 Hz, 1H), 4.64 (d, J = 12.3 Hz, 1H), 3.97 – 3.92 (m, 1H), 3.84 (dd, $J_1 = J_2 = 2.5$ Hz, 1H), 3.68 (dd, $J_1 = 10.8$ Hz, $J_2 = 5.1$ Hz, 1H), 3.60 (dd, $J_1 = 10.8$ Hz, $J_2 = 2.1$ Hz, 1H), 3.58 (dd, $J_1 = J_2 = 9.6$ Hz, 1H), 3.51 (s, 3H), 3.44 (dd, $J_1 = 9.3$ Hz, $J_2 = 3.2$ Hz, 1H), 3.36 (s, 3H), 3.32 (dd, $J_1 = 8.9$ Hz, $J_2 = 6.4$ Hz, 1H), 3.14 (dd, $J_1 = 8.9$ Hz, $J_2 = 7.0$ Hz, 1H), 2.65 – 2.50 (m, 2H), 1.93 – 1.83 (m, 1H), 1.23 (t, J = 7.5 Hz, 3H), 0.90 (d, J = 6.7 Hz, 3H), 0.88 (d, J = 6.7 Hz, 3H).

Assignment: δ = 7.36 (Bn, ϕ), 7.30 (Bn, ϕ), 7.24 (Bn, ϕ), 5.37 (H¹), 4.68 (Bn, CH₂), 4.65 (Bn, CH₂), 3.94 (H⁵), 3.83 (H²), 3.66 (CH₂), 3.60 (CH₂), 3.57 (H⁴), 3.51 (OCH₃), 3.43 (H³), 3.35 (OCH₃), 3.32 (Leu, CH₂), 3.14 (Leu, CH₂), 2.55 (SEt, CH₂), 1.88 (Leu, CH), 1.22 (SEt, CH₃), 0.88 (Leu, CH₃).

^{13}C -NMR (125 MHz, CDCl_3 , 300 K): δ = 127.24 (Bn, ϕ), 127.36 (Bn, ϕ), 128.17 (Bn, ϕ), 81.85 (C^3), 81.43 (C^1), 78.25 (Leu, $\underline{\text{C}}\text{H}_2$), 76.59 (C^4), 75.53 (C^2), 71.74 (C^5), 71.66 (Bn, $\underline{\text{C}}\text{H}_2$), 69.94 ($\underline{\text{C}}\text{H}_2$), 60.47 ($\text{O}\underline{\text{C}}\text{H}_3$), 57.29 ($\text{O}\underline{\text{C}}\text{H}_3$), 28.46 (Leu, $\underline{\text{C}}\text{H}$), 25.06 (SEt, $\underline{\text{C}}\text{H}_2$), 19.30 (Leu, $\underline{\text{C}}\text{H}_3$), 14.84 (SEt, $\underline{\text{C}}\text{H}_3$).

ESI-MS: m/z : 421.3 [$\text{M}+\text{Na}^+$], MW calcd. for $\text{C}_{21}\text{H}_{34}\text{O}_5\text{S}$: 398.2.

8.3.23 Synthesis of ethyl-2-*O*-benzyl-6-*O*-isopropyl-3,4-di-*O*-methyl-1-thio- α -D-mannopyranoside (**33**)



CDA deprotection of ethyl-2-*O*-benzyl-3,4-*O*-[1',2'-dimethoxycyclohexan-1',2'-diyl]-6-*O*-isopropyl-1-thio- α -D-mannopyranoside **30** was carried out as outlined in 8.3.10. Subsequent methylation at 3 and 4 positions as described in section 8.3.1 using methyl iodide afforded **33** in 70 % yield. Activation of the S*Et* group in the presence of MeI caused the formation of methyl-mannopyranoside as byproduct. Before purification by flash column chromatography, the excess of toxic alkyl halide was destroyed with a 15 % solution of ammonium hydroxide.

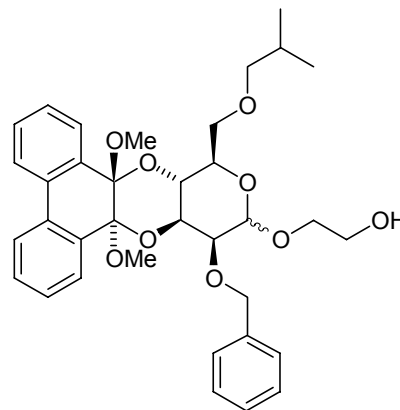
$^1\text{H-NMR}$ (500 MHz, CD_3CN , 300 K): δ = 7.44 – 7.31 (m, 5H), 5.42 (s, 1H), 4.70 (d, J = 11.9 Hz, 1H), 4.62 (d, J = 11.9 Hz, 1H), 3.92 (s, 1H), 3.87 – 3.83 (m, 1H), 3.66 – 3.56 (m, 3H), 3.51 – 3.38 (m, 5H), 3.36 (s, 3H), 2.69 – 2.55 (m, 2H), 1.27 (t, J = 7.3 Hz, 3H), 1.16 – 1.13 (m, 6H).

Assignment: δ = 7.41 (Bn, ϕ), 7.40 (Bn, ϕ), 7.34 (Bn, ϕ), 5.42 (H^1), 4.70 (Bn, CH_2), 4.62 (Bn, CH_2), 3.92 (H^2), 3.85 (H^5), 3.62 (iPr, CH), 3.60 (CH_2), 3.48 (OCH_3), 3.45 (H^4), 3.41 (H^3), 3.36 (OCH_3), 2.65 (SEt, CH_2), 2.60 (SEt, CH_2), 1.27 (SEt, CH_3), 1.14 (iPr, CH_3).

$^{13}\text{C-NMR}$ (125 MHz, CD_3CN , 300 K): δ = 128.72 (Bn, ϕ), 128.33 (Bn, ϕ), 128.04 (Bn, ϕ), 82.38 (C^3), 82.10 (C^1), 76.84 (C^4), 76.56 (C^2), 72.42 (C^5), 72.19 (Bn, CH_2), 72.00 (iPr, CH), 67.48 (CH_2), 60.13 (OCH_3), 56.82 (OCH_3), 25.34 (SEt, CH_2), 21.74 (iPr, CH_3), 14.76 (SEt, CH_3).

ESI-MS: m/z : 407.3 [M+Na⁺], MW calcd. for C₂₀H₃₂O₅S: 384.2.

8.3.24 Synthesis of [2'-hydroxyethyl]-2-*O*-benzyl-3,4-*O*-[9',10'-dimethoxyphenanthrene-9',10'-diyl]-6-*O*-isobutyl- α,β -D-mannopyranoside (**34**)



Ehyl-2-*O*-benzyl-3,4-*O*-[9',10'-dimethoxyphenanthrene-9',10'-diyl]-6-*O*-isobutyl-1-thio- α -D-mannopyranoside **31** was reacted with Br₂ as outlined in 8.3.4. Successively, the fresh prepared mannosyl bromide as glycosyl donor was coupled to anhydrous ethylene glycol in 5: 1 DCM/THF solution (8.3.6). The addition of THF was needed to dissolve the ethylene glycol and to create an homogenous system. Purification by flash column chromatography afforded **34** in 90 % yield with an 1:1 α/β ratio. The two conformers were on purpose collected together.

β :

¹H-NMR (500 MHz, CD₃CN, 300 K): δ = 7.83 (d, *J* = 7.6 Hz, 2H), 7.61 (d, *J* = 7.9 Hz, 1H), 7.59 – 7.54 (m, 3H), 7.45 (t, *J* = 7.6 Hz, 2H), 7.37 – 7.25 (m, 5H), 5.08 (d, *J* = 12.2 Hz, 1H), 4.91 (d, *J* = 12.2 Hz, 1H), 4.86 (s, 1H), 4.80 (s, 1H), 4.47 (t, *J* = 9.8 Hz, 1H), 4.18 (d, *J* = 11.6 Hz, 1H), 4.16 (s, 1H), 4.00 – 3.90 (m, 2H), 3.85 – 3.74 (m, 5H), 3.43 – 3.31 (m, 2H), 2.91 (s, 3H), 2.88 (s, 3H), 1.95 – 1.86 (m, 1H), 0.97 – 0.91 (m, 6H).

Assignment: δ = 7.83 (PDA, H^{4,5}), 7.61 (PDA, H¹), 7.57 (PDA, H⁸), 7.56 (Bn, ϕ), 7.45 (PDA, H^{3,6}), 7.35 (PDA, H^{2,7}), 7.31 (Bn, ϕ), 7.27 (Bn, ϕ), 5.08 (Bn, CH₂), 4.91 (Bn, CH₂), 4.86 (OH), 4.80 (H¹), 4.47 (H⁴), 4.18 (H³), 4.16 (H²), 3.97 (hydroxyethyl, CH₂), 3.93 (CH₂), 3.83 (CH₂), 3.79 (H⁵), 3.76 (hydroxyethyl, CH₂), 3.76 (hydroxyethyl, CH₂), 3.41 (Leu, CH₂), 3.34 (Leu, CH₂), 2.91 (PDA, CH₃), 2.88 (PDA, CH₃), 1.90 (Leu, CH), 0.94 (Leu, CH₃).

^{13}C -NMR (125 MHz, CD_3CN , 300 K): $\delta = 129.17$ (PDA, $\text{C}^{3,6}$), 128.44 (Bn, ϕ), 128.07 (Bn, ϕ), 127.42 (Bn, ϕ), 127.07 (PDA, $\text{C}^{2,7}$), 125.64 (PDA, C^1), 125.43 (PDA, C^8), 124.26 (PDA, $\text{C}^{4,5}$), 102.14 (C^1), 78.84 (Leu, $\underline{\text{C}}\text{H}_2$), 76.84 (C^2), 74.87 (C^5), 74.48 (Bn, $\underline{\text{C}}\text{H}_2$), 72.39 (C^3), 71.68 (hydroxyethyl, $\underline{\text{C}}\text{H}_2$), 69.81 ($\underline{\text{C}}\text{H}_2$), 65.12 (C^4), 61.50 (hydroxyethyl, $\underline{\text{C}}\text{H}_2$), 48.51 (PDA, $\underline{\text{C}}\text{H}_3$), 48.47 (PDA, $\underline{\text{C}}\text{H}_3$), 28.68 (Leu, $\underline{\text{C}}\text{H}$), 18.72 (Leu, $\underline{\text{C}}\text{H}_3$).

α :

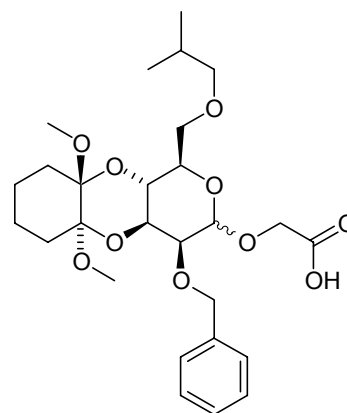
^1H -NMR (500 MHz, CD_3CN , 300 K): $\delta = 7.85$ (d, $J = 7.6$ Hz, 2H), 7.66 (d, $J = 7.3$ Hz, 1H), 7.60 (d, $J = 7.3$ Hz, 1H), 7.53 – 7.44 (m, 4H), 7.41 – 7.32 (m, 5H), 5.02 (d, $J = 11.6$ Hz, 1H), 4.97 (s, 1H), 4.79 (d, $J = 11.6$ Hz, 1H), 4.50 – 4.40 (m, 2H), 4.05 – 3.98 (m, 2H), 3.84 – 3.54 (m, 6H), 3.40 – 3.28 (m, 2H), 2.87 (s, 3H), 2.86 (s, 3H), 1.94 – 1.84 (m, 1H), 0.96 – 0.89 (m, 6H).

Assignment: $\delta = 7.85$ (PDA, $\text{H}^{4,5}$), 7.66 (PDA, H^1), 7.60 (PDA, H^8), 7.50 (Bn, ϕ), 7.47 (PDA, $\text{H}^{3,6}$), 7.38 (Bn, ϕ), 7.37 (PDA, $\text{H}^{2,7}$), 7.34 (Bn, ϕ), 5.02 (Bn, $\underline{\text{C}}\text{H}_2$), 4.97 (H^1), 4.79 (Bn, $\underline{\text{C}}\text{H}_2$), 4.47 (H^4), 4.44 (H^3), 4.02 (H^5), 3.99 (H^2), 3.82 ($\underline{\text{C}}\text{H}_2$), 3.77 (hydroxyethyl, $\underline{\text{C}}\text{H}_2$), 3.67 (hydroxyethyl, $\underline{\text{C}}\text{H}_2$), 3.59 (hydroxyethyl, $\underline{\text{C}}\text{H}_2$), 3.37 (Leu, $\underline{\text{C}}\text{H}_2$), 3.31 (Leu, $\underline{\text{C}}\text{H}_2$), 2.87 (PDA, $\underline{\text{C}}\text{H}_3$), 2.86 (PDA, $\underline{\text{C}}\text{H}_3$), 1.88 (Leu, $\underline{\text{C}}\text{H}$), 0.93 (Leu, $\underline{\text{C}}\text{H}_3$).

^{13}C -NMR (125 MHz, CD_3CN , 300 K): $\delta = 129.43$ (PDA, $\text{C}^{3,6}$), 128.63 (Bn, ϕ), 128.35 (Bn, ϕ), 127.90 (Bn, ϕ), 127.46 (PDA, $\text{C}^{2,7}$), 125.75 (PDA, C^1), 125.67 (PDA, C^8), 124.60 (PDA, $\text{C}^{4,5}$), 99.94 (C^1), 78.57 (Leu, $\underline{\text{C}}\text{H}_2$), 76.96 (C^2), 73.29 (Bn, $\underline{\text{C}}\text{H}_2$), 71.15 (C^5), 70.43 (C^3), 70.08 (hydroxyethyl, $\underline{\text{C}}\text{H}_2$), 69.45 ($\underline{\text{C}}\text{H}_2$), 65.07 (C^4), 61.40 (hydroxyethyl, $\underline{\text{C}}\text{H}_2$), 48.88 (PDA, $\underline{\text{C}}\text{H}_3$), 28.68 (Leu, $\underline{\text{C}}\text{H}$), 19.19 (Leu, $\underline{\text{C}}\text{H}_3$).

ESI-MS: $m/z = 629.3$ [$\text{M} + \text{Na}^+$], MW calcd. for $\text{C}_{35}\text{H}_{42}\text{O}_9$: 606.3.

8.3.25 Synthesis of [carboxymethyl]-2-*O*-benzyl-3,4-*O*-[1',2'-dimethoxycyclohexan-1',2'-diyl]-6-*O*-isobutyl- α,β -D-mannopyranoside (**35**)



Ethyl-2-*O*-benzyl-3,4-*O*-[1',2'-dimethoxycyclohexan-1',2'-diyl]-6-*O*-isobutyl-1-thio- α -D-mannopyranoside **29** was either reacted with Br₂, as outlined in 8.3.4, and successively the fresh prepared mannosyl bromide as glycosyl donor was coupled to anhydrous glycolic acid methyl ester (8.3.6) to give preferentially the β -anomer or **29** was reacted directly with glycolic acid methyl ester as described in 8.3.5 to give preferentially the α -anomer. Hydrolysis of the methyl ester in 10 mL of 1:1 solution of 1 M NaOH and MeOH for 1 hour afforded quantitatively α,β **35** which were purified by HPLC.

β :

¹H-NMR (500 MHz, CD₃CN, 300 K): δ = 7.48 (d, *J* = 7.4 Hz, 2H), 7.36 (t, *J* = 7.4 Hz, 2H), 7.31 (t, *J* = 7.4 Hz, 1H), 4.85 (d, *J* = 11.7 Hz, 1H), 4.74 (d, *J* = 11.7 Hz, 1H), 4.72 (s, 1H), 4.30 – 4.26 (m, 2H), 4.15 (t, *J* = 10.2 Hz, 1H), 3.93 (d, *J* = 2.7 Hz, 1H), 3.92 – 3.89 (dd, *J*₁ = 2.7 Hz, *J*₂ = 10.4 Hz, 1H), 3.65 – 3.62 (dd, *J*₁ < 2 Hz, *J*₂ = 19.0 Hz, 1H), 3.59 – 3.56 (m, 1H), 3.50 – 3.45 (m, 1H), 3.28 – 3.25 (dd, *J*₁ = 6.7 Hz, *J*₂ = 9.3 Hz, 1H), 3.21 – 3.18 (m, 7H), 1.87 – 1.68 (m, 3H), 1.66 – 1.58 (m, 2H), 1.54 – 1.48 (m, 2H), 1.44 – 1.31 (m, 2H), 0.88 (s, 3H), 0.87 (s, 3H).

Assignment: δ = 7.48 (Bn, ϕ), 7.36 (Bn, ϕ), 7.31 (Bn, ϕ), 4.85 (Bn, CH₂), 4.74 (Bn, CH₂), 4.72 (H¹), 4.27 (Asp, CH₂), 4.15 (H⁴), 3.93 (H²), 3.90 (H³), 3.63 (CH₂), 3.57 (CH₂), 3.47 (H⁵), 3.26 (Leu, CH₂), 3.19 (Leu, CH₂), 3.19 (CDA, CH₃), 3.18 (CDA,

$\underline{\text{CH}}_3$), 1.82 (Leu, $\underline{\text{CH}}$), 1.78 (CDA, $\underline{\text{CH}}_2$), 1.71 (CDA, $\underline{\text{CH}}_2$), 1.50 (CDA, $\underline{\text{CH}}_2$), 1.37 (CDA, $\underline{\text{CH}}_2$), 0.89 (Leu, $\underline{\text{CH}}_3$), 0.87 (Leu, $\underline{\text{CH}}_3$).

^{13}C -NMR (125 MHz, CD_3CN , 300 K): $\delta = 128.46$ (Bn, ϕ), 128.13 (Bn, ϕ), 127.67 (Bn, ϕ), 101.07 (C^1), 78.41 (Leu, $\underline{\text{CH}}_2$), 76.84 (C^2), 74.85 (C^5), 74.04 (Bn, $\underline{\text{CH}}_2$), 71.58 (C^3), 69.24 ($\underline{\text{CH}}_2$), 65.38 (Asp, $\underline{\text{CH}}_2$), 64.36 (C^4), 46.59 (CDA, $\underline{\text{CH}}_3$), 28.74 (Leu, $\underline{\text{CH}}$), 27.23 (CDA, $\underline{\text{CH}}_2$), 21.61 (CDA, $\underline{\text{CH}}_2$), 19.07 (Leu, $\underline{\text{CH}}_3$).

α :

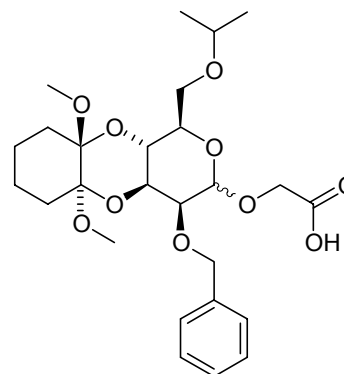
^1H -NMR (500 MHz, CD_3CN , 300 K): $\delta = 7.46$ (d, $J = 7.0$ Hz, 2H), 7.40 – 7.37 (m, 2H), 7.34 – 7.31 (m, 1H), 4.94 (s, 1H), 4.82 (d, $J = 11.5$ Hz, 1H), 4.64 (d, $J = 11.5$ Hz, 1H), 4.24 (t, $J = 10.2$ Hz, 1H), 4.19 – 4.17 (m, 3H), 3.82 – 3.81 (m, 1H), 3.79 – 3.75 (m, 1H), 3.59 – 3.57 (m, 2H), 3.28 – 3.25 (dd, $J_1 = 6.6$ Hz, $J_2 = 9.1$ Hz, 1H), 3.21 – 3.20 (m, 7H), 1.88 – 1.72 (m, 3H), 1.70 – 1.62 (m, 2H), 1.56 – 1.47 (m, 2H), 1.47 – 1.34 (m, 2H), 0.90 (d, $J = 6.7$ Hz, 6H).

Assignment: $\delta = 7.45$ (Bn, ϕ), 7.38 (Bn, ϕ), 7.32 (Bn, ϕ), 4.94 (H^1), 4.82 (Bn, $\underline{\text{CH}}_2$), 4.64 (Bn, $\underline{\text{CH}}_2$), 4.23 (H^4), 4.18 (Asp, $\underline{\text{CH}}_2$), 4.17 (H^3), 3.81 (H^2), 3.77 (H^5), 3.58 ($\underline{\text{CH}}_2$), 3.26 (Leu, $\underline{\text{CH}}_2$), 3.20 (Leu, $\underline{\text{CH}}_2$), 3.20 (CDA, $\underline{\text{CH}}_3$), 1.82 (Leu, $\underline{\text{CH}}$), 1.80 (CDA, $\underline{\text{CH}}_2$), 1.67 (CDA, $\underline{\text{CH}}_2$), 1.52 (CDA, $\underline{\text{CH}}_2$), 1.40 (CDA, $\underline{\text{CH}}_2$), 0.90 (Leu, $\underline{\text{CH}}_3$).

^{13}C -NMR (125 MHz, CD_3CN , 300 K): $\delta = 128.56$ (Bn, ϕ), 128.23 (Bn, ϕ), 127.97 (Bn, ϕ), 99.12 (C^1), 78.45 (Leu, $\underline{\text{CH}}_2$), 76.61 (C^2), 72.90 (Bn, $\underline{\text{CH}}_2$), 71.82 (C^5), 69.76 (C^3), 69.37 ($\underline{\text{CH}}_2$), 64.53 (C^4), 63.70 (Asp, $\underline{\text{CH}}_2$), 46.64 (CDA, $\underline{\text{CH}}_3$), 28.74 (Leu, $\underline{\text{CH}}$), 27.31 (CDA, $\underline{\text{CH}}_2$), 21.66 (CDA, $\underline{\text{CH}}_2$), 19.08 (Leu, $\underline{\text{CH}}_3$).

ESI-MS: m/z : 547.4 [$\text{M}+\text{Na}^+$], MW calcd. for $\text{C}_{27}\text{H}_{40}\text{O}_{10}$: 524.3.

8.3.26 Synthesis of [carboxymethyl]-2-*O*-benzyl-3,4-*O*-[1',2'-dimethoxycyclohexan-1',2'-diyl]-6-*O*-isopropyl- α,β -D-mannopyranoside (**36**)



Ethyl-2-*O*-benzyl-3,4-*O*-[1',2'-dimethoxycyclohexan-1',2'-diyl]-6-*O*-isopropyl-1-thio- α -D-mannopyranoside **30** was either reacted with Br₂, as outlined in 8.3.4, and successively the fresh prepared mannosyl bromide as glycosyl donor was coupled to anhydrous glycolic acid methyl ester (8.3.6) to give preferentially the β -anomer or **30** was reacted directly with glycolic acid methyl ester as described in 8.3.5 to give preferentially the α -anomer. Hydrolysis of the methyl ester in 10 mL of 1:1 solution of 1 M NaOH and MeOH for 1 hour afforded quantitatively α,β **36** which were purified by HPLC.

β :

¹H-NMR (500 MHz, CD₃CN, 300 K): δ = 7.50 (d, *J* = 7.5 Hz, 2H), 7.37 (t, *J* = 7.5 Hz, 2H), 7.34 – 7.29 (m, 1H), 4.87 (d, *J* = 11.6 Hz, 1H), 4.81 – 4.68 (m, 3H), 4.36 – 4.23 (m, 2H), 4.18 (t, *J* = 12.0 Hz, 1H), 3.98 – 3.85 (m, 2H), 3.73 – 3.53 (m, 3H), 3.50 – 3.42 (m, 1H), 3.22 (s, 3H), 3.20 (s, 3H), 1.85 – 1.58 (m, 4H), 1.58 – 1.33 (m, 4H), 1.13 (d, *J* = 5.0 Hz, 6H).

Assignment: δ = 7.50 (Bn, ϕ), 7.37 (Bn, ϕ), 7.31 (Bn, ϕ), 4.86 (Bn, CH₂), 4.76 (Bn, CH₂), 4.73 (H¹), 4.29 (Asp, CH₂), 4.18 (H⁴), 3.93 (H²), 3.91 (H³), 3.68 (CH₂), 3.64 (iPr, CH), 3.57 (CH₂), 3.46 (H⁵), 3.22 (CDA, CH₃), 3.20 (CDA, CH₃), 1.77 (CDA, CH₂), 1.65 (CDA, CH₂), 1.52 (CDA, CH₂), 1.40 (CDA, CH₂), 1.13 (iPr, CH₃).

^{13}C -NMR (125 MHz, CD_3CN , 300 K): $\delta = 128.44$ (Bn, ϕ), 128.21 (Bn, ϕ), 127.72 (Bn, ϕ), 101.28 (C^1), 76.99 (C^2), 75.29 (C^5), 74.16 (Bn, $\underline{\text{CH}_2}$), 72.04 (iPr, $\underline{\text{CH}}$), 71.74 (C^3), 66.50 ($\underline{\text{CH}_2}$), 65.77 (Asp, $\underline{\text{CH}_2}$), 64.40 (C^4), 46.60 (CDA, $\underline{\text{CH}_3}$), 27.28 (CDA, $\underline{\text{CH}_2}$), 21.67 (iPr, $\underline{\text{CH}_3}$), 21.57 (CDA, $\underline{\text{CH}_2}$).

α :

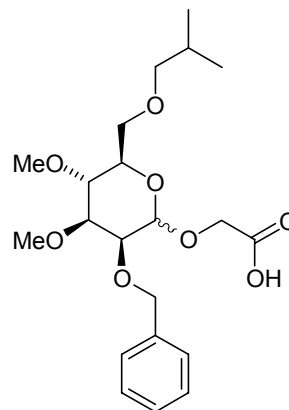
^1H -NMR (500 MHz, CD_3CN , 300 K): $\delta = 7.46$ (d, $J = 7.2$ Hz, 2H), 7.39 (t, $J = 7.2$ Hz, 2H), 7.36 – 7.31 (m, 1H), 4.93 (s, 1H), 4.82 (d, $J = 11.6$ Hz, 1H), 4.64 (d, $J = 11.6$ Hz, 1H), 4.25 (t, $J = 10.2$ Hz, 1H), 4.20 – 4.13 (m, 3H), 3.81 (s, 1H), 3.76 – 3.71 (m, 1H), 3.67 – 3.51 (m, 3H), 3.22 (s, 3H), 3.20 (s, 3H), 1.84 – 1.60 (m, 4H), 1.57 – 1.34 (m, 4H), 1.17 – 1.07 (m, 6H).

Assignment: $\delta = 7.46$ (Bn, ϕ), 7.39 (Bn, ϕ), 7.33 (Bn, ϕ), 4.93 (H^1), 4.82 (Bn, $\underline{\text{CH}_2}$), 4.64 (Bn, $\underline{\text{CH}_2}$), 4.25 (H^4), 4.17 (Asp, $\underline{\text{CH}_2}$), 4.16 (H^3), 3.81 (H^2), 3.74 (H^5), 3.62 (iPr, $\underline{\text{CH}}$), 3.58 ($\underline{\text{CH}_2}$), 3.22 (CDA, $\underline{\text{CH}_3}$), 3.20 (CDA, $\underline{\text{CH}_3}$), 1.77 (CDA, $\underline{\text{CH}_2}$), 1.66 (CDA, $\underline{\text{CH}_2}$), 1.52 (CDA, $\underline{\text{CH}_2}$), 1.40 (CDA, $\underline{\text{CH}_2}$), 1.13 (iPr, $\underline{\text{CH}_3}$).

^{13}C -NMR (125 MHz, CD_3CN , 300 K): $\delta = 128.61$ (Bn, ϕ), 128.38 (Bn, ϕ), 127.97 (Bn, ϕ), 99.22 (C^1), 76.76 (C^2), 72.98 (Bn, $\underline{\text{CH}_2}$), 72.00 (C^5), 72.00 (iPr, $\underline{\text{CH}}$), 69.75 (C^3), 66.21 ($\underline{\text{CH}_2}$), 64.26 (C^4), 63.65 (Asp, $\underline{\text{CH}_2}$), 46.46 (CDA, $\underline{\text{CH}_3}$), 27.28 (CDA, $\underline{\text{CH}_2}$), 21.67 (iPr, $\underline{\text{CH}_3}$), 21.56 (CDA, $\underline{\text{CH}_2}$).

ESI-MS: m/z : 533.3 [$\text{M}+\text{Na}^+$], MW calcd. for $\text{C}_{26}\text{H}_{38}\text{O}_{10}$: 510.2.

8.3.27 Synthesis of [carboxymethyl]-2-*O*-benzyl-6-*O*-isobutyl-3,4-di-*O*-methyl- α,β -D-mannopyranoside (**39**)



Ethyl-2-*O*-benzyl-6-*O*-isobutyl-3,4-di-*O*-methyl-1-thio- α -D-mannopyranoside **32** was either reacted with Br₂, as outlined in 8.3.4, and successively the fresh prepared mannosyl bromide as glycosyl donor was coupled to anhydrous glycolic acid methyl ester (8.3.6) to give preferentially the β -anomer or **32** was reacted directly with glycolic acid methyl ester as described in 8.3.5 to give preferentially the α -anomer. Hydrolysis of the methyl ester in 10 mL of 1:1 solution of 1 M NaOH and MeOH for 1 hour afforded quantitatively α,β **39** which were purified by HPLC.

β :

¹H-NMR (500 MHz, CD₃CN, 300 K): δ = 7.44 (d, *J* = 7.9 Hz, 2H), 7.41 – 7.35 (m, 2H), 7.31 (t, *J* = 7.6 Hz, 1H), 4.87 (d, *J* = 11.9 Hz, 1H), 4.75 (d, *J* = 11.9 Hz, 1H), 4.60 (s, 1H), 4.31 – 4.27 (m, 2H), 4.06 (d, *J* = 3.7 Hz, 1H), 3.67 – 3.54 (m, 2H), 3.46 (s, 3H), 3.43 – 3.37 (m, 4H), 3.34 – 3.25 (m, 3H), 3.22 – 3.16 (m, 1H), 1.89 – 1.80 (m, 1H), 0.92 (d, *J* = 5.8 Hz, 3H), 0.90 (d, *J* = 5.8 Hz, 3H).

Assignment: δ = 7.44 (Bn, ϕ), 7.38 (Bn, ϕ), 7.32 (Bn, ϕ), 4.87 (Bn, $\underline{\text{CH}}_2$), 4.75 (Bn, $\underline{\text{CH}}_2$), 4.61 (H¹), 4.29 (Asp, $\underline{\text{CH}}_2$), 4.05 (H²), 3.62 ($\underline{\text{CH}}_2$), 3.46 (O $\underline{\text{CH}}_3$), 3.39 (O $\underline{\text{CH}}_3$), 3.39 (H⁴), 3.32 (Leu, $\underline{\text{CH}}_2$), 3.30 (H⁵), 3.28 (H³), 3.19 (Leu, $\underline{\text{CH}}_2$), 1.85 (Leu, $\underline{\text{CH}}$), 0.91 (Leu, $\underline{\text{CH}}_3$).

¹³C-NMR (125 MHz, CD₃CN, 300 K): δ = 128.37 (Bn, ϕ), 128.22 (Bn, ϕ), 127.81 (Bn, ϕ), 101.25 (C¹), 83.95 (C³), 78.28 (Leu, $\underline{\text{CH}}_2$), 76.37 (C⁴), 75.73 (C⁵), 74.94 (C²), 74.46

(Bn, $\underline{\text{CH}}_2$), 70.07 ($\underline{\text{CH}}_2$), 65.69 (Asp, $\underline{\text{CH}}_2$), 60.11 ($\text{O}\underline{\text{CH}}_3$), 56.84 ($\text{O}\underline{\text{CH}}_3$), 28.74 (Leu, $\underline{\text{CH}}$), 19.12 (Leu, $\underline{\text{CH}}_3$).

α :

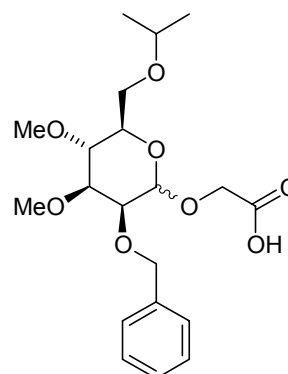
$^1\text{H-NMR}$ (500 MHz, CD_3CN , 300 K): $\delta = 7.43 - 7.36$ (m, 4H), 7.36 - 7.30 (m, 1H), 4.98 (s, 1H), 4.67 (s, 2H), 4.15 (s, 2H), 3.91 (s, 1H), 3.63 - 3.53 (m, 3H), 3.52 - 3.43 (m, 5H), 3.40 (s, 3H), 3.34 - 3.28 (m, 1H), 3.21 - 3.16 (m, 1H), 1.90 - 1.79 (m, 1H), 0.92 (d, $J = 6.1$ Hz, 3H), 0.90 (d, $J = 6.1$ Hz, 3H).

Assignment: $\delta = 7.39$ (Bn, ϕ), 7.38 (Bn, ϕ), 7.32 (Bn, ϕ), 4.98 (H^1), 4.67 (Bn, $\underline{\text{CH}}_2$), 4.15 (Asp, $\underline{\text{CH}}_2$), 3.91 (H^2), 3.58 ($\underline{\text{CH}}_2$), 3.57 (H^5), 3.48 (H^3), 3.47 ($\text{O}\underline{\text{CH}}_3$), 3.47 (H^4), 3.40 ($\text{O}\underline{\text{CH}}_3$), 3.30 (Leu, $\underline{\text{CH}}_2$), 3.18 (Leu, $\underline{\text{CH}}_2$), 1.84 (Leu, $\underline{\text{CH}}$), 0.90 (Leu, $\underline{\text{CH}}_3$).

$^{13}\text{C-NMR}$ (125 MHz, CD_3CN , 300 K): $\delta = 128.69$ (Bn, ϕ), 128.13 (Bn, ϕ), 127.95 (Bn, ϕ), 98.07 (C^1), 81.61 (C^3), 78.20 (Leu, $\underline{\text{CH}}_2$), 76.39 (C^4), 74.74 (C^2), 72.80 (Bn, $\underline{\text{CH}}_2$), 72.47 (C^5), 70.02 ($\underline{\text{CH}}_2$), 63.61 (Asp, $\underline{\text{CH}}_2$), 60.13 ($\text{O}\underline{\text{CH}}_3$), 56.99 ($\text{O}\underline{\text{CH}}_3$), 28.74 (Leu, $\underline{\text{CH}}$), 19.00 (Leu, $\underline{\text{CH}}_3$).

ESI-MS: m/z : 435.2 [$\text{M} + \text{Na}^+$], MW calcd. for $\text{C}_{21}\text{H}_{32}\text{O}_8$: 412.2.

8.3.28 Synthesis of [carboxymethyl]-2-*O*-benzyl-6-*O*-isopropyl-3,4-di-*O*-methyl- α,β -D-mannopyranoside (**40**)



Ethyl-2-*O*-benzyl-6-*O*-isopropyl-3,4-di-*O*-methyl-1-thio- α -D-mannopyranoside **33** was either reacted with Br₂, as outlined in 8.3.4, and successively the fresh prepared mannosyl bromide as glycosyl donor was coupled to anhydrous glycolic acid methyl ester (8.3.6) to give preferentially the β -anomer or **33** was reacted directly with glycolic acid methyl ester as described in 8.3.5 to give preferentially the α -anomer. Hydrolysis of the methyl ester in 10 mL of 1:1 solution of 1 M NaOH and MeOH for 1 hour afforded quantitatively α,β **40** which were purified by HPLC.

β :

¹H-NMR (500 MHz, CD₃CN, 300 K): δ = 7.44 (d, *J* = 7.6 Hz, 2H), 7.39 (t, *J* = 7.6 Hz, 2H), 7.32 (t, *J* = 7.6 Hz, 1H), 4.86 (d, *J* = 11.4 Hz, 1H), 4.75 (d, *J* = 11.4 Hz, 1H), 4.60 (s, 1H), 4.34 – 4.26 (m, 2H), 4.05 (d, *J* = 3.4 Hz, 1H), 3.69 – 3.56 (m, 3H), 3.47 (s, 3H), 3.41 – 3.36 (m, 4H), 3.29 – 3.25 (m, 2H), 1.16 – 1.13 (m, 6H).

Assignment: δ = 7.44 (Bn, ϕ), 7.39 (Bn, ϕ), 7.32 (Bn, ϕ), 4.86 (Bn, $\underline{\text{CH}}_2$), 4.75 (Bn, $\underline{\text{CH}}_2$), 4.60 (H¹), 4.30 (Asp, $\underline{\text{CH}}_2$), 4.05 (H²), 3.68 ($\underline{\text{CH}}_2$), 3.64 (iPr, $\underline{\text{CH}}$), 3.58 ($\underline{\text{CH}}_2$), 3.47 (O $\underline{\text{CH}}_3$), 3.39 (O $\underline{\text{CH}}_3$), 3.39 (H⁴), 3.27 (H⁵), 3.27 (H³), 1.15 (iPr, $\underline{\text{CH}}_3$).

¹³C-NMR (125 MHz, CD₃CN, 300 K): δ = 128.44 (Bn, ϕ), 128.22 (Bn, ϕ), 127.79 (Bn, ϕ), 101.39 (C¹), 84.10 (C³), 76.34 (C⁴), 75.90 (C⁵), 74.94 (C²), 74.72 (Bn, $\underline{\text{CH}}_2$), 72.09 (iPr, $\underline{\text{CH}}$), 67.40 ($\underline{\text{CH}}_2$), 65.93 (Asp, $\underline{\text{CH}}_2$), 60.15 (O $\underline{\text{CH}}_3$), 56.85 (O $\underline{\text{CH}}_3$), 21.75 (iPr, $\underline{\text{CH}}_3$).

α :

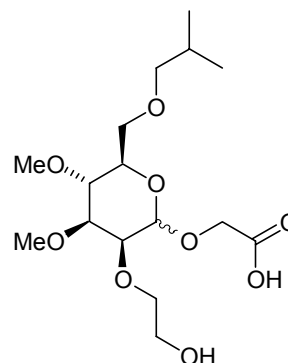
$^1\text{H-NMR}$ (500 MHz, CD_3CN , 300 K): $\delta = 7.42 - 7.30$ (m, 5H), 4.97 (s, 1H), 4.67 (s, 2H), 4.15 (s, 2H), 3.91 (s, 1H), 3.65 – 3.41 (m, 9H), 3.40 (s, 3H), 1.16 – 1.10 (m, 6H).

Assignment: $\delta = 7.41$ (Bn, ϕ), 7.40 (Bn, ϕ), 7.33 (Bn, ϕ), 4.97 (H^1), 4.67 (Bn, $\underline{\text{CH}_2}$), 4.15 (Asp, $\underline{\text{CH}_2}$), 3.91 (H^2), 3.62 (iPr, $\underline{\text{CH}}$), 3.58 ($\underline{\text{CH}_2}$), 3.55 (H^5), 3.48 (OCH_3), 3.47 (H^3), 3.46 (H^4), 3.40 (OCH_3), 1.14 (iPr, $\underline{\text{CH}}$).

$^{13}\text{C-NMR}$ (125 MHz, CD_3CN , 300 K): $\delta = 128.69$ (Bn, ϕ), 128.22 (Bn, ϕ), 128.01 (Bn, ϕ), 98.21 (C^1), 81.78 (C^3), 76.37 (C^4), 74.75 (C^2), 72.86 (Bn, $\underline{\text{CH}_2}$), 72.58 (C^5), 72.01 (iPr, $\underline{\text{CH}}$), 67.24 ($\underline{\text{CH}_2}$), 63.59 (Asp, $\underline{\text{CH}_2}$), 60.07 (OCH_3), 57.05 (OCH_3), 21.68 (iPr, $\underline{\text{CH}_3}$).

ESI-MS: m/z : 421.3 [$\text{M}+\text{Na}^+$], MW calcd. for $\text{C}_{20}\text{H}_{30}\text{O}_8$: 398.2.

8.3.29 Synthesis of [carboxymethyl]-2-*O*-[2'-hydroxyethyl]-6-*O*-isobutyl-3,4-di-*O*-methyl- α,β -D-mannopyranoside (44)



Ethyl-2-*O*-benzyl-6-*O*-isobutyl-3,4-di-*O*-methyl-1-thio- α -D-mannopyranoside **32** was either reacted with Br₂, as outlined in 8.3.4, and successively the fresh prepared mannosyl bromide as glycosyl donor was coupled to anhydrous glycol aldehyde dimethyl acetal (8.3.6) to give preferentially the β -anomer or **32** was reacted directly with glycol aldehyde dimethyl acetal as described in 8.3.5 to give preferentially the α -anomer. The benzyl group was then cleaved as outline in 8.3.14 and the residue coupled with bromoethyl-2-benzyl ether under Williamson conditions described in 8.3.1. A solution of [2',2'-dimethoxyethyl]-2-*O*-[2'-benzyloxyethyl]-6-*O*-isobutyl-3,4-di-*O*-methyl-D-mannopyranoside **42** (0.2 mmol, α,β anomers were kept in different flasks) in a mixture of 10 mL 2 N aqueous HCl and 10 mL THF was stirred at room temperature for 1 hour until completion of the reaction (TLC). The solution was neutralized with NaHCO₃, the aldehyde extracted with ether and the organic extract concentrated. The residue was then dissolved in 8 mL *tert*-BuOH and 3 mL 2-methyl-2-butene. An equiv. of NaClO₂ (18.0 mg, 0.2 mmol) together with 0.3 g (2.52 mmol) sodium dihydrogenphosphate were dissolved in 3 mL of H₂O and added dropwise to the previous solution. At completion of the reaction (3 hours) the solution was treated with an aqueous Na₂SO₃ to destroy the excess of NaClO₂. The solvent was evaporated and the aqueous solution was extracted with EtOAc (5 x 15 mL). The organic extract was dried (Na₂SO₄), concentrated and the residue used in the following reaction without purification. The benzyl group was then cleaved as outline in 8.3.14 and both α,β anomers purified by HPLC.

β:

¹H-NMR (500 MHz, CDCl₃, 300 K): δ = 4.52 (s, 1H), 4.35 (d, J = 16.5 Hz, 1H), 4.35 – 4.30 (m, 2H), 4.30 (d, J = 16.5 Hz, 1H), 3.85 – 3.79 (m, 1H), 3.78 – 3.58 (m, 4H), 3.52 (s, 3H), 3.51 – 3.45 (m, 4H), 3.34 – 3.26 (m, 2H), 3.22 – 3.14 (m, 2H), 1.86 (m, 1H), 0.89 (d, J = 6.7 Hz, 3H), 0.88 (d, J = 6.7 Hz, 3H).

Assignment: δ = 4.52 (H¹), 4.30 (Asp, CH₂), 3.99 (Ser, CH₂), 3.95 (H²), 3.82 (Ser, CH₂), 3.72 (Ser, CH₂), 3.66 (CH₂), 3.61 (CH₂), 3.52 (OCH₃), 3.51 (OCH₃), 3.50 (H⁴), 3.32 (H⁵), 3.29 (Leu, CH₂), 3.20 (H³), 3.17 (Leu, CH₂), 1.86 (Leu, CH), 0.88 (Leu, CH₃).

¹³C-NMR (125 MHz, CDCl₃, 300 K): δ = 100.44 (C¹), 83.94 (C³), 78.63 (Leu, CH₂), 76.26 (C⁴), 75.81 (C²), 75.64 (C⁵), 74.00 (Ser, CH₂), 69.60 (CH₂), 66.37 (Asp, CH₂), 61.86 (Ser, CH₂), 60.78 (OCH₃), 58.41 (OCH₃), 28.29 (Leu, CH), 19.24 (Leu, CH₃).

α:

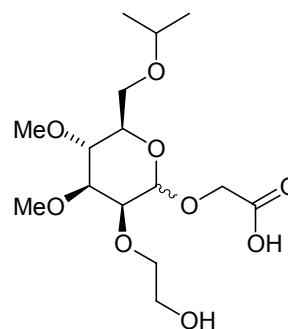
¹H-NMR (500 MHz, CD₃CN, 300 K): δ = 4.93 (s, 1H), 4.15 (s, 2H), 3.83 (s, 1H), 3.74 – 3.54 (m, 7H), 3.51 – 3.39 (m, 8H), 3.34 – 3.27 (m, 1H), 3.22 – 3.16 (m, 1H), 1.92 – 1.81 (m, 1H), 0.92 (d, J = 6.4 Hz, 3H), 0.91 (d, J = 6.4 Hz, 3H).

Assignment: δ = 4.93 (H¹), 4.15 (Asp, CH₂), 3.83 (H²), 3.68 (Ser, CH₂), 3.65 (Ser, CH₂), 3.61 (Ser, CH₂), 3.58 (Ser, CH₂), 3.57 (CH₂), 3.57 (H⁵), 3.48 (OCH₃), 3.47 (OCH₃), 3.47 (H³), 3.42 (H⁴), 3.30 (Leu, CH₂), 3.19 (Leu, CH₂), 1.86 (Leu, CH), 0.92 (Leu, CH₃).

¹³C-NMR (125 MHz, CDCl₃, 300 K): δ = 98.37 (C¹), 81.70 (C³), 78.30 (Leu, CH₂), 76.63 (C⁴), 75.94 (C²), 72.94 (Ser, CH₂), 72.39 (C⁵), 70.07 (CH₂), 63.71 (Asp, CH₂), 61.37 (Ser, CH₂), 60.10 (OCH₃), 57.60 (OCH₃), 28.72 (Leu, CH), 19.01 (Leu, CH₃).

ESI-MS: *m/z*: 389.1 [M+Na⁺], MW calcd. for C₁₆H₃₀O₉: 366.2.

8.3.30 Synthesis of [carboxymethyl]-2-*O*-[2'-hydroxyethyl]-6-*O*-isopropyl-3,4-di-*O*-methyl- α,β -D-mannopyranoside (**46**)



Ethyl-2-*O*-benzyl-6-*O*-isopropyl-3,4-di-*O*-methyl-1-thio- α -D-mannopyranoside **33** was either reacted with Br₂, as outlined in 8.3.4, and successively the fresh prepared mannosyl bromide as glycosyl donor was coupled to anhydrous glycol aldehyde dimethyl acetal (8.3.6) to give preferentially the β -anomer or **33** was reacted directly with glycol aldehyde dimethyl acetal as described in 8.3.5 to give preferentially the α -anomer. The benzyl group was then cleaved as outline in 8.3.14 and the residue coupled with bromoethyl-2-benzyl ether under Williamson conditions described in 8.3.1. A solution of [2',2'-dimethoxyethyl]-2-*O*-[2'-benzyloxyethyl]-6-*O*-isopropyl-3,4-di-*O*-methyl-D-mannopyranoside **45** (0.2 mmol, α,β anomers were kept in different flasks) in a mixture of 10 mL 2 N aqueous HCl and 10 mL THF was stirred at room temperature for 1 hour until completion of the reaction (TLC). The solution was neutralized with NaHCO₃, the aldehyde extracted with ether and the organic extract concentrated. The residue was then dissolved in 8 mL *tert*-BuOH and 3 mL 2-methyl-2-butene. An equiv. of NaClO₂ (18.0 mg, 0.2 mmol) together with 0.3 g (2.52 mmol) sodium dihydrogenphosphate were dissolved in 3 mL of H₂O and added dropwise to the previous solution. At completion of the reaction (3 hours) the solution was treated with an aqueous Na₂SO₃ to destroy the excess of NaClO₂. The solvent was evaporated and the aqueous solution was extracted with EtOAc (5 x 15 mL). The organic extract was dried (Na₂SO₄), concentrated and the residue used in the following reaction without purification. The benzyl group was then cleaved as outline in 8.3.14 and both α,β anomers purified by HPLC.

β:

¹H-NMR (500 MHz, CDCl₃, 300 K): δ = 4.55 (s, 1H), 4.32 – 4.23 (m, 2H), 3.94 (d, J = 2.7 Hz, 1H), 3.81 – 3.72 (m, 2H), 3.67 – 3.55 (m, 5H), 3.48 (s, 3H), 3.47 (s, 3H), 3.51 (t, J = 10.2 Hz, 1H), 3.26 – 3.20 (m, 2H), 1.18 – 1.14 (m, 6H).

Assignment: δ = 4.55 (H¹), 4.27 (Asp, CH₂), 3.94 (H²), 3.77 (Ser, CH₂), 3.66 (CH₂), 3.63 (iPr, CH), 3.61 (Ser, CH₂), 3.58 (CH₂), 3.48 (OCH₃), 3.47 (OCH₃), 3.36 (H⁴), 3.25 (H³), 3.22 (H⁵), 1.16 (iPr, CH₃).

¹³C-NMR (125 MHz, CDCl₃, 300 K): δ = 100.54 (C¹), 84.20 (C³), 76.53 (C⁴), 75.88 (C²), 75.73 (C⁵), 74.70 (Ser, CH₂), 72.14 (iPr, CH), 67.26 (CH₂), 65.78 (Asp, CH₂), 61.38 (Ser, CH₂), 60.20 (OCH₃), 57.64 (OCH₃), 21.68 (iPr, CH₃).

α:

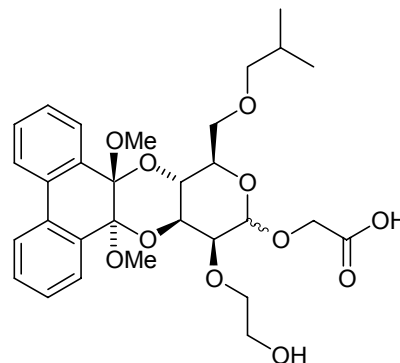
¹H-NMR (500 MHz, CDCl₃, 300 K): δ = 4.92 (s, 1H), 4.15 (s, 2H), 3.83 (s, 1H), 3.72 – 3.51 (m, 8H), 3.50 – 3.38 (m, 8H), 1.18 – 1.13 (m, 6H).

Assignment: δ = 4.92 (H¹), 4.15 (Asp, CH₂), 3.83 (H²), 3.69 (Ser, CH₂), 3.64 (Ser, CH₂), 3.62 (Ser, CH₂), 3.62 (iPr, CH), 3.58 (Ser, CH₂), 3.58 (CH₂), 3.54 (H⁵), 3.48 (OCH₃), 3.48 (OCH₃), 3.46 (H³), 3.44 (H⁴), 1.15 (iPr, CH₃).

¹³C-NMR (125 MHz, CDCl₃, 300 K): δ = 98.41 (C¹), 81.72 (C³), 76.60 (C⁴), 76.17 (C²), 73.12 (Ser, CH₂), 72.46 (C⁵), 72.10 (iPr, CH), 67.23 (CH₂), 63.86 (Asp, CH₂), 61.35 (Ser, CH₂), 60.22 (OCH₃), 57.72 (OCH₃), 21.75 (iPr, CH₃).

ESI-MS: *m/z*: 375.1 [M+Na⁺], MW calcd. for C₁₅H₂₈O₉: 352.2.

8.3.31 Synthesis of [carboxymethyl]-2-*O*-[2'-hydroxyethyl]-3,4-*O*-[9',10'-dimethoxyphenanthrene-9',10'-diyl]-6-*O*-isobutyl- α,β -D-mannopyranoside (49)



[2'-hydroxyethyl]-2-*O*-benzyl-3,4-*O*-[9',10'-dimethoxy-phenanthrene-9',10'-diyl]-6-*O*-isobutyl- α,β -D-mannopyranoside **34** (6.5 mmol) and imidazole (19.5 mmol) were dissolved in 25 mL DMF and the solution was stirred at room temperature. Successively, *tert*-butyl diphenyl silyl chloride (TBDPSCl, 8.5 mmol) was added dropwise. Stirring was continued for 3 hours until completion of the reaction, followed by TLC. The solvent was evaporated under vacuum and the residue purified by flash column chromatography (gradient elution: hexane/EtOAc 9:1 to hexane/EtOAc 4:1) to give the title compound as a colorless oil (5.5 mmol, 85 %). The benzyl group at position 2 was then cleaved as outline in 8.3.14 and the residue coupled with bromoethyl-2-benzyl ether under Williamson conditions described in 8.3.1. TBDPS removal was carried out overnight under stirring in 20 mL THF using 2 eq. of tetrabutylammonium fluoride (TBAF) of a 1 M TBAF solution in THF. The solvent was evaporated and the residue purified by flash column chromatography (gradient elution: hexane/EtOAc 6:1 to hexane/EtOAc 4:1) (96 %). The free primary alcohol present in [2'-hydroxyethyl]-2-*O*-[2'-benzyloxyethyl]-6-*O*-isopropyl-3,4-di-*O*-methyl-D-mannopyranoside **48** (0.2 mmol, α,β anomers were kept in different flasks) was then oxidized to aldehyde as described in 8.3.7. The residue was then dissolved in 8 mL *tert*-BuOH and 3 mL 2-methyl-2-butene. An equiv. of NaClO₂ (18.0 mg, 0.2 mmol) together with 0.3 g (2.52 mmol) sodium dihydrogenphosphate were dissolved in 3 mL of H₂O and added dropwise to the previous solution. At completion of the reaction (3 hours) the solution was treated with an aqueous Na₂SO₃ to destroy the excess of NaClO₂. The solvent was evaporated and the aqueous solution was extracted with

EtOAc (5 x 15 mL). The organic extract was dried (Na_2SO_4), concentrated and the residue used in the following reaction without purification. The benzyl group was then cleaved as outline in 8.3.14 and both α,β anomers purified by HPLC.

β :

$^1\text{H-NMR}$ (500 MHz, CD_3CN , 300 K): δ = 7.84 (d, J = 7.3 Hz, 2H), 7.61 (d, J = 7.6 Hz, 1H), 7.58 (d, J = 7.6 Hz, 1H), 7.51 – 7.45 (m, 2H), 7.40 – 7.34 (m, 2H), 4.81 (s, 1H), 4.41 – 4.28 (m, 3H), 4.16 – 4.11 (m, 1H), 4.08 (s, 1H), 3.94 – 3.78 (m, 4H), 3.75 – 3.65 (m, 3H), 3.39 – 3.29 (m, 2H), 2.86 (s, 3H), 2.85 (s, 3H), 1.94 – 1.85 (m, 1H), 0.96 – 0.91 (m, 6H).

Assignment: δ = 7.84 (PDA, $\text{H}^{4,5}$), 7.61 (PDA, H^1), 7.58 (PDA, H^8), 7.47 (PDA, $\text{H}^{3,6}$), 7.36 (PDA, $\text{H}^{2,7}$), 4.81 (H^1), 4.36 (Asp, CH_2), 4.34 (Asp, CH_2), 4.31 (H^4), 4.14 (H^3), 4.08 (H^2), 3.90 (hydroxyethyl, CH_2), 3.85 (CH_2), 3.81 (CH_2), 3.69 (hydroxyethyl, CH_2), 3.68 (H^5), 3.36 (Leu, CH_2), 3.32 (Leu, CH_2), 2.86 (PDA, CH_3), 2.85 (PDA, CH_3), 1.90 (Leu, CH), 0.94 (Leu, CH_3).

$^{13}\text{C-NMR}$ (125 MHz, CD_3CN , 300 K): δ = 129.57 (PDA, $\text{C}^{3,6}$), 127.47 (PDA, $\text{C}^{2,7}$), 125.77 (PDA, $\text{C}^{1,8}$), 124.64 (PDA, $\text{C}^{4,5}$), 100.66 (C^1), 78.76 (Leu, CH_2), 77.30 (C^2), 74.82 (C^5), 74.65 (hydroxyethyl, CH_2), 71.69 (C^3), 69.31 (CH_2), 65.71 (Asp, CH_2), 64.73 (C^4), 61.27 (hydroxyethyl, CH_2), 48.84 (PDA, CH_3), 28.68 (Leu, CH), 18.98 (Leu, CH_3).

α :

$^1\text{H-NMR}$ (500 MHz, CD_3CN , 300 K): δ = 7.85 (d, J = 8.2 Hz, 2H), 7.64 – 7.58 (m, 2H), 7.51 – 7.45 (m, 2H), 7.41 – 7.33 (m, 2H), 5.03 (s, 1H), 4.44 – 4.34 (m, 2H), 4.26 (s, 2H), 4.02 – 3.96 (m, 2H), 3.93 – 3.72 (m, 5H), 3.65 – 3.59 (m, 1H), 3.39 – 3.27 (m, 4H), 2.87 (s, 3H), 2.85 (s, 3H), 1.93 – 1.84 (m, 1H), 0.96 – 0.90 (m, 6H).

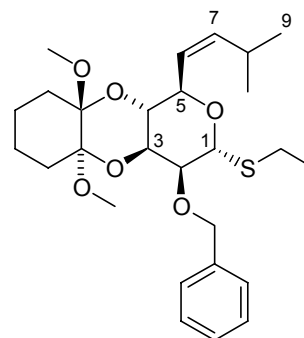
Assignment: δ = 7.85 (PDA, $\text{H}^{4,5}$), 7.62 (PDA, H^1), 7.59 (PDA, H^8), 7.48 (PDA, $\text{H}^{3,6}$), 7.37 (PDA, $\text{H}^{2,7}$), 5.03 (H^1), 4.41 (H^4), 4.37 (H^3), 4.26 (Asp, CH_2), 3.99 (H^2), 3.99 (H^5), 3.89 (hydroxyethyl, CH_2), 3.85 (hydroxyethyl, CH_2), 3.83 (CH_2), 3.78 (CH_2),

3.75 (hydroxyethyl, $\underline{\text{CH}_2}$), 3.63 (hydroxyethyl, $\underline{\text{CH}_2}$), 3.36 (Leu, $\underline{\text{CH}_2}$), 3.31 (Leu, $\underline{\text{CH}_2}$), 2.87 (PDA, $\underline{\text{CH}_3}$), 2.85 (PDA, $\underline{\text{CH}_3}$), 1.90 (Leu, $\underline{\text{CH}}$), 0.94 (Leu, $\underline{\text{CH}_3}$).

^{13}C -NMR (125 MHz, CD_3CN , 300 K): δ = 129.49 (PDA, $\text{C}^{3,6}$), 127.46 (PDA, $\text{C}^{2,7}$), 125.73 (PDA, $\text{C}^{1,8}$), 124.54 (PDA, $\text{C}^{4,5}$), 99.85 (C^1), 78.59 (Leu, $\underline{\text{CH}_2}$), 77.51 (C^2), 73.55 (hydroxyethyl, $\underline{\text{CH}_2}$), 71.75 (C^5), 70.13 (C^3), 69.32 ($\underline{\text{CH}_2}$), 64.54 (C^4), 63.82 (Asp, $\underline{\text{CH}_2}$), 61.39 (hydroxyethyl, $\underline{\text{CH}_2}$), 48.96 (PDA, $\underline{\text{CH}_3}$), 28.71 (Leu, $\underline{\text{CH}}$), 19.05 (Leu, $\underline{\text{CH}_3}$).

ESI-MS: m/z = 597.3 [$\text{M}+\text{Na}^+$], MW calcd. for $\text{C}_{30}\text{H}_{38}\text{O}_{11}$: 574.2.

8.3.32 Synthesis of α -D-manno-Non-6-enopyranoside, ethyl-6,7,8,9-tetra-deoxy-2-O-benzyl-3,4-O-[1',2'-dimethoxycyclohexan-1',2'-diyl]-8-methyl-1-thio (50)



The free primary alcohol in ethyl-2-O-benzyl-3,4-O-[1',2'-dimethoxycyclohexan-1',2'-diyl]-1-thio- α -D-manno-pyranoside **28** was oxidized to aldehyde following the general procedure 8.3.7. The aldehyde was then reacted with isobutyl triphenylphosphonium chloride salt (8.3.8) under conditions described in 8.3.9 with good Z/E selectivity (>10: 1).

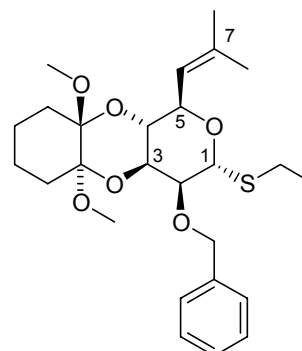
$^1\text{H-NMR}$ (500 MHz, CDCl_3 , 300 K): δ = 7.47 – 7.26 (m, 5H), 5.48 (t, J = 10.4 Hz, 1H), 5.29 (t, J = 10.4 Hz, 1H), 5.24 (s, 1H), 4.93 (d, J = 12.2 Hz, 1H), 4.80 (t, J = 9.2 Hz, 1H), 4.68 (d, J = 12.2 Hz, 1H), 4.23 – 4.11 (m, 2H), 3.82 (s, 1H), 3.23 (s, 3H), 3.20 (s, 3H), 2.76 – 2.54 (m, 3H), 1.88-1.65 (m, 4H), 1.56 – 1.35 (m, 4H), 1.25 (t, J = 7.3 Hz, 3H), 0.99 – 0.94 (m, 6H).

Assignment: δ = 7.45 (Bn, ϕ), 7.34 (Bn, ϕ), 7.28 (Bn, ϕ), 5.48 (H^7), 5.29 (H^6), 5.24 (H^1), 4.93 (Bn, CH_2), 4.80 (H^5), 4.68 (Bn, CH_2), 4.18 (H^3), 4.15 (H^4), 3.82 (H^2), 3.23 (CDA, CH_3), 3.20 (CDA, CH_3), 2.73 (H^8), 2.61 (SEt, CH_2), 1.78 (CDA, CH_2), 1.54 (CDA, CH_2), 1.40 (CDA, CH_2), 1.25 (SEt, CH_3), 0.97 (CH_3).

$^{13}\text{C-NMR}$ (125 MHz, CDCl_3 , 300 K): δ = 128.58 (Bn, ϕ), 128.48 (Bn, ϕ), 127.84 (Bn, ϕ), 144.06 (C^7), 123.83 (C^6), 84.32 (C^1), 78.49 (C^2), 73.24 (Bn, CH_2), 70.57 (C^3), 68.59 (C^4), 68.00 (C^5), 47.01 (CDA, CH_3), 46.81 (CDA, CH_3), 27.88 (C^8), 27.32 (CDA, CH_2), 25.86 (SEt, CH_2), 23.34 (CH_3), 21.73 (CDA, CH_2), 15.34 (SEt, CH_3).

ESI-MS: m/z = 515.4 [$\text{M}+\text{Na}^+$], MW calcd. for $\text{C}_{27}\text{H}_{40}\text{O}_6\text{S}$: 492.3.

8.3.33 Synthesis of α -D-manno-Oct-6-enopyranoside, ethyl-6,7,8-trideoxy-2-O-benzyl-3,4-O-[1',2'-dimethoxycyclohexan-1',2'-diyl]-7-methyl-1-thio (51)



The free primary alcohol in ethyl-2-O-benzyl-3,4-O-[1',2'-dimethoxycyclohexan-1',2'-diyl]-1-thio- α -D-manno-pyranoside **28** was oxidized to aldehyde following the general procedure 8.3.7. The aldehyde was then reacted with isopropyl triphenylphosphonium iodide salt (8.3.8) under conditions described in 8.3.9.

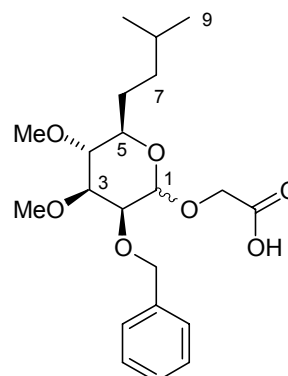
$^1\text{H-NMR}$ (500 MHz, CDCl_3 , 300 K): δ = 7.48 – 7.26 (m, 5H), 5.28 (d, J = 8.9 Hz, 1H), 5.21 (s, 1H), 4.94 (d, J = 11.9 Hz, 1H), 4.74 (t, J = 8.9 Hz, 1H), 4.69 (d, J = 11.9 Hz, 1H), 4.24 (t, J = 9.5 Hz, 1H), 4.17 (d, J = 11.3 Hz, 1H), 3.84 (s, 1H), 3.25 (s, 6H), 2.73 – 2.57 (m, 2H), 1.95 – 1.65 (m, 10H), 1.60 – 1.36 (m, 4H), 1.26 (t, J = 7.3 Hz, 3H).

Assignment: δ = 7.46 (Bn, ϕ), 7.35 (Bn, ϕ), 7.28 (Bn, ϕ), 5.28 (H^6), 5.21 (H^1), 4.94 (Bn, CH_2), 4.74 (H^5), 4.69 (Bn, CH_2), 4.24 (H^4), 4.17 (H^3), 3.84 (H^2), 3.25 (CDA, CH_3), 2.68 (SEt, CH_2), 2.62 (SEt, CH_2), 1.81 (CDA, CH_2), 1.79 (CH_3), 1.76 (CDA, CH_2), 1.76 (CH_3), 1.54 (CDA, CH_2), 1.41 (CDA, CH_2), 1.26 (SEt, CH_3).

$^{13}\text{C-NMR}$ (125 MHz, CDCl_3 , 300 K): δ = 128.69 (Bn, ϕ), 128.38 (Bn, ϕ), 127.76 (Bn, ϕ), 122.18 (C^6), 84.34 (C^1), 78.68 (C^2), 73.32 (Bn, CH_2), 70.71 (C^3), 69.08 (C^4), 68.33 (C^5), 47.02 (CDA, CH_3), 27.44 (CDA, CH_2), 26.38 (CH_3), 25.98 (SEt, CH_2), 21.78 (CDA, CH_2), 19.25 (CH_3), 15.30 (SEt, CH_3).

ESI-MS: m/z = 501.5 [$\text{M}+\text{Na}^+$], MW calcd. for $\text{C}_{26}\text{H}_{38}\text{O}_6\text{S}$: 478.3.

8.3.34 Synthesis of α,β -D-manno-Non-pyranoside, [carboxymethyl]-6,7,8,9-tetra-deoxy-2-*O*-benzyl-3,4-di-*O*-methyl-8-methyl (56)



The double bond present in α -D-manno-Non-6-enopyranoside, ethyl-6,7,8,9-tetra-deoxy-2-*O*-benzyl-3,4-*O*-[1',2'-dimethoxycyclohexan-1',2'-diyl]-8-methyl-1-thio **50** was reduced with *para*-toluenesulfonylhydrazide following the procedure described in 8.3.12 or by hydrogenation with poisoned Pd/C as outlined in 8.3.13. CDA deprotection was carried out as outlined in 8.3.10. Subsequent methylation at 3 and 4 positions as described in section 8.3.1 using methyl iodide afforded the desired α -D-manno-Non-pyranoside, ethyl-6,7,8,9-tetra-deoxy-2-*O*-benzyl-3,4-di-*O*-methyl-8-methyl-1-thio **54** in 90 % yield. Before purification by flash column chromatography, the excess of toxic alkyl halide was destroyed with a 15 % solution of ammonium hydroxide. To obtain preferentially the β -anomer, α -D-manno-Non-pyranoside, ethyl-6,7,8,9-tetra-deoxy-2-*O*-benzyl-3,4-di-*O*-methyl-8-methyl-1-thio **54** was reacted firstly with *N*-bromosuccinimide (section 8.3.2) and secondly with thionyl chloride (section 8.3.3) and successively the fresh prepared mannosyl chloride as glycosyl donor was coupled to anhydrous glycolic acid methyl ester (8.3.6). Note that the direct activation of SEt with Br₂ as outlined in 8.3.4 did not work in this case. To obtain preferentially the α -anomer, **54** was reacted directly with glycolic acid methyl ester as described in 8.3.5. Hydrolysis of the methyl ester in 10 mL of 1:1 solution of 1 M NaOH and MeOH for 1 hour afforded quantitatively α,β **56** which were purified by HPLC.

β :

¹H-NMR (500 MHz, CD₃CN, 300 K): δ = 7.43 (d, J = 7.6 Hz, 2H), 7.38 (t, J = 7.6 Hz, 2H), 7.31 (t, J = 7.6 Hz, 1H), 4.86 (d, J = 11.9 Hz, 1H), 4.75 (d, J = 11.9 Hz, 1H), 4.57 (s, 1H), 4.31 – 4.24 (m, 2H), 4.04 (d, J = 2.5 Hz, 1H), 3.48 (s, 3H), 3.38 (s, 3H), 3.25

– 3.20 (m, 1H), 3.13 – 3.07 (m, 2H), 1.87 – 1.79 (m, 1H), 1.62 – 1.52 (m, 1H), 1.52 – 1.38 (m, 2H), 1.32 – 1.22 (m, 1H), 0.94 – 0.89 (m, 6H).

Assignment: δ = 7.43 (Bn, ϕ), 7.38 (Bn, ϕ), 7.31 (Bn, ϕ), 4.86 (Bn, $\underline{\text{CH}}_2$), 4.75 (Bn, $\underline{\text{CH}}_2$), 4.57 (H^1), 4.27 (Asp, $\underline{\text{CH}}_2$), 4.04 (H^2), 3.48 (OCH_3), 3.38 (OCH_3), 3.23 (H^3), 3.10 (H^5), 3.10 (H^4), 1.82 ($\underline{\text{CH}}_2^6$), 1.57 (H^8), 1.47 ($\underline{\text{CH}}_2^6$), 1.42 ($\underline{\text{CH}}_2^7$), 1.26 ($\underline{\text{CH}}_2^7$), 0.92 ($\underline{\text{CH}}_3$), 0.91 ($\underline{\text{CH}}_3$).

^{13}C -NMR (125 MHz, CD_3CN , 300 K): δ = 128.49 (Bn, ϕ), 128.29 (Bn, ϕ), 127.80 (Bn, ϕ), 101.09 (C^1), 84.12 (C^3), 80.47 (C^4), 75.78 (C^5), 74.98 (C^2), 74.67 (Bn, $\underline{\text{CH}}_2$), 65.60 (Asp, $\underline{\text{CH}}_2$), 60.23 (OCH_3), 56.71 (OCH_3), 34.73 ($\underline{\text{CH}}_2^7$), 29.53 ($\underline{\text{CH}}_2^6$), 27.99 (C^8), 22.44 ($\underline{\text{CH}}_3$), 21.96 ($\underline{\text{CH}}_3$).

α :

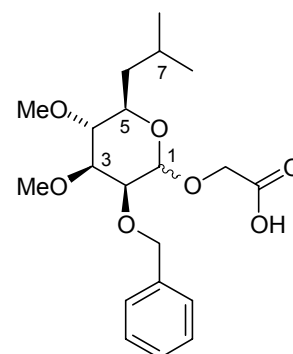
^1H -NMR (500 MHz, CD_3CN , 300 K): δ = 7.41 – 7.30 (m, 5H), 4.94 (s, 1H), 4.67 (s, 2H), 4.13 (s, 2H), 3.90 (s, 1H), 3.50 – 3.38 (m, 8H), 3.16 (t, J = 10.4 Hz, 1H), 1.82 – 1.75 (m, 1H), 1.61 – 1.52 (m, 1H), 1.49 – 1.37 (m, 2H), 1.28 – 1.19 (m, 1H), 0.94 – 0.89 (m, 6H).

Assignment: δ = 7.39 (Bn, ϕ), 7.33 (Bn, ϕ), 4.94 (H^1), 4.67 (Bn, $\underline{\text{CH}}_2$), 4.13 (Asp, $\underline{\text{CH}}_2$), 3.90 (H^2), 3.48 (OCH_3), 3.40 (OCH_3), 3.44 (H^3), 3.40 (H^5), 3.16 (H^4), 1.78 ($\underline{\text{CH}}_2^6$), 1.56 (H^8), 1.43 ($\underline{\text{CH}}_2^6$), 1.40 ($\underline{\text{CH}}_2^7$), 1.23 ($\underline{\text{CH}}_2^7$), 0.92 ($\underline{\text{CH}}_3$), 0.91 ($\underline{\text{CH}}_3$).

^{13}C -NMR (125 MHz, CD_3CN , 300 K): δ = 128.58 (Bn, ϕ), 128.09 (Bn, ϕ), 127.98 (Bn, ϕ), 97.94 (C^1), 81.64 (C^3), 80.48 (C^4), 74.79 (C^2), 72.85 (Bn, $\underline{\text{CH}}_2$), 72.30 (C^5), 63.57 (Asp, $\underline{\text{CH}}_2$), 60.15 (OCH_3), 56.89 (OCH_3), 34.76 ($\underline{\text{CH}}_2^7$), 29.60 ($\underline{\text{CH}}_2^6$), 28.14 (C^8), 22.45 ($\underline{\text{CH}}_3$), 22.00 ($\underline{\text{CH}}_3$).

ESI-MS: m/z : 419.3 [$\text{M}+\text{Na}^+$], MW calcd. for $\text{C}_{21}\text{H}_{32}\text{O}_7$: 396.2.

8.3.35 Synthesis of α,β -D-manno-Oct-pyranoside, [carboxymethyl]-6,7,8-trideoxy-2-*O*-benzyl-3,4-di-*O*-methyl-7-methyl (57)



The double bond present in α -D-manno-Oct-6-enopyranoside, ethyl-6,7,8-trideoxy-2-*O*-benzyl-3,4-*O*-[1',2'-dimethoxycyclohexan-1',2'-diy]-7-methyl-1-thio **51** was reduced with *para*-toluenesulfonylhydrazide following the procedure described in 8.3.12 or by hydrogenation with poisoned Pd/C as outlined in 8.3.13. CDA deprotection was carried out as outlined in 8.3.10. Subsequent methylation at 3 and 4 positions as described in section 8.3.1 using methyl iodide afforded the desired α -D-manno-Oct-pyranoside, ethyl-6,7,8-trideoxy-2-*O*-benzyl-3,4-di-*O*-methyl-7-methyl-1-thio **55** in 90 % yield. Before purification by flash column chromatography, the excess of toxic alkyl halide was destroyed with a 15 % solution of ammonium hydroxide. To obtain preferentially the β -anomer, **55** was reacted firstly with *N*-bromosuccinimide (section 8.3.2) and secondly with thionyl chloride (section 8.3.3) and successively the fresh prepared mannosyl chloride as glycosyl donor was coupled to anhydrous glycolic acid methyl ester (8.3.6). Note that the direct activation of SET with Br₂ as outlined in 8.3.4 did not work in this case. To obtain preferentially the α -anomer, **55** was reacted directly with glycolic acid methyl ester as described in 8.3.5. Hydrolysis of the methyl ester in 10 mL of 1:1 solution of 1 M NaOH and MeOH for 1 hour afforded quantitatively α,β **57** which were purified by HPLC.

β :

¹H-NMR (500 MHz, CD₃CN, 300 K): δ = 7.44 (d, J = 7.3 Hz, 2H), 7.38 (t, J = 7.3 Hz, 2H), 7.32 (t, J = 7.3 Hz, 1H), 4.85 (d, J = 11.9 Hz, 1H), 4.75 (d, J = 11.9 Hz, 1H), 4.58 (s, 1H), 4.30 – 4.23 (m, 2H), 4.05 (d, J = 2.7 Hz, 1H), 3.47 (s, 3H), 3.38 (s, 3H), 3.26

– 3.16 (m, 2H), 3.07 (t, $J = 9.2$ Hz, 1H), 1.91 – 1.81 (m, 1H), 1.60 – 1.54 (m, 1H), 1.49 – 1.43 (m, 1H), 0.98 – 0.88 (m, 6H).

Assignment: $\delta = 7.44$ (Bn, ϕ), 7.38 (Bn, ϕ), 7.32 (Bn, ϕ), 4.85 (Bn, $\underline{\text{CH}_2}$), 4.75 (Bn, $\underline{\text{CH}_2}$), 4.58 (H^1), 4.27 (Asp, $\underline{\text{CH}_2}$), 4.05 (H^2), 3.47 (OCH_3), 3.38 (OCH_3), 3.24 (H^3), 3.19 (H^5), 3.07 (H^4), 1.86 (H^7), 1.58 ($\underline{\text{CH}_2}^6$), 1.47 ($\underline{\text{CH}_2}^6$), 0.96 ($\underline{\text{CH}_3}$), 0.91 ($\underline{\text{CH}_3}$).

^{13}C -NMR (125 MHz, CD_3CN , 300 K): $\delta = 128.53$ (Bn, ϕ), 128.30 (Bn, ϕ), 127.80 (Bn, ϕ), 101.07 (C^1), 84.19 (C^3), 80.93 (C^4), 74.98 (C^2), 74.72 (Bn, $\underline{\text{CH}_2}$), 73.76 (C^5), 65.58 (Asp, $\underline{\text{CH}_2}$), 60.21 (OCH_3), 56.75 (OCH_3), 40.89 ($\underline{\text{CH}_2}^6$), 24.65 (C^7), 23.38 ($\underline{\text{CH}_3}$), 21.13 ($\underline{\text{CH}_3}$).

α :

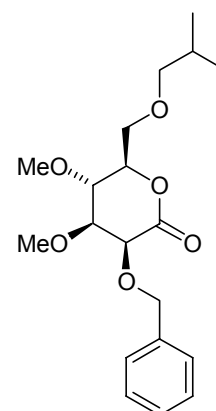
^1H -NMR (500 MHz, CD_3CN , 300 K): $\delta = 7.41$ – 7.31 (m, 5H), 4.93 (s, 1H), 4.67 (s, 2H), 4.20 – 4.13 (m, 2H), 3.91 (s, 1H), 3.51 (t, $J = 9.5$ Hz, 1H), 3.49 – 3.45 (m, 4H), 3.40 (s, 3H), 3.12 (t, $J = 9.2$ Hz, 1H), 1.89 – 1.79 (m, 1H), 1.59 – 1.52 (m, 1H), 1.46 – 1.39 (m, 1H), 0.98 – 0.88 (m, 6H).

Assignment: $\delta = 7.39$ (Bn, ϕ), 7.33 (Bn, ϕ), 4.93 (H^1), 4.67 (Bn, $\underline{\text{CH}_2}$), 4.16 (Asp, $\underline{\text{CH}_2}$), 3.91 (H^2), 3.51 (H^5), 3.48 (OCH_3), 3.47 (H^3), 3.40 (OCH_3), 3.12 (H^4), 1.84 (H^7), 1.55 ($\underline{\text{CH}_2}^6$), 1.42 ($\underline{\text{CH}_2}^6$), 0.95 ($\underline{\text{CH}_3}$), 0.90 ($\underline{\text{CH}_3}$).

^{13}C -NMR (125 MHz, CD_3CN , 300 K): $\delta = 128.60$ (Bn, ϕ), 128.17 (Bn, ϕ), 128.00 (Bn, ϕ), 97.93 (C^1), 81.51 (C^3), 80.95 (C^4), 74.81 (C^2), 72.91 (Bn, $\underline{\text{CH}_2}$), 70.34 (C^5), 63.58 (Asp, $\underline{\text{CH}_2}$), 60.17 (OCH_3), 56.99 (OCH_3), 41.24 ($\underline{\text{CH}_2}^6$), 24.60 (C^7), 23.62 ($\underline{\text{CH}_3}$), 21.29 ($\underline{\text{CH}_3}$).

ESI-MS: m/z : 405.3 [$\text{M}+\text{Na}^+$], MW calcd. for $\text{C}_{20}\text{H}_{30}\text{O}_7$: 382.2.

8.3.36 Synthesis of D-mannonic acid, 2-*O*-benzyl-6-*O*-isobutyl-3,4-di-*O*-methyl, 5-lactone (**58**)



The SET group in ethyl-2-*O*-benzyl-6-*O*-isobutyl-3,4-di-*O*-methyl-1-thio- α -D-mannopyranoside **32** was cleaved as described in 8.3.2. The free mannopyranose was then oxidized to lactone dissolving it in DMSO/Ac₂O 2:1 (15 mL) and stirring and heating the solution at 70 °C for 2 hours. The Ac₂O was then evaporated, the residue dissolved in ethyl ether (20 mL) and the organic extract washed with water (3 x 10 mL), dried (Na₂SO₄) and concentrated. Purification by flash column chromatography afforded **58** in 95 % yield.

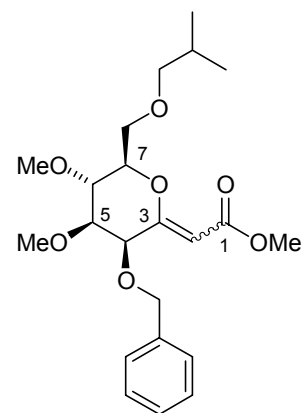
¹H-NMR (500 MHz, CDCl₃, 300 K): δ = 7.41 (d, *J* = 7.6 Hz, 2H), 7.37 (t, *J* = 7.6 Hz, 2H), 7.34 – 7.30 (m, 1H), 5.06 (d, *J* = 12.3 Hz, 1H), 4.62 (d, *J* = 12.3 Hz, 1H), 4.28 (s, 1H), 4.18 – 4.13 (m, 1H), 3.81 (s, 1H), 3.69 – 3.63 (m, 2H), 3.56 (d, *J* = 7.5 Hz, 1H), 3.53 (s, 3H), 3.42 (s, 3H), 3.31 – 3.25 (m, 2H), 1.92 – 1.84 (m, 1H), 0.91 (d, *J* = 7.2 Hz, 6H).

Assignment: δ = 7.41 (Bn, ϕ), 7.37 (Bn, ϕ), 7.32 (Bn, ϕ), 5.06 (Bn, $\underline{\text{CH}}_2$), 4.62 (Bn, $\underline{\text{CH}}_2$), 4.28 (H²), 4.16 (H⁵), 3.81 (H³), 3.66 ($\underline{\text{CH}}_2$), 3.56 (H⁴), 3.53 (O $\underline{\text{CH}}_3$), 3.42 (O $\underline{\text{CH}}_3$), 3.28 (Leu, $\underline{\text{CH}}_2$), 1.88 (Leu, $\underline{\text{CH}}$), 0.91 (Leu, $\underline{\text{CH}}_3$).

¹³C-NMR (125 MHz, CDCl₃, 300 K): δ = 128.75 (Bn, ϕ), 128.35 (Bn, ϕ), 128.32 (Bn, ϕ), 79.97 (C³), 78.98 (Leu, $\underline{\text{C}}_2$), 78.89 (C⁵), 77.90 (C⁴), 75.54 (C²), 73.33 (Bn, $\underline{\text{C}}_2$), 70.72 ($\underline{\text{C}}_2$), 59.20 (O $\underline{\text{C}}_3$), 57.97 (O $\underline{\text{C}}_3$), 28.59 (Leu, $\underline{\text{C}}_1$), 19.72 (Leu, $\underline{\text{C}}_3$).

ESI-MS: m/z : 375.3 $[M+Na^+]$, MW calcd. for $C_{19}H_{28}O_6$: 352.2.

8.3.37 Synthesis of D-manno-Oct-2-enonic acid, 3,7-anhydro-4-*O*-benzyl-2-deoxy-8-*O*-isobutyl-5,6-di-*O*-methyl, methyl ester (**59**)



A solution of lactone **58** (1 mmol) and methoxycarbonylmethylene-triphenylphosphorane (670 mg, 2 mmol), which was prepared following 8.3.11, in toluene (15 mL) was placed in a standard stainless steel vessel under an argon atmosphere and heated for 24 hours at 140 °C. After cooling, the solvent was removed under vacuum, and the residue was taken up in dichloromethane and placed on a silica gel column. Elution with a 6: 1 mixture of hexane/ethyl acetate gave analytically pure olefins **59** in 60 % yield. The ratio between the two isomers was 3:1. It was not possible to distinguish between E and Z and to assign the resonances for the least populated isomer. The two isomers were on purpose collected together.

$^1\text{H-NMR}$ (500 MHz, CDCl_3 , 300 K): δ = 7.44 – 7.29 (m, 5H), 5.21 (s, 1H), 4.74 (d, J = 12.3 Hz, 1H), 4.57 (d, J = 12.3 Hz, 1H), 4.22 – 4.15 (m, 1H), 3.88 – 3.74 (m, 3H), 3.71 (s, 3H), 3.56 – 3.42 (m, 9H), 3.34 – 3.28 (m, 1H), 1.98 – 1.87 (m, 1H), 0.99 – 0.90 (m, 6H).

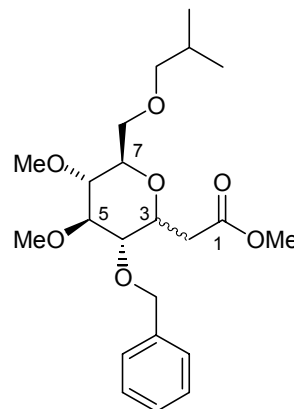
Assignment: δ = 7.37 (Bn, ϕ), 7.32 (Bn, ϕ), 5.21 (H^2), 4.74 (Bn, CH_2), 4.57 (Bn, CH_2), 4.19 (H^7), 3.85 (H^4), 3.81 (CH_2), 3.77 (CH_2), 3.71 (COOMe, CH_3), 3.53 (OCH_3), 3.51 (H^6), 3.51 (H^5), 3.47 (OCH_3), 3.45 (Leu, CH_2), 3.31 (Leu, CH_2), 1.93 (Leu, CH), 0.94 (Leu, CH_3).

$^{13}\text{C-NMR}$ (125 MHz, CDCl_3 , 300 K): δ = 128.91 (Bn, ϕ), 128.34 (Bn, ϕ), 128.28 (Bn, ϕ), 99.72 (C^2), 85.14 (C^5), 79.18 (C^6), 79.18 (Leu, CH_2), 77.91 (C^4), 77.91 (C^7), 71.91

(Bn, $\underline{\text{C}}\text{H}_2$), 69.57 ($\underline{\text{C}}\text{H}_2$), 59.53 ($\underline{\text{O}}\text{C}\underline{\text{H}}_3$), 58.85 ($\underline{\text{O}}\text{C}\underline{\text{H}}_3$), 51.39 (COOMe, $\underline{\text{C}}\text{H}_3$), 28.81 (Leu, $\underline{\text{C}}\text{H}$), 19.72 (Leu, $\underline{\text{C}}\text{H}_3$).

ESI-MS: m/z : 431.3 [$\text{M}+\text{Na}^+$], MW calcd. for $\text{C}_{22}\text{H}_{32}\text{O}_7$: 408.2.

8.3.38 Synthesis of D-gluco-Octonic acid, 3,7-anhydro-4-*O*-benzyl-2-deoxy-8-*O*-isobutyl-5,6-di-*O*-methyl, methyl ester (**60**)



Olefins **59** (0.1 mmol) were dissolved in 10 mL of dry methanol. To this solution was added nickel dichloride (3.75 mg, 0.016 mmol) and the solution was cooled to 0 °C. Sodium borohydride (11.5 mg, 0.3 mmol) was added to the mixture and it turned black. After 1 hour, the mixture was passed through a plug of celite and rinsed with 2 x 5 mL of methanol. The solvent was evaporated and the filtrate dissolved in 15 mL of Et₂O and 5 mL of H₂O. The phases were separated and the aqueous phase was extracted with 2 x 15 mL Et₂O. The combined organic phases were washed with 5 mL of brine, dried over Na₂SO₄, filtered, concentrated under vacuum and the residue purified by column chromatography using hexane/EtOAc 5:1 as eluant to afford **60** in 90 % yield with an α/β ratio of 2:1.

β :

¹H-NMR (500 MHz, CDCl₃, 300 K): δ = 7.41 – 7.28 (m, 5H), 4.92 (d, J = 11.4 Hz, 1H), 4.63 (d, J = 11.4 Hz, 1H), 3.72 – 3.54 (m, 12H), 3.38 – 3.14 (m, 6H), 2.76 – 2.69 (dd, J = 11.4 and 4.2 Hz, 1H), 2.50 – 2.44 (dd, J = 11.3 and 7.9 Hz, 1H), 1.95 – 1.85 (m, 1H), 0.94 – 0.89 (m, 6H).

Assignment: δ = 7.35 (Bn, ϕ), 7.31 (Bn, ϕ), 4.92 (Bn, CH₂), 4.63 (Bn, CH₂), 3.69 (OCH₃), 3.67 (H³), 3.64 (CH₂⁸), 3.62 (COOMe, CH₃), 3.58 (CH₂⁸), 3.57 (OCH₃), 3.34 (H⁵), 3.31 (Leu, CH₂), 3.26 (H⁷), 3.23 (H⁶), 3.21 (H⁴), 3.17 (Leu, CH₂), 2.73 (CH₂²), 2.46 (CH₂²), 1.29 (Leu, CH), 0.93 (Leu, CH₃), 0.91 (Leu, CH₃).

^{13}C -NMR (125 MHz, CDCl_3 , 300 K): $\delta = 128.40$ (Bn, ϕ), 128.20 (Bn, ϕ), 89.54 (C^5), 81.43 (C^4), 80.88 (C^6), 79.50 (C^7), 78.92 (Leu, $\underline{\text{C}}\text{H}_2$), 76.26 (C^3), 75.29 (Bn, $\underline{\text{C}}\text{H}_2$), 70.13 ($\underline{\text{C}}\text{H}_2^8$), 61.31 ($\text{O}\underline{\text{C}}\text{H}_3$), 60.81 ($\text{O}\underline{\text{C}}\text{H}_3$), 51.99 (COOMe, $\underline{\text{C}}\text{H}_3$), 37.93 ($\underline{\text{C}}\text{H}_2^2$), 30.10 (Leu, $\underline{\text{C}}\text{H}$), 19.95 (Leu, $\underline{\text{C}}\text{H}_3$), 19.81 (Leu, $\underline{\text{C}}\text{H}_3$).

α :

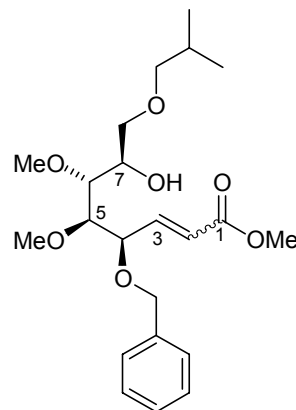
^1H -NMR (500 MHz, CDCl_3 , 300 K): $\delta = 7.38 - 7.30$ (m, 5H), 4.71 - 4.59 (m, 3H), 3.67 - 3.49 (m, 13H), 3.37 - 3.31 (m, 2H), 3.25 (t, $J = 9.5$ Hz, 1H), 3.15 - 3.10 (m, 1H), 2.77 - 2.72 (dd, $J = 14.8$ and 5.2 Hz, 1H), 2.69 - 2.63 (dd, $J = 15.1$ and 9.3 Hz, 1H), 1.96 - 1.87 (m, 1H), 0.94 - 0.89 (m, 6H).

Assignment: $\delta = 7.35$ (Bn, ϕ), 7.31 (Bn, ϕ), 4.69 (Bn, $\underline{\text{C}}\text{H}_2$), 4.64 (Bn, $\underline{\text{C}}\text{H}_2$), 4.62 (H^3), 3.66 ($\text{O}\underline{\text{C}}\text{H}_3$), 3.64 (COOMe, $\underline{\text{C}}\text{H}_3$), 3.63 (H^4), 3.58 ($\underline{\text{C}}\text{H}_2^8$), 3.57 ($\text{O}\underline{\text{C}}\text{H}_3$), 3.52 (H^7), 3.34 (H^5), 3.33 (Leu, $\underline{\text{C}}\text{H}_2$), 3.25 (H^6), 3.13 (Leu, $\underline{\text{C}}\text{H}_2$), 2.75 ($\underline{\text{C}}\text{H}_2^2$), 2.65 ($\underline{\text{C}}\text{H}_2^2$), 1.90 (Leu, $\underline{\text{C}}\text{H}$), 0.93 (Leu, $\underline{\text{C}}\text{H}_3$), 0.90 (Leu, $\underline{\text{C}}\text{H}_3$).

^{13}C -NMR (125 MHz, CDCl_3 , 300 K): $\delta = 128.13$ (Bn, ϕ), 128.08 (Bn, ϕ), 84.77 (C^5), 80.15 (C^6), 79.43 (C^4), 79.04 (Leu, $\underline{\text{C}}\text{H}_2$), 73.86 (Bn, $\underline{\text{C}}\text{H}_2$), 72.74 (C^7), 71.94 (C^3), 70.27 ($\underline{\text{C}}\text{H}_2^8$), 61.42 ($\text{O}\underline{\text{C}}\text{H}_3$), 60.95 ($\text{O}\underline{\text{C}}\text{H}_3$), 52.34 (COOMe, $\underline{\text{C}}\text{H}_3$), 32.83 ($\underline{\text{C}}\text{H}_2^2$), 28.78 (Leu, $\underline{\text{C}}\text{H}$), 20.02 (Leu, $\underline{\text{C}}\text{H}_3$), 19.76 (Leu, $\underline{\text{C}}\text{H}_3$).

ESI-MS: m/z : 410.2 [$\text{M} + \text{Na}^+$], MW calcd. for $\text{C}_{22}\text{H}_{34}\text{O}_7$: 433.3.

8.3.39 Synthesis of D-manno-Oct-2-enonic acid, 4-O-benzyl-2,3-deoxy-8-O-isobutyl-5,6-di-O-methyl, methyl ester (**61**)



The SET group in ethyl-2-*O*-benzyl-6-*O*-isobutyl-3,4-di-*O*-methyl-1-thio- α -D-mannopyranoside **32** was cleaved as described in 8.3.2. To a solution of the free mannopyranose (0.46 mmol) and acid-washed Zn dust (0.6 gr, 9.25 mmol, 20 equiv.) in anhydrous toluene (10 mL) were added at room temperature tributylphosphine (0.57 mL, 2.31 mmol, 5 equiv.) and methyl bromoacetate (0.22 mL, 2.31 mmol, 5 equiv.). The mixture was heated at reflux and the reaction monitored by TLC. After 48 hours, the mixture was concentrated and chromatographic purification on silica gel (7:1 hexane/EtOAc) afforded **61** in 60 % yield with an E/Z ratio of 1:1. The isomers on purpose were collected together.

$^1\text{H-NMR}$ (500 MHz, CDCl_3 , 300 K): δ = 7.42 – 7.16 (m, 10H), 7.10 (dd, J = 15.9 and 6.7 Hz, 1H), 6.33 (dd, J = 11.3 and 10.1 Hz, 1H), 6.22 (d, J = 15.9 Hz 1H), 6.10 (d, J = 11.3 Hz, 1H), 5.43 (dd, J = 9.5 and 6.4 Hz, 1H), 4.65 (d, J = 11.6 Hz, 1H), 4.61 (d, J = 11.6 Hz, 1H), 4.53 (d, J = 11.6 Hz, 1H), 4.40 (d, J = 11.6 Hz, 1H), 4.23 (t, J = 7.6 Hz, 1H), 3.95 – 3.86 (m, 2H), 3.81 (s, 3H), 3.76 (s, 3H), 3.69 – 3.44 (m, 14H), 3.38 (s, 3H), 3.35 (s, 3H), 3.34 – 3.21 (m, 4H), 1.97 – 1.85 (m, 2H), 0.99 – 0.88 (m, 12H).

E:

Assignment: δ = 7.10 (H^3), 6.22 (H^2), 4.65 (Bn, CH_2), 4.40 (Bn, CH_2), 4.23 (H^4), 3.88 (H^7), 3.81 (COOMe, CH_3), 3.61 (CH_2), 3.60 (H^5), 3.56 (H^6), 3.46 (OCH_3), 3.35 (OCH_3), 3.31 (Leu, CH_2), 3.24 (Leu, CH_2), 1.91 (Leu, CH), 0.94 (Leu, CH_3).

^{13}C -NMR (125 MHz, CDCl_3 , 300 K): $\delta = 147.23$ (C^3), 123.87 (C^2), 82.90 (C^5), 80.20 (C^6), 78.56 (Leu, $\underline{\text{C}}\text{H}_2$), 78.11 (C^4), 71.86 ($\underline{\text{C}}\text{H}_2$), 71.51 (Bn, $\underline{\text{C}}\text{H}_2$), 69.82 (C^7), 61.27 ($\text{O}\underline{\text{C}}\text{H}_3$), 60.52 ($\text{O}\underline{\text{C}}\text{H}_3$), 52.01 (COOMe , $\underline{\text{C}}\text{H}_3$), 28.80 (Leu, $\underline{\text{C}}\text{H}$), 19.69 (Leu, $\underline{\text{C}}\text{H}_3$).

Z:

Assignment: $\delta = 6.33$ (H^3), 6.10 (H^2), 5.43 (H^4), 4.61 (Bn, $\underline{\text{C}}\text{H}_2$), 4.53 (Bn, $\underline{\text{C}}\text{H}_2$), 3.91 (H^7), 3.76 (COOMe , $\underline{\text{C}}\text{H}_3$), 3.69 (H^5), 3.61 ($\underline{\text{C}}\text{H}_2$), 3.49 (H^6), 3.51 ($\text{O}\underline{\text{C}}\text{H}_3$), 3.38 ($\text{O}\underline{\text{C}}\text{H}_3$), 3.31 (Leu, $\underline{\text{C}}\text{H}_2$), 3.24 (Leu, $\underline{\text{C}}\text{H}_2$), 1.91 (Leu, $\underline{\text{C}}\text{H}$), 0.94 (Leu, $\underline{\text{C}}\text{H}_3$).

^{13}C -NMR (125 MHz, CDCl_3 , 300 K): $\delta = 146.83$ (C^3), 123.37 (C^2), 82.50 (C^5), 80.64 (C^6), 78.56 (Leu, $\underline{\text{C}}\text{H}_2$), 74.43 (C^4), 71.86 ($\underline{\text{C}}\text{H}_2$), 71.38 (Bn, $\underline{\text{C}}\text{H}_2$), 70.22 (C^7), 61.09 ($\text{O}\underline{\text{C}}\text{H}_3$), 60.34 ($\text{O}\underline{\text{C}}\text{H}_3$), 51.74 (COOMe , $\underline{\text{C}}\text{H}_3$), 28.80 (Leu, $\underline{\text{C}}\text{H}$), 19.69 (Leu, $\underline{\text{C}}\text{H}_3$).

ESI-MS: m/z : 433.3 [$\text{M}+\text{Na}^+$], MW calcd. for $\text{C}_{22}\text{H}_{34}\text{O}_7$: 410.2.

8.4 Conformational analysis of the cyclodextrin mimetics

8.4.1 NMR Spectroscopy

The spectra were acquired in H₂O (10 % D₂O), pH \cong 5.5 at T = 293 K (otherwise indicated) with Bruker DMX500 and DMX600 spectrometer and calibrated using 3-(trimethylsilyl)propionic acid-d₄ sodium salt as external reference.¹⁹⁴ Water suppression was achieved using WATERGATE.¹⁹⁵ The assignment of all proton and carbon resonances was carried out *via* standard procedures^{196,197} using double-quantum-filtered (DQF) COSY^{198,199} and heteronuclear (¹H-¹³C, ¹⁵N) single-quantum coherence (HSQC)²⁰⁰⁻²⁰³ with echo/antiecho coherence selection and decoupling during acquisition. Sequential assignment was accomplished by through bond connectivities from heteronuclear multibond correlation (HMBC)²⁰⁴⁻²⁰⁶ spectra with low-pass J-filter to suppress one-bond correlations, no decoupling during acquisition and echo/antiecho coherence selection. Multiplicities are given (obtained from 1D spectra) as s (singlet), d (doublet), t (triplet), dd (doublet of doublets), m (multiplet), br (broad). Data were processed on a Bruker X32 workstation using the UXMNMR-software. Proton distances were calculated using the two spin approximation from rotating frame nuclear Overhauser enhancement (ROESY)^{207,208} spectra with cw spinlock for mixing, $\tau_{\text{mix}} = 80\text{-}150$ ms, and phase sensitive using States-TPPI method. The offset correction, integration and calibration of the ROE cross peaks were achieved using the program SYBYL (Version 6.6, Tripos, Inc. MO, USA). ROE connectivities were calibrated based upon fixed geometric distances between protons within the pyranose ring hold in the ⁴C₁ conformation. Homonuclear coupling constants were determined from one dimensional spectra and from exclusive COSY (E.COSY)²⁰⁹ cross peaks. In the case of ³J(CH₂-NH) the use of the Karplus equation (A = 9.4 Hz, B = -1.1 Hz, C = 0.4 Hz, phase shift $\sigma = -60$) gave approximate values for the correspondent ' ϕ ' angle of the Gum sugar amino acid.

8.4.2 Computer simulations

The structure calculations were performed on Silicon Graphics computers. Energy minimization (EM) and molecular dynamic (MD) calculations were carried out with

the program DISCOVER using the CVFF force field,²¹⁰ and a dielectric constant of 80. After EM using steepest descent and conjugate gradient the system was heated gradually starting from 300 K up to 800 K and subsequently cooled down to 300 K using at every temperature 5 ps steps, each by direct scaling of velocities. Configurations were saved every 25 ps for another 500 ps. All the structures coming from MD simulations were minimized using again steepest descent and conjugate gradient algorithms. During molecular modeling simulations no restraints were taken into account. The structures were at the end evaluated based upon the NOE and the dihedral restraints derived from ³J coupling constants.

8.5 Binding studies of the cyclodextrin mimetics

Complexation was monitored by recording ¹H NMR spectra for samples with different host/guest ratios which vary from 0.25 to 10. The host/guest ratio corresponding to each sample was deduced from direct integration of the NMR signal. The ¹H spin-lattice relaxation time (T_1) was measured by an inversion recovery pulse sequence (180°-τ-90°). The data were analyzed by the UXNMR T_1/T_2 relaxation menu and fitted using the equation $I(t) = I(0) * [1 - 2A * \exp(-t/T_1)]$. Diffusion coefficients were obtained from pseudo-2D diffusion experiment with first order compensation of convection flux.¹⁷¹ The diffusion measured on one proton was calculated obtaining the intensity $I(\text{grad})$ of the signal of this nucleus at various gradient values. The data were fitted by the UXNMR T_1/T_2 relaxation menu using the equation $I(\text{grad}) = I(0) * \exp[-1e-5 * D * (\text{DELTA} - d/3) * (2\pi * \gamma * d * G)^2]$ where $d = 6$ ms, $\text{DELTA} = 42$ ms and the g factor (Hz/Gauss) was calibrated based upon the extrapolated diffusion coefficient of the water peak at 293 K.¹⁷¹

8.6 Biological evaluation of the mannose-based library

Adhesion buffer: Click's RPMI medium, 1% BSA, 1.0 mM CaCl₂, 1.0 mM MgCl₂.

Tris buffer Saline (TBS-buffer): Tris (14 mM), NaCl (137 mM), KCl (2.7 mM), Glucose (2.0 mM), 1% BSA, Mn²⁺ (1.0 mM).

Medium for 38C13 β 1- and 38C13 β 7-cells: Click's RPMI medium (0.5 L), FCS (35 mL), glutamine (5 mL), β -mercaptoethanol (1000 X, 0.5 mL).

Medium for Jurkat cells: Click's RPMI medium (0.5 L), FCS (35 mL), glutamine (5 mL).

38C13 β 7-cells: B lymphoma cells from C3H/He mice, infected with L β 7SN virus and selected with G418.

8.6.1 38C13 β 1- and 38C13 β 7-cells in culture

2/3 of the cell solution were daily separated from the rest and diluted with new medium. The cell cultures were constantly kept at 37 °C.

8.6.2 MAdCAM-1 and VCAM supernatant

293T cells (embryonic fibroblasts from kidney) were transfected with pCDNA3.1 IgG MAdCAM-1 or pCDNA3.1 IgG VCAM, respectively and the supernatants were collected after two to three days.

8.6.3 Coating of 96-well plates with MAdCAM-1 and VCAM

96-well plates were coated with donkey anti-human IgG (Jackson ImmunoResearch Laboratories Inc.) (0.5 μ g in 100 μ L PBS/well) overnight at 4 °C. The plates were purged with adhesion buffer (1x 100 μ L/well) and incubated 30 min at RT with 25-150 μ L/well MAdCAM- or VCAM-supernatant (depending on the concentration).

8.6.4 Preparation of the 96-well plates

The plates coated with MAdCAM-1 or VCAM were washed with adhesion buffer (1 x 100 μ L/well) and blocked with adhesion buffer for 1 h at RT.

8.6.5 Preparation of the cells

The cell suspension (12.5 mL) was centrifuged for 3 min at 1500 Upm, washed with PBS (1 x 5 mL) and again centrifuged for 3 min at 1500 Upm. The cells were resuspended in adhesion buffer (3 mM) and incubated for 30 min at 37 °C with a dye (6 µL H33342, Calbiochem, La Jolla, CA). The suspension was centrifuged for 3 min at 1500 Upm, purged with PBS/1 mM EDTA (5 mL), again centrifuged for 3 min at 1500 Upm and resuspended in PBS (10 mL).

After counting the cells, the suspension was centrifuged for 3 min at 1500 Upm. The cells were suspended in a defined amount of adhesion buffer to reach a final cell concentration of 8×10^5 cells/mL.

8.6.6 Performance of the cell adhesion assay

The cell suspension (350 µL, 8×10^5 cells/mL) was incubated with the compound (3.5 µL of the stock solution: 1 mg compound in 10 µL DMSO) for 10 min at 37 °C and aliquots were put on the plate with a pipette (100 µL/well). The plates were centrifuged for 10 min at 15 g and analyzed by fluorimetry using Cytofluor 2300 (Millipore, Bedford, MA). After incubation for 30 min at 37 °C, the wells were checked visually for precipitation. The plates were washed in a PBS bath and the wells were sealed with a wrap. After inverse centrifugation for 10 min at 50 g the wrap was removed and the remaining liquid was carefully removed in vacuum. The wells were filled with adhesion buffer (100 µL/well) and quantified by fluorimetry.

8.7 Conformational analysis of the mannose-based library

8.7.1 NMR Spectroscopy

The spectra were acquired in CD₃CN or CDCl₃ at T = 300 K (otherwise indicated) with Bruker DMX500 spectrometer and calibrated using the solvent as internal reference. The assignment of all proton and carbon resonances was carried out *via* standard procedures^{196,197} using double-quantum-filtered (DQF) COSY^{198,199} and heteronuclear (¹H-¹³C) single-quantum coherence (HSQC)²⁰⁰⁻²⁰³ with echo/antiecho coherence selection and decoupling during acquisition. Sequential assignment was

accomplished by through bond connectivities from heteronuclear multibond correlation (HMBC)²⁰⁴⁻²⁰⁶ with low-pass J-filter to suppress one-bond correlations, no decoupling during acquisition and echo/antiecho coherence selection, and from HSQC-COSY experiments. Multiplicities are given (obtained from 1D spectra) as s (singlet), d (doublet), t (triplet), dd (doublet of doublets), m (multiplet). Data were processed on a Bruker X32 workstation using the XWINNMR-software. Proton distances were calculated using the nuclear Overhauser enhancement (NOESY)²¹¹ with $\tau_{\text{mix}} = 200$ ms, and phase sensitive using States-TPPI method. The integration and calibration of the NOE cross peaks were achieved using the program SYBYL (Version 6.6, Tripos, Inc. MO, USA). NOE connectivities were calibrated based upon fixed geometric distances between protons within the pyranose ring hold in the 4C_1 conformation. Homonuclear coupling constants were determined from one dimensional spectra.

8.7.2 Computer simulations

The structure calculations were performed on Silicon Graphics computers. Energy minimization (EM) and molecular dynamic (MD) calculations were carried out in vacuum with the program DISCOVER using the CVFF force field.²¹⁰ After EM using steepest descent and conjugate gradient the system was heated gradually starting from 300 K up to 800 K and subsequently cooled down to 300 K using at every temperature 5 ps steps, each by direct scaling of velocities. Configurations were saved every 25 ps for another 1.25 ns. All the structures coming from MD simulations were minimized using again steepest descent and conjugate gradient algorithms. During molecular modeling simulations no restraints were taken into account. The structures were evaluated at the end based upon the NOE data.

9 References

- (1) Heyns, K.; Paulsen, H. *Chem. Ber.* **1955**, *88*, 188-195.
- (2) Gruner, S. A. W.; Locardi, E.; Lohof, E.; Kessler, H. *Chem. Rev.* **2002**, *102*, 491-514.
- (3) Lohof, E.; Burkhart, F.; Born, M. A.; Planker, E.; Kessler, H. In *Advances in Amino Acid Mimetics and Peptidomimetics*; Abell, A., Ed.; JAI Press Inc.: Stanford, Connecticut, 1999; Vol. 2, pp 263-292.
- (4) Graf von Roedern, E.; Kessler, H. *Angew. Chem. Int. Ed. Engl.* **1994**, *33*, 687-689.
- (5) McDevitt, J. P.; Lansbury, P. T. *J. Am. Chem. Soc.* **1996**, *118*, 3818-3828.
- (6) Sofia, M. J.; Hunter, R.; Chan, T. Y.; Vaughn, A.; Dulina, R.; Wang, H.; Gange, D. *J. Org. Chem.* **1998**, *63*, 2802-2803.
- (7) Ramamoorthy, P. S.; Gervay, J. *J. Org. Chem.* **1997**, *62*, 7801-7805.
- (8) Fügedi, P.; Peto, C.; Wlasichuk, K. In *8th European Carbohydrate Symposium*, 1995.
- (9) Sabesan, S. *Tetrahedron Lett.* **1997**, *38*, 3127-3130.
- (10) Fuchs, E. F.; Lehmann, J. *J. Chem. Ber.* **1975**, *108*, 2254-2260.
- (11) Fuchs, E. F.; Lehmann, J. *Carbohydr. Res.* **1976**, *49*, 267-273.
- (12) Nicolaou, K. C.; Flörke, H.; Egan, M. G.; Barth, T.; Estevez, V. A. *Tetrahedron Lett.* **1995**, *36*, 1775-1778.
- (13) Goodnow Jr., R. A.; Tam, S.; Pruess, D. L.; McComas, W. W. *Tetrahedron Lett.* **1997**, *38*, 3199-3202.
- (14) Goodnow Jr., R. A.; Richou, A.-R.; Tam, S. *Tetrahedron Lett.* **1997**, *38*, 3195-3198.
- (15) Locardi, E.; Stöckle, M.; Gruner, S.; Kessler, H. In *20th International Carbohydrate Symposium*, 2000; p 51.
- (16) Locardi, E.; Stöckle, M.; Gruner, S.; Kessler, H. *J. Am. Chem. Soc.* **2001**, *123*, 8189-8196.
- (17) Schneider, H.-J.; Hacket, F.; Rüdiger, V. *Chem. Rev.* **1998**, *98*, 1755-1785.
- (18) Rekharsky, M. V.; Inoue, Y. *Chem. Rev.* **1998**, *98*, 1875-1917.

- (19) Uekama, K.; Hirayama, F.; Irie, T. *Chem. Rev.* **1998**, *98*, 2045-2076.
- (20) Loftsson, T.; Brewster, M. E. *Journal of Pharmaceutical Sciences* **1996**, *85*, 1017-1169.
- (21) Szejtli, J. *Chem. Rev.* **1998**, *98*, 1743-1753.
- (22) Hirschmann, R.; Nicolaou, K. C.; Pietranico, S.; Leahy, E. M.; Salvino, J.; Arison, B.; Cichy, B. M. A.; Spoons, P. G.; Shakespeare, W. C.; Sprengeler, P. A.; Hamley, P.; Smith III, A. B.; Reisine, T.; Raynor, K.; Maechler, L.; Donaldson, C.; Vale, W.; Freidinger, R. M.; Cascieri, M. R.; Strader, C. D. *J. Am. Chem. Soc.* **1993**, *115*, 12550-12568.
- (23) Hirschmann, R.; Sprengeler, P. A.; Kawasaki, T.; Leahy, J. W.; Shakespeare, W. C.; Smith III, A. B. *Tetrahedron* **1993**, *49*, 3665-3676.
- (24) Olson, G. L.; Bolin, D. R.; Bonner, M. P.; Bös, M.; Cook, C. M.; Fry, D. C.; Graves, B. J.; Hatada, M.; Hill, D. E.; Kahn, M.; Madison, V. S.; Rusiecki, V. K.; Sarabu, R.; Sepinwall, J.; Vincent, G. P.; Voss, M. E. *J. Med. Chem.* **1993**, *36*, 3039-3049.
- (25) Bélanger, P. C.; Dufresne, C. *Can. J. Chem.* **1986**, *64*, 1514-1520.
- (26) Hirschmann, R.; Hynes, J.; Cichy-Knight, M. A.; van Rijn, R. D.; Sprengeler, P. A.; Spoons, P. G.; Shakespeare, W. C.; Pietranico-Cole, S.; Barbosa, J.; Liu, J.; Yao, W.; Rohrer, S.; Smith III, A. B. *J. Med. Chem.* **1998**, *41*, 1382-1391.
- (27) Papageorgiou, C.; Haltiner, R.; Bruns, C.; Petcher, T. J. *Bioorg. Med. Chem. Lett.* **1992**, *2*, 135-140.
- (28) Boer, J.; Gottschling, D.; Schuster, A.; Semmrich, M.; Holzmann, B.; Kessler, H. *J. Med. Chem.* **2001**, *44*, 2586-2592.
- (29) Boer, J.; Gottschling, D.; Schuster, A.; Holzmann, B.; Kessler, H. *Angew. Chem. Int. Ed. Engl.* **2001**, *40*, 3870-3873.
- (30) von Andrian, U. H.; Mackay, C. R. *New Eng. J. Med.* **2000**, *343*, 1020-1034.
- (31) Hynes, R. O. *Cell* **1992**, *69*, 11-25.
- (32) Curley, G. P.; Blum, H.; Humphries, M. J. *Cell. Mol. Life Sci.* **1999**, *56*, 427-441.
- (33) Hantgan, R. R.; Mousa, S. A. *Thromb. Res.* **1998**, *89*, 271-279.
- (34) Fan, S.; Mackman, N.; Cui, M.; Edgington, T. S. *J. Immunol.* **1995**, *154*, 3266-3274.

- (35) Arroyo, A. G.; Yang, J. T.; Rayburn, H.; Hynes, R. O. *Immunity* **1999**, *11*, 555-566.
- (36) Hamann, A.; Andrew, D. P.; Joblansky, D. W.; Holzmann, B.; Butcher, E. C. *J. Immunol.* **1994**, *152*, 3282-3293.
- (37) Humphries, M. J. *J. Cell Sci.* **1990**, *97*, 585-592.
- (38) Newham, P.; Humphries, M. J. *Mol. Med. Today* **1996**, *2*, 304-313.
- (39) Gardner, J. M.; Hynes, R. O. *Cell* **1985**, *42*, 439-448.
- (40) Pytela, R.; Pierschbacher, M. D.; Ruoslahti, E. *Cell* **1985**, *40*, 191-198.
- (41) Pytela, R.; Pierschbacher, M. D.; Ginsberg, M. H.; Plow, E. F.; Ruoslahti, E. *Science* **1986**, *231*, 1559-1562.
- (42) Dedhar, S.; Gray, V. *J. Cell Biol.* **1990**, *110*, 2185-2193.
- (43) Goodman, S. L.; Hölzemann, G.; Sulyok, G. A. G.; Kessler, H. *J. Med. Chem.* **2002**, *45*, 1045-1051.
- (44) Wayner, E. A.; Garcia-Pardo, A.; Humphries, M. J.; McDonald, J. A.; Carter, W. G. *J. Cell Biol.* **1989**, *109*, 1321-1330.
- (45) Mould, A. P.; Wheldon, L. A.; Komoriya, A.; Wayner, E. A.; Yamada, K. M.; Humphries, M. J. *J. Biol. Chem.* **1990**, *265*, 4020-4024.
- (46) Komoriya, A.; Green, L. J.; Mervic, M.; Yamada, S. S.; Yamada, K. M.; Humphries, M. J. *J. Biol. Chem.* **1991**, *266*, 15075-15079.
- (47) Ruegg, C.; Postigo, A. A.; Sikorski, E. E.; Butcher, E. C.; Pytela, R.; Erle, D. J. *J. Cell Biol.* **1992**, *117*, 179-189.
- (48) Chan, B. M.; Elices, M. J.; Murphy, E.; Hemler, M. E. *J. Biol. Chem.* **1992**, *267*, 8366-8370.
- (49) Clements, J. M.; Newham, P.; Shepherd, M.; Gilbert, R.; Dudgeon, T. J.; Needham, L. A.; Edwards, R. M.; Berry, L.; Brass, A.; Humphries, M. J. *J. Cell Sci.* **1994**, *107*, 2127-2135.
- (50) Osborn, L.; Vassallo, C.; Benjamin, C. D. *J. Exp. Med.* **1992**, *176*, 99-107.
- (51) Osborn, L.; Vassallo, C.; Browning, B. G.; Tizard, R.; Haskard, D. O.; Benjamin, C. D.; Douglas, I.; Kirchhausen, T. *J. Cell Biol.* **1994**, *124*, 601-608.
- (52) Renz, M. E.; Chiu, H. H.; Jones, S.; Fox, J.; Kim, K. J.; Presta, L. G.; Fong, S. *J. Cell Biol.* **1994**, *125*, 1395-1406.
- (53) Vonderheide, R. H.; Springer, T. A. *J. Exp. Med.* **1992**, *175*, 1433-1442.

- (54) Vonderheide, R. H.; Tedder, T. F.; Springer, T. A.; Staunton, D. E. *J. Cell Biol.* **1994**, *125*, 215-222.
- (55) Chiu, H. H.; Crowe, D. T.; Renz, M. E.; Presta, L. G.; Jones, S.; Weissman, L.; Fong, S. *J. Immunol.* **1995**, *155*, 5257-5267.
- (56) Berlin, C.; Berg, E. L.; Briskin, M. J.; Andrew, D. P.; Kilshaw, P. J.; Holzmann, B.; Weissman, I. L.; Hamann, A.; Butcher, E. C. *Cell* **1993**, *74*, 185-195.
- (57) Briskin, M. J.; McEvoy, L. M.; Butcher, E. C. *Nature* **1993**, *363*, 461-464.
- (58) Briskin, M. J.; Rott, L.; Butcher, E. C. *J. Immunol.* **1996**, *156*, 719-726.
- (59) Erle, D. J.; Briskin, M. J.; Butcher, E. C.; Garcia-Pardo, A.; Lazarovits, A. I.; Tidswell, M. *J. Immunol.* **1994**, *153*, 517-528.
- (60) Hemler, M. E. *Ann. Rev. Immunol.* **1990**, *8*, 365-400.
- (61) Chuluyan, H. E.; Issekutz, A. C. *Springer Semin. Immunopathology* **1995**, *16*, 391-404.
- (62) Postigo, A. A.; Sanchez-Mateos, P.; Lazarovits, A. I.; Sanchez-Madrid, F.; de Landazuri, M. O. *J. Immunol.* **1993**, *151*, 2471-2483.
- (63) Kilger, G.; Holzmann, B. *J. Mol. Med.* **1995**, *73*, 347-354.
- (64) Bargatze, R. F.; Jutila, M. A.; Butcher, E. C. *Immunity* **1995**, *3*, 99-108.
- (65) Andrew, D. P.; Berlin, C.; Honda, S.; Yoshino, T.; Hamann, A.; Holzmann, B.; Kilshaw, P. J.; Butcher, E. C. *J. Immunol.* **1994**, *153*, 3847-3861.
- (66) Holzmann, B.; Weissman, I. L. *Embo J.* **1989**, *8*, 1735-1741.
- (67) Holzmann, B.; McIntyre, B. W.; Weissman, I. L. *Cell* **1989**, *56*, 37-46.
- (68) Hu, M. C.; Crowe, D. T.; Weissman, I. L.; Holzmann, B. *Proc. Natl. Acad. Sci. USA* **1992**, *89*, 8254-8258.
- (69) Picarella, D.; Hurlbut, P.; Rottman, J.; Shi, X.; Butcher, E.; Ringler, D. J. *J. Immunol.* **1997**, *158*, 2099-20106.
- (70) Yang, X. D.; Sytwu, H. K.; McDevitt, H. O.; Michie, S. A. *Diabetes* **1997**, *46*, 1542-1547.
- (71) Connor, E. M.; Eppihimer, M. J.; Morise, Z.; Granger, D. N.; Grisham, M. B. *J. Leukocyte Biol.* **1999**, *65*, 349-355.
- (72) Tanaka, H.; Kuwashima, N. *Kekkan to Naihi* **1995**, *5*, 561-570.
- (73) Viney, J. L.; Joenes, S.; Chiu, H. H.; Lagrimas, B.; Renz, M. E.; Presta, L. G.; Jackson, D.; Hillan, K. J.; Lew, S.; Fong, S. *J. Immunol.* **1996**, *157*, 2488-2497.

- (74) Tan, K.; Casanovas, J. M.; Liu, J. H.; Briskin, M. J.; Springer, T. A.; Wang, J. H. *Structure* **1998**, *6*, 793-801.
- (75) Wang, J. H.; Pepinsky, R. B.; Stehle, T.; Liu, J. H.; Karpusas, M.; Browning, B.; Osborn, L. *Proc. Natl. Acad. Sci. USA* **1995**, *92*, 5714-5718.
- (76) Jones, E. Y.; Harlos, K.; Bottomley, M. J.; Robinson, R. C.; Driscoll, P. C.; Edwards, R. M.; Clements, J. M.; Dudgeon, T. J.; Stuart, D. I. *Nature* **1995**, *373*, 539-544.
- (77) Xiong, J.-P.; Stehle, T.; Diefenbach, B.; Zhang, R.; Dunker, R.; Scott, D. L.; Joachimiak, A.; Goodman, S. L.; Arnaout, M. A. *Science* **2001**, *294*, 339-345.
- (78) Xiong, J.-P.; Stehle, T.; Zhang, R.; Joachimiak, A.; Frech, M.; Goodman, S. L.; Arnaout, M. A. *Science* **2002**, *296*, 151-155.
- (79) Dechantsreiter, M. A.; Planker, E.; Mathä, B.; Lohof, E.; Hölzemann, G.; Jonczyk, A.; Goodman, S. L.; Kessler, H. *J. Med. Chem.* **1999**, *42*, 3033 - 3040.
- (80) Gottschalk, K. E.; Günther, R.; Kessler, H. *ChemBioChem* **2002**, *3*, 470-473.
- (81) Gottschalk, K. E.; Kessler, H. *Angew. Chem. Int. Ed.* **2002**, in print.
- (82) Lohof, E.; Born, M. A.; Kessler, H. In *Synthesis of Peptides and Peptidomimetics*; Goodman, M., Felix, A., Moroder, L., Toniolo, C., Eds.; Georg Thieme Verlag: Stuttgart, 2001; Vol. E22b, in press.
- (83) Williamson, A. R.; Zamenhof, S. *J. Biol. Chem.* **1963**, *238*, 2255-2258.
- (84) Heyns, K.; Kiessling, G.; Lindenberg, W.; Paulsen, H.; Webster, M. E. *Chem. Ber.* **1959**, *92*, 2435-2438.
- (85) Waltho, J. P.; Williams, D. H.; Selva, E.; Ferrari, P. *J. Chem. Soc. Perkin Trans. I* **1987**, *9*, 2103-2107.
- (86) Knapp, S. *Chem. Rev.* **1995**, *95*, 1859-1876.
- (87) Knapp, S.; Jaramillo, C.; Freeman, B. *J. Org. Chem.* **1994**, *59*, 4800-4804.
- (88) Watanabe, K. A.; Falco, E. A.; Fox, J. J. *J. Am. Chem. Soc.* **1972**, *94*, 3272-3274.
- (89) Coutsogeorgopoulos, C.; Bloch, A.; Watanabe, K. A.; Fox, J. J. *J. Med. Chem.* **1975**, *18*, 771-776.
- (90) Fox, J. J.; Kuwada, Y.; Watanabe, K. A. *Tetrahedron Lett.* **1968**, *57*, 6029-6032.

- (91) Lichtenthaler, F. W.; Morino, T.; Mezel, H. M. *Tetrahedron Lett.* **1975**, *16*, 665-668.
- (92) Kotick, M. P.; Klein, R. S.; Watanabe, K. A.; Fox, J. J. *Carbohydr. Res.* **1969**, *11*, 369-377.
- (93) Siehl, D. L.; Subramanian, M. V.; Walters, E. W.; Lee, S.-F.; Anderson, R. J.; Toschi, A. G. *Plant. Physiol.* **1996**, *110*, 753-758.
- (94) Nakajima, M.; Itoi, K.; Takamatsu, Y.; Kinoshita, T. i.; Okazaki, T.; Kawakubo, K.; Shindo, M.; Honma, T.; Tohjigamori, M.; Haneishi, T. *J. Antibiot.* **1991**, *44*, 293-300.
- (95) Haruyama, H.; Takayama, T.; Kinoshita, T.; Kondo, M.; Nakajima, M.; Haneishi, T. *J. Chem. Soc. Perkin Trans. 1* **1991**, *7*, 1637-1640.
- (96) Umezawa, H.; Aoyagi, T.; Komiyama, T.; Morishima, H.; Hamada, M.; Takeuchi, T. *J. Antibiot.* **1974**, *27*, 963-969.
- (97) Graf von Roedern, E.; Lohof, E.; Hessler, G.; Hoffmann, M.; Kessler, H. *J. Am. Chem. Soc.* **1996**, *118*, 10156-10167.
- (98) Smith, M. D.; Long, D. D.; Claridge, T. D. W.; Marquess, D. G.; Fleet, G. W. J. *J. Chem. Soc., Chem. Commun.* **1998**, *18*, 2039-2040.
- (99) Long, D. D.; Smith, M. D.; Marquess, D. G.; Claridge, T. D. W.; Fleet, G. W. J. *Tetrahedron Lett.* **1998**, *39*, 9293-9296.
- (100) Long, D. D.; Hungerford, N. L.; Smith, M. D.; Brittain, D. E. A.; Marquess, D. G.; Claridge, T. D. W.; Fleet, G. W. J. *Tetrahedron Lett.* **1999**, *40*, 2195-2198.
- (101) Claridge, T. D. W.; Long, D. D.; Hungerford, N. L.; Smith, M. D.; Aplin, R. T.; Marquess, D. G.; Fleet, G. W. J. *Tetrahedron Lett.* **1999**, *40*, 2199-2203.
- (102) Watterson, M. P.; Pickering, L.; Smith, M. D.; Hudson, S. H.; Marsh, P. R.; Mordaunt, J. E.; Watkin, D. J.; Newman, C. J.; Fleet, G. W. J. *Tetrahedron Asymmetry* **1999**, *10*, 1855-1859.
- (103) Smith, M. D.; Fleet, G. W. J. *J. Peptide Sci.* **1999**, 425-441.
- (104) Hungerford, N. L.; Claridge, T. D. W.; Watterson, M. P.; Aplin, R. T.; Moreno, A.; Fleet, G. W. J. *J. Chem. Soc. Perkin Trans. 1* **2000**, 3666-3679.
- (105) Smith, M. D.; Long, D. D.; Martin, A.; Marquess, D. G.; Claridge, T. D. W.; Fleet, G. W. J. *Tetrahedron Lett.* **1999**, *40*, 2191-2194.

- (106) Gruner, S. A. W.; Truffault, V.; Voll, G.; Locardi, E.; Stöckle, M.; Kessler, H. *Chem. Eur. J.* **2002**, *8*, 4365-4376.
- (107) Lohof, E.; Planker, E.; Mang, C.; Burkart, F.; Dechantsreiter, M. A.; Haubner, R.; Wester, H.-J.; Schwaiger, M.; Hölzemann, G.; Goodman, S. L.; Kessler, H. *Angew. Chem. Int. Ed. Engl.* **2000**, *39*, 2761-2764.
- (108) Gruner, S. A. W.; Kéri, G.; Schwab, R.; Venetianer, A.; Kessler, H. *Org. Lett.* **2001**, *3*, 3723-3725.
- (109) Haubner, R.; Wester, H.-J.; Burkhart, F.; Senekowitsch-Schmidtke, R.; Goodman, S. L.; Kessler, H.; Schwaiger, M. *J. Nucl. Med.* **2001**, *42*, 326-336.
- (110) Haubner, R.; Wester, H.-J.; Weber, W. A.; Mang, C.; Ziegler, S. I.; Goodman, S. L.; Senekowitsch-Schmidtke, R.; Kessler, H.; Schwaiger, M. *Cancer Res.* **2001**, *61*, 1781-1785.
- (111) Drouillat, B.; Kellam, B.; Dekany, G.; Starr, M. S.; Toth, I. *Bioorg. Med. Chem. Lett.* **1997**, *7*, 2247-2250.
- (112) Kirshenbaum, K.; Zuckermann, R. N.; Dill, K. A. *Curr. Opin. Struct. Biol.* **1999**, *9*, 530-535.
- (113) Soth, M. J.; Nowick, J. S. *Curr. Opin. Chem. Biol.* **1997**, *1*, 120-129.
- (114) Seeberger, P. H.; Haase, W.-C. *Chem. Rev.* **2000**, *100*, 4349-4393.
- (115) Seeberger, P. H. *Solid support oligosaccharide synthesis and combinatorial carbohydrate libraries*; Wiley: New York, 2001.
- (116) Fuchs, E. F.; Lehmann, J. *Chem. Ber.* **1976**, *109*, 267-273.
- (117) Yoshimura, J.; Ando, H.; Sato, T.; Tsuchida, S.; Hashimoto, H. *Bull. Chem. Soc. Jpn.* **1976**, *49*, 2511-2514.
- (118) Wessel, H. P.; Mitchell, C.; Lobato, C. M.; Schmid, G. *Angew. Chem. Int. Ed. Engl.* **1995**, *34*, 2712-2713.
- (119) Suhara, Y.; Hildreth, J. E. K.; Ichikawa, Y. *Tetrahedron Lett.* **1996**, *37*, 1575-1578.
- (120) Suhara, Y.; Ichikawa, M.; Hildreth, J. E. K.; Ichikawa, Y. *Tetrahedron Lett.* **1996**, *37*, 2549-2552.
- (121) Müller, C.; Kitas, E.; Wessel, H. P. *J. Chem. Soc., Chem. Commun.* **1995**, *23*, 2425-2426.

- (122) Szabo, L.; Smith, B. L.; McReynolds, K. D.; Parrill, A. L.; Morris, E. R.; Gervay, J. *J. Org. Chem.* **1998**, *63*, 1074-1078.
- (123) van Well, R. M.; Overkleeft, H. S.; Overhand, M.; Vang Carstenen, E.; van der Marel, G. A.; van Boom, J. H. *Tetrahedron Lett.* **2000**, *41*, 9331-9335.
- (124) Stöckle, M.; Voll, G.; Günther, R.; Lohof, E.; Locardi, E.; Gruner, S.; Kessler, H. *Org. Lett.* **2002**, *4*, 2501-2504.
- (125) Bols, M. *Carbohydrate Building Blocks*; Wiley: New York, 1996.
- (126) Wunberg, T.; Kallus, C.; Opatz, T.; Henke, S.; Schmidt, W.; Kunz, H. *Angew. Chem. Int. Ed.* **1998**, *37*, 2503-2505.
- (127) Schweizer, F.; Hindsgaul, O. *Curr. Opin. Chem. Biol.* **1999**, *3*, 291-298.
- (128) Hirschmann, R.; Nicolaou, K. C.; Pietranico, S.; Salvino, J.; Leahy, E. M.; Sprengler, P. A.; Furst, G.; Smith III, A. B. *J. Am. Chem. Soc.* **1992**, *114*, 9217-9218.
- (129) Hirschmann, R.; Yao, W.; Cascieri, M. A.; Strader, C. D.; Maechler, L.; Cichy, M. A.; Jr., J. H.; van Rijn, R. D.; Sprengler, P. A.; Smith III, A. B. *J. Med. Chem.* **1996**, *39*, 2441-2448.
- (130) Nicolaou, K. C.; Trujillo, J. I.; Chibale, K. *Tetrahedron* **1997**, *53*, 8751-8778.
- (131) Brazeau, P.; Vale, W.; Burgus, R.; Guillemain, R. *Can. J. Biochem.* **1974**, *52*, 1067-1072.
- (132) Gurrath, M.; Müller, G.; Kessler, H.; Aumailley, M.; Timpl, R. *Eur. J. Biochem.* **1992**, *210*, 911-921.
- (133) Pfaff, M.; Tangemann, K.; Müller, B.; Gurrath, M.; Müller, G.; Kessler, H.; Timpl, R.; Engel, J. *J. Biol. Chem.* **1994**, *269*, 20233-22038.
- (134) Haubner, R.; Gratias, R.; Diefenbach, B.; Goodman, S. L.; Jonczyk, A.; Kessler, H. *J. Am. Chem. Soc.* **1996**, *118*, 7461.
- (135) Haubner, R.; Finsinger, D.; Kessler, H. *Angew. Chem. Int. Ed. Engl.* **1997**, *36*, 1374-1389.
- (136) Wermuth, J.; Goodman, S. L.; Jonczyk, A.; Kessler, H. *J. Am. Chem. Soc.* **1997**, *119*, 1328-1335.
- (137) Moitessier, N.; Minoux, H.; Maigret, B.; Chretien, F.; Chapleur, Y. *Lett. Pept. Sci.* **1998**, *5*, 75-78.
- (138) Moitessier, N.; Dufour, S.; Chretien, F.; Thiery, J. P.; Maigret, B.; Chapleur, Y. *Bioorg. Med. Chem.* **2001**, *9*, 511-523.

- (139) Le Diguarher, T.; Boudon, A.; Elwell, C.; Paterson, D. E.; Billington, D. C. *Bioorg. Med. Chem. Lett.* **1996**, *6*, 1983-1988.
- (140) Dinh, T. G.; Smith, C. D.; Du, X.; Armstrong, R. W. *J. Med. Chem.* **1998**, *41*, 981-987.
- (141) Lockhoff, O. *Angew. Chem. Int. Ed.* **1999**, *37*, 3436-3439.
- (142) Smith III, A. B.; Sasho, S.; Barwis, B. A.; Sprengeler, P.; Barbosa, J.; Hirschmann, R.; Cooperman, B. S. *Bioorg. Med. Chem. Lett.* **1998**, *8*, 3133-3136.
- (143) Gottschling, D.; Boer, J.; Schuster, A.; Holzmann, B.; Kessler, H. *Angew. Chem. Int. Ed. Engl.* **2002**, *41*, 3007-3011.
- (144) Gottschling, D.; Boer, J.; Marinelli, L.; Voll, G.; Haupt, M.; Schuster, A.; Holzmann, B.; Kessler, H. *ChemBioChem* **2002**, *3(6)*, 575-578.
- (145) Locardi, E.; Boer, J.; Modlinger, A.; Schuster, A.; Holzmann, B.; Kessler, H. *J. Med. Chem.* **2002**, submitted.
- (146) Davis, N. J.; Flitsch, S. L. *Tetrahedron Lett.* **1993**, *34*, 1181-1184.
- (147) Anelli, P. L.; Biffi, C.; Montanari, F.; Quici, S. *J. Org. Chem.* **1987**, *52*, 2559-2562.
- (148) de Nooy, A. E. J.; Besemer, A. C. *Tetrahedron* **1995**, *51*, 8023-8032.
- (149) de Nooy, A. E. J.; Besemer, A. C.; van Bekkum, H. *Carbohydr. Res.* **1995**, *269*, 89-98.
- (150) Ehrlich, A.; Rothmund, S.; Brudel, M.; Beyermann, M.; Carpino, L. A.; Bienert, M. *Tetrahedron Lett.* **1993**, *34*, 4781-4784.
- (151) Ehrlich, A.; Heyne, H. U.; Winter, R.; Beyermann, M.; Haber, H.; Carpino, L. A.; Bienert, M. *J. Org. Chem.* **1996**, *61*, 8831-8838.
- (152) Carpino, L. A.; El-Faham, A.; Albericio, F. *Tetrahedron Lett.* **1994**, *35*, 2279-2282.
- (153) Carpino, L. A.; El-Faham, A.; Minor, C. A.; Albericio, F. *J. Chem. Soc., Chem. Commun.* **1994**, 201-203.
- (154) Brady, S. F.; Varga, S. L.; Freidinger, R. M.; Schwenk, D. A.; Mendlowski, M.; Holly, F. W.; Veber, D. F. *J. Org. Chem.* **1979**, *44*, 3101-3105.
- (155) Zimmer, S.; Hoffmann, E.; Jung, G.; Kessler, H. *Liebigs Ann. Chem.* **1993**, 497-501.

- (156) Zimmer, S.; Hoffmann, E.; Jung, G.; Kessler, H. In *Peptides 1992*; Schneider, C. H., Eberle, A. N., Eds.; ESCOM Science Publishers, 1993; pp 393-394.
- (157) Shioiri, T.; Ninomiya, K.; Yamada, S.-I. *J. Am. Chem. Soc.* **1972**, *94*, 6203-6205.
- (158) Carpino, L. A. *J. Am. Chem. Soc.* **1993**, *115*, 4397-4398.
- (159) Khan, A. R.; Forgo, P.; Stine, K. J.; D'Souza, V. T. *Chem. Rev.* **1998**, *98*, 1977-1996.
- (160) Lehmann, J.; Kleinpeter, E.; Krechl, J. *J. Inclusion. Phenom.* **1991**, *10*, 233-239.
- (161) Salvatierra, D.; Diez, C.; Jaime, C. *J. Inclusion. Phenom.* **1997**, *27*, 215-231.
- (162) Butkus, E.; Jose, J. C.; Berg, U. *J. Inclusion. Phenom.* **1996**, *26*, 209-218.
- (163) Davies, D. M.; Savage, J. R. *J. Chem. Soc. Perkin Trans. 2* **1994**, 1525-1530.
- (164) Inoue, Y.; Okuda, T.; Kuan, F. H.; Chujo, R. *Carbohydr. Res.* **1984**, *129*, 9-20.
- (165) Inoue, Y.; Kuan, F. H.; Chujo, R. *Bull. Chem. Soc. Jpn.* **1987**, *60*, 2539-2545.
- (166) Behr, J. P.; Lehn, J. M. *J. Am. Chem. Soc.* **1976**, *98*, 1743-1747.
- (167) Mock, W. M.; Shih, N.-Y. *J. Am. Chem. Soc.* **1989**, *111*, 2697-2699.
- (168) Hilmersson, G.; Rebek, J. *Magn. Reson. Chem.* **1998**, *36*, 663-669.
- (169) Rymden, R.; Carlfors, J.; Stilbs, P. *J. Inclusion. Phenom.* **1983**, *1*, 159-167.
- (170) Gafni, A.; Cohen, Y.; Katakly, R.; Palmer, S.; Parker, D. *J. Chem. Soc. Perkin Trans. 2* **1998**, 19-23.
- (171) Diercks, T. In *Institut für Organische Chemie und Biochemie*; Technische Universität München: München, 1999; pp 1-266.
- (172) Chen, L.; Tilley, J. W.; Huang, T.-N.; Miklowski, D.; Trilles, R.; Guthrie, R. W.; Luk, K.; Hanglow, A.; Rowan, K.; Schwinge, V.; Wolitzky, B. *Bioorg. Med. Chem. Lett.* **2000**, *10*, 725-727.
- (173) Chen, L.; Tilley, J. W.; Guthrie, R. W.; Mennona, F.; Huang, T.-N.; Kaplan, G.; Trilles, R.; Miklowski, D.; Huby, N.; Schwinge, V.; Wolitzky, B.; Rowan, K. *Bioorg. Med. Chem. Lett.* **2000**, *10*, 729-733.
- (174) Tilley, J. W.; Kaplan, G.; Rowan, K.; Schwinge, V.; Wolitzky, B. *Bioorg. Med. Chem. Lett.* **2000**, *11*, 1-4.
- (175) Ashwell, S.; Banker, A. L.; Bicksler, J. J.; Dressen, D. B.; Cannon, C.; Giberson, J.; Grant, F. F.; Konradi, A. W.; Leeson, P. D.; Lombardo, L. J.; Pleiss, M.

- A.; Sarantakis, D.; Thompson, T.; Thorsett, E. D.; Vandever, C.; Yang, C. In *Abstr. Pap. Am. Chem. Soc.*, 2000; Vol. 220th, p 138.
- (176) Hagmann, W. K.; Durette, P. L.; Lanza, T.; Kevin, N. J.; de Laszlo, S. E.; Kopka, I. E.; Young, D.; Magriotis, P. A.; Li, B.; Lin, L. S.; Yang, G.; Kamenecka, T.; Chang, L. L.; Wilson, J.; MacCoss, M.; Mills, S. G.; van Riper, G.; McCauley, E.; Egger, L. A.; Kidambi, U.; Lyons, K.; Vincent, S.; Stearns, R.; Colletti, A.; Teffera, J.; Tong, S.; Fenyk-Melody, J.; Owens, K.; Levorse, D.; Kim, P.; Schmidt, J. A.; Mumford, R. A. *Bioorg. Med. Chem. Lett.* **2001**, *11*, 2709-2713.
- (177) Harriman, G. C. B.; Schwender, C. F.; Gallant, D. L.; Cochran, N. A.; Briskin, M. J. *Bioorg. Med. Chem. Lett.* **2000**, *10*, 1497-1499.
- (178) Grice, P.; Ley, S. V.; Pietruszka, J.; Priepke, H. W. M.; Warriner, S. L. *J. Chem. Soc. Perkin Trans. 1* **1997**, 351-363.
- (179) Douglas, N. L.; Ley, S. V.; Osborn, H. M. I.; Owen, D. R.; Priepke, H. W. M.; Warriner, S. L. *Synlett* **1996**, 793-794.
- (180) Williamson, W. *Justus Liebigs Ann. Chem.* **1851**, *77*, 37-49.
- (181) Johnstone, R. A. W.; Rose, M. E. *Tetrahedron* **1979**, *35*, 2169-2173.
- (182) Gridley, J. J.; Osborn, H. M. I. *J. Chem. Soc. Perkin Trans. 1* **2000**, 1471-1491.
- (183) Praly, J. P.; Lemieux, R. U. *Can. J. Chem.* **1987**, *65*, 213-223.
- (184) Paulsen, H.; Lockhoff, O. *Chem. Ber.* **1981**, *114*, 3102-3114.
- (185) Perlin, A. S.; Casu, B. *Tetrahedron Lett.* **1969**, 2921-2924.
- (186) Bock, K.; Pedersen, C. *J. Chem. Soc. Perkin Trans. 2* **1974**, 293-297.
- (187) Dalcanale, E.; Montanari, F. *J. Org. Chem.* **1986**, *51*, 567-569.
- (188) Lakhri, M.; Chapleur, Y. *Angew. Chem. Int. Ed. Engl.* **1996**, *35*, 750-752.
- (189) Sato, F.; Sato, S.; Sato, M. *J. Organomet. Chem.* **1976**, *122*, C25-C27.
- (190) Sato, F.; Sato, S.; Sato, M. *J. Organomet. Chem.* **1977**, *131*, C26-C28.
- (191) Dheilly, L.; Fréchet, C.; Beaupère, D.; Uzan, R.; Demailly, G. *Carbohydr. Res.* **1992**, *224*, 301-306.
- (192) Shroff, H. N.; Schwender, C. F.; Baxter, A. D.; Brookfield, F.; Payne, L. J.; Cochran, N. A.; Gallant, D. L.; Briskin, M. J. *Bioorg. Med. Chem. Lett.* **1998**, *8*, 1601-1606.
- (193) Lipinski, C. A. *Chimia* **1998**, *52*, 503.

- (194) Wishart, D. S.; Bigam, C. G.; Yao, J.; Abildgaard, F.; Dyson, H. J.; Oldfield, E.; Markley, J. L.; Sykes, B. D. *J. Biomol. NMR* **1995**, *6*, 135-140.
- (195) Piotto, M.; Saudek, V.; Sklenar, V. *J. Biomol. NMR* **1992**, *2*, 661-666.
- (196) Kessler, H.; Seip, S. In *Two-Dimensional NMR-Spectroscopy, Applications for Chemists and Biochemists*; Croasmun, W. R., Carlson, M. K., Eds.; VCH: New York, 1994; pp 619-654.
- (197) Kessler, H.; Schmitt, W. In *Encyclopedia of Nuclear Magnetic Resonance*; Grant, D. M., Harris, R. K., Eds.; Wiley&Sons: New York, 1996; Vol. 6, pp 3527-3537.
- (198) Piantini, U.; Sørensen, O. W.; Ernst, R. R. *J. Am. Chem. Soc.* **1982**, *104*, 6800-6801.
- (199) Rance, M.; Sørensen, O. W.; Bodenhausen, G.; Wagner, G.; Ernst, R. R.; Wüthrich, K. *Biochem. Biophys. Res. Commun.* **1983**, *117*, 479-485.
- (200) Müller, L. *J. Am. Chem. Soc.* **1979**, *101*, 4481-4484.
- (201) Bodenhausen, G.; Ruben, D. J. *Chem. Phys. Letter* **1980**, *69*, 185-189.
- (202) Bax, A.; Ikura, M.; Kay, L. E.; Torchia, D. A.; Tschudin, R. *J. Magn. Reson.* **1990**, *86*, 304-318.
- (203) Norwood, T. J.; Boyd, J.; Heritage, J. E.; Soffe, N.; Campbell, I. D. *J. Magn. Reson.* **1990**, *87*, 488-501.
- (204) Bax, A.; Summers, M. F. *J. Am. Chem. Soc.* **1986**, *108*, 2093-2094.
- (205) Bermel, W.; Wagner, K.; Griesinger, C. *J. Magn. Reson.* **1989**, *83*, 223-232.
- (206) Kessler, H.; Schmieder, P.; Köck, M.; Kurz, M. *J. Magn. Reson.* **1990**, *88*, 615-618.
- (207) Bothner-By, A. A.; Stevens, R. L.; Lee, J.; Warren, C. D.; Jeanloz, R. W. *J. Am. Chem. Soc.* **1984**, *106*, 811-813.
- (208) Kessler, H.; Griesinger, C.; Kerssebaum, R.; Wagner, K.; Ernst, R. R. *J. Am. Chem. Soc.* **1987**, *109*, 607-609.
- (209) Griesinger, C.; Sørensen, O. W.; Ernst, R. R. *J. Am. Chem. Soc.* **1985**, *107*, 6394-6396.
- (210) Hagler, A. T.; Lifson, S.; Dauber, P. *J. Am. Chem. Soc.* **1979**, *101*, 5122-5130.
- (211) Kumar, A.; Ernst, R. R.; Wüthrich, K. *Biochem. Biophys. Res. Commun.* **1980**, *95*, 1-6.